

Utrecht university

Migration of heavy metals in soils by evaporation

Earth sciences, Geochemistry

Zeinab Safar

Content list

<i>Abstract:</i>	4
<i>Introduction</i>	6
2. <i>Literature</i>	9
2.1 <i>Introduction:</i>	9
2.2 <i>Saudi Arabia and mineralogical properties of its soil:</i>	10
2.3 <i>The effect of wetting- drying cycles:</i>	11
2.4 <i>Heavy metal retention mechanisms:</i>	11
2.4.1 <i>Adsorption mechanism:</i>	12
2.4.2 <i>Surface complexation and precipitation:</i>	15
2.4.3 <i>Fixation of heavy metal:</i>	16
2.4.4 <i>Heavy metal competitive behavior:</i>	16
2.5 <i>Individual retention behavior of selected heavy metals:</i>	17
2.5.1 <i>Cd:</i>	17
2.5.2 <i>Cr:</i>	18
2.6.3 <i>Pb</i>	19
2.5.5 <i>Cu:</i>	20
2.5.5 <i>Zn:</i>	20
2.5.6 <i>Ni:</i>	21
3. <i>Materials and methods:</i>	22
3.1 <i>Soil characterization:</i>	22
3.2 <i>Experimental setup:</i>	23
3.3 <i>XRF analysis:</i>	24
3.4 <i>XRD analysis:</i>	25
4. <i>Results and discussion:</i>	26
4.1 <i>Soil characteristics:</i>	26
4.2 <i>Experimental results:</i>	29
4.3 <i>Cr:</i>	32
4.3.1 <i>The Cr migration and speciation behavior in the clay soil samples:</i>	32
4.3.2 <i>The Cr migration and speciation behavior in the sand soil samples:</i>	33
4.4 <i>Cu:</i>	35
4.4.1 <i>The Cu migration and speciation behavior in the clay soil samples:</i>	35

4.4.2	<i>The Cu migration and speciation behavior in the sand soil samples:</i>37
4.5	<i>Ni:</i>38
4.5.1	<i>The Ni migration and speciation behavior in the clay soil samples:</i>38
4.5.2	<i>The Ni migration and speciation behavior in the sand soil samples:</i>40
4.6	<i>Zn:</i>41
4.6.1	<i>The Zn migration and speciation behavior in the clay soil samples:</i>41
4.7	<i>Pb:</i>44
4.7.1	<i>The Pb migration and speciation behavior in the clay soil samples:</i>44
4.7.2	<i>The Pb migration and speciation behavior in the sand soil samples:</i>46
4.8	<i>Cd:</i>47
4.8.1	<i>The Cd migration and speciation behavior in the clay soil samples:</i>47
4.8.2	<i>The Cd migration and speciation behavior in the sand soil samples:</i>49
4.9	<i>The change in alkali metals and other elements present in the soils:</i>50
5.	<i>Final considerations and conclusions</i>52
	<i>Acknowledgement:</i>55
	<i>References:</i>56
	<i>Appendix A: pictures of the samples after evaporation</i>58
	<i>Appendix B: graph of relative distribution of the heavy metals through the soil columns</i>59
	<i>Appendix C-1 : Micro XRF data of the sand</i>66
	<i>Appendix C-2 :Micro XRF data of the clay</i>80
	<i>Some of the surface sample pictures:</i>94
	<i>Appendix D: XRD data (sand)</i>96
	<i>Appendix E: concentrations alkali metals of other elements present in the soil</i> 105

Abstract:

The heavy metals behave differently in the soil depending on soil type, composition and also on the environment surrounding the soil. In the arid and semiarid environments, evaporation has predominance on precipitation. Heavy metals may accumulate in the soil, due to anthropogenic activities causing contamination of the soils. These heavy metals may migrate upward, with the evaporating soil pore water in different forms, reaching the top soil and the surface. The heavy metals at the soil surface may cause health hazard, to the people contacting the soil even in low concentration. Because the heavy metals could be bonded on the surface of the clay particles and fly away with the wind as dust particles, which can be inhaled by people.

The aim of this thesis is to study the migration and complexation of the heavy metals by evaporation. Two different soil types, sandy and clayey soils, from Saudi Arabia were chosen for this study.

The soils have high pH and contain high amounts of Fe, and Al hydroxides, but they are totally different in all other characteristics, like organic matter and moisture content, grain size distribution etc.

In the laboratory, both soil samples were contaminated with heavy metals in 7 separate soil reactors for each soil type, by introducing a solution of heavy metals through the soil sample columns until water saturation. The samples were left to age during three weeks after saturation. After contamination and ageing, the concentrations of the heavy metals were measured in one sample of each soil type, these samples were sliced in three slices for the measurement of the heavy metals. The heavy metals concentrations in the slices were incubated according to Aqua Regia procedure and measured with ICP OES technique.

The rest of the soil samples were evaporated in different evaporation stages, a set of samples were dried during three weeks, other set was dried for five weeks and the last set was dried for seven weeks. A salt layer was accumulated at the surface of the samples that became thicker after each evaporation step.

The samples were divided into different number of slices and the surface layer was separated. The windblown dust on the reactor ceiling and caught in water tubes were also analyzed by extraction with 67% HNO₃. The concentrations of the heavy metals and other elements present in the soil were measured in all of the slices, in the surface layer and the dust particles as well.

The bottom, middle and the surface slices of each sample were analyzed with Micro XRF(X-ray fluorescence). These slices of the sand sample were also analyzed with XRD (X- ray diffraction) technique, to investigate the speciation of the heavy metals in different slices.

The heavy metals behave differently in the two soil types, since the soil characteristics are different. The heavy metals generally migrate upward faster in the sand than in the clay. This is due to the fact that the sand is coarser grained, and it has lower capacity to adsorb heavy metals, compared to the clay sample. But since it contains high amounts of Fe and Al hydroxides and hydroxides that can adsorb the heavy metals by inner-sphere adsorption mechanism, the metals could also be retained in the sand sample.

The heavy metals are retained and accumulated in the lower slices of the samples, by inner-sphere adsorption onto the soil constituents like Fe, Mn and Al oxides and hydroxides, and complexation with dissolved organic matter in the case of the clay sample.

In both soil samples, the heavy metals are migrated upward mostly in dissolved carbonate, sulfate and chloride complexes and precipitated as the pore water was dried. The heavy metals could bind to the clay particles by non-specific (outer-sphere) adsorption. In this case they can also migrate upward by exchange with other ions, the competitive behavior of the metals may play an important role in the migration of the metals if they are adsorbed electrostatically on the clay particles. The more electronegative metals with larger radius will exchange the lesser electronegative, and smaller radius metal. This might cause the faster migration of the Ni, and in lesser extent the Zn, Cr and Cd compared with the stronger binding, and slower migrating Cu and Pb. The heavy metals concentrations in the dust particles of the two soil type were also totally different. The metal concentrations were significantly higher in the dust particles of the sand soil, than in the clay dust particles. The metals could bind to the clay particles by exchangeable adsorption, and may cause health hazard. Most of them, like Cd are toxic even at very low concentrations.

Introduction

Soil is one of the key elements for the ecosystems. It provides the nutrient bearing environment for plant life and is of essential importance for degradation and transfer of biomass. Soil is a very complex heterogeneous medium, which consist of solid phases, the soil matrix, containing minerals and organic matter and fluid phases, the soil water and soil air, which interact with each other and with ions entering the soil system. The ability of the soil to retain heavy metals from aqueous solution is of special interest. It has consequences for many issues, like agriculture, environmental questions such as remediation of polluted soils and waste deposition [1]. Accumulation of heavy metals in the polluted soils can also have impact on human's health. Since men come in contact with soils though many activities.

Heavy metal ions are the most toxic inorganic pollutants which occur in soils and can be of natural or anthropogenic origin. Some of them are toxic even if their concentration is very low and their toxicity increases with accumulation in water and soils [1].

Disposal of metals contaminated industrial effluent, sewage sludge, mining activities, application of fertilizers and pesticides in agriculture and municipal waste land filling contributed to a continuous accumulation of heavy metals in soils [2].

Most of these contamination sources produce relatively high concentrations of heavy metals, which can reach orders of mg/kg in concentration. Figure 1 shows a table with listed heavy metal concentrations of an industrial area and sewage sludge as example of heavy metal contamination concentrations.

figure 1: Example of concentrations of heavy metal contamination sources [4].

Heavy metals (mg/kg) studied in samples collected small-scale industrial areas of Kanpur city.

	Fe	Mn	Zn	Cu	Cd	Ni	Pb	Cr
USEPA Std. (MSW)	-	-	-	281	3.3	7.5	34	76
Compost Std. (MSW, India)	-	-	-	300	5	50	100	50
PIA ^a (no. of samples)								
SW (12)	1884.57	173.14	232.93	20.10	1.42	26.11	107.11	1323.45
S (12)	871.64	40.86	346.04	8.19	1.03	10.98	55.49	859.24
RD (12)	1083.99	75.09	144.49	15.23	1.17	18.00	85.53	939.71
JJA ^b								
SW (12)	2340.32	444.81	131.82	28.38	1.12	396.68	19.20	733.61
S (12)	1689.48	266.34	77.21	13.39	1.66	11.85	8.21	393.30
RD (12)	838.22	188.59	43.00	12.19	1.07	22.90	3.50	406.92
Landfill (3)	953.43	176.13	32.93	6.47	1.50	1.61	4.10	23.50
Ganga bed sediment (2)	245.87	46.00	134.00	23.00	0.60	0.68	1.70	66.00

SW, solid waste samples; S, soil samples; RD, road dust samples.

^a Panki Industrial Area.

^b Jajmau Industrial Area.

The heavy metals accumulated in the polluted soils behave differently depending on the environmental conditions and soil properties. The soils have different characteristics in different environments. For instance in wet climatic areas the soils are muddy and rich in organic matter and soil moisture content and have a relatively low to natural pH. While in the arid and semi arid climatic regions, the soils are more calcareous and characterized with high pH, relatively low organic matter and low soil moisture content. This difference in characteristics is due to the fact that the soils are influenced by the climate conditions. In arid environments the evaporation has predominance over precipitation. The soil water will be transported to the top soil due to the atmospheric demand for evaporation and capillarity, creating latent heat flux and causing more drying effect on the top and the surface of the soil.

Evaporation takes place at the soil surface for initially wet conditions but eventually also occurs below the surface as the soil dries. This has a significant effect on the surface energy balance since the energy required for the phase change must be transferred from the soil surface to the subsurface evaporation sites mainly by conduction, which requires an increase of soil heat flux density and temperature gradient [8]. Concurrently water vapor diffuses upward from these evaporation sites to the soil surface. This vapor transfer is supplied by liquid water flow from layers below the evaporation zone [8].

The process of evaporation can be divided into three stages: (a) when the soil is wet, evaporation occurs at the potential rate, hence the only limitation is the atmospheric demand; (b) when the soil becomes dryer, water cannot be supplied to the soil surface fast enough to meet the evaporative demand, and so the rate of evaporation decreases as the thickness of the dry layer increase; (c) the rate of evaporation becomes very small compared to the potential demand [5].

Analysis of field studies of soil drying, suggests that the dispersion flux of the water vapor near the soil surface, which is seldom considered in soil drying models, can make a significant contribution to the total water flux [11].

In a study under arid conditions, the existence of a dry soil layer is reported, from surface to 25 cm depth through which the water transport was mainly in vapor form, whereas water transport in liquid form dominated below this layer. Later studies, based on field measurements and numerical simulations, reported the existence of an evaporation zone, at the bottom of the dry soil surface layer, which is thicker for fine-textured soils than for coarse-textured soils. The relative roles of vapor and liquid fluxes on water transport from the inner soil to the soil/ atmosphere interface was explored using a numerical model. The results indicate that, while vapor diffusion dominates total moisture transport near the soil surface, liquid transport controls evaporation at daily time scales in the deeper layers of the soil, for all but the dry soils [11]. Other studies suggested that the contraction and the expansion of air near the surface could transport water vapor by convection (in addition to diffusion and Brownian motion).

The coupled transport of water liquid and vapor and energy in the unsaturated zone effects contaminant transport and volatilization [11].

Evaporation takes place even at temperatures well below the boiling point of water.

When the water evaporates the non volatile constituents of the water remain at the site of evaporation [10].

The evaporation of water from soils containing dissolved salts or chemicals leads to a concentration of these substances at or near surface [19].

The concentration profile which develops with time depend upon both the upward evaporative flux of water, which concentrates salts, for example, at the surface, and the diffusive- dispersive flux, which tends to move salts downward against the upward flux of water [19].

Under evaporative conditions, solutes which are initially in the soil will accumulate near the surface with increasing time [19]. Under field conditions where macropores may be present, it is likely that evaporation will take place not only at the soil surface but within the top few centimeters of the soil. Under field conditions, precipitation of solutes may also take place at or near the soil surface [19].

The aim of this research is to investigate the upward movement and the speciation of the heavy metals in the metal contaminated soils by evaporation, which is the dominating process in arid and semi arid environments. Exposure to toxic heavy metals, if they are accumulated at the soil surface of contaminated soils, can cause health problems for people contacting these soils (like children or farmers). They can also be inhaled with the dust coming from the soil surface by blowing air, depending on the binding form with the soil particles. Two types of soil samples from Saudi Arabia are chosen to study this behavior of the heavy metals.

2. Literature

2.1 Introduction:

In soils the heavy metals mobility is low compared to other elements. This is due to the capacity of the soil to adsorb heavy metals. The mobility of the metals depends on the interaction with the solid phases during transport by water through the pores. The metals are immobilized either by forming low solubility precipitates, by adsorption or both [2,23].

The general term for the retention of the heavy metals is sorption. This term is preferred, because the retention mechanism is often unknown. According to Bradle et al: 'sorption involves the loss of metal ion from an aqueous to a contiguous solid phase and consists of three important processes; adsorption, surface precipitation and fixation' [1].

Soil components, amount of heavy metals added and environmental factors like hydrological, mineralogical and chemical properties of the soil affect the degree of heavy metal sorption in the soils. The main sorption surfaces are clay particles, Fe, Al and Mn (hydro) oxides and organic matter [2, 23].

Generally the principle soil characteristics that determine the capacity to retain the heavy metals are pH, dissolved organic matter content, cation exchange capacity, specific surface area, carbonate content and Iron oxides content. The presence of carbonates at high pH (>7) leads to an increase of the soil heavy metal retention capacity. In this case the metals retain in the soil mainly as carbonate salts or scavenged in the carbonate matrix. As the pH decreases, the carbonates will dissolve and ionic exchange will be the principle retention mechanism of heavy metals [23].

The soils in arid regions contain often silicates, carbonates, and sulfate minerals that are relatively sensitive to dissolution reactions with percolating water. They are often at the early stages of Jackson- Sherman weathering sequence (table 1).

The evaporation rates in the arid zone exceed the precipitation rates on annual basis. Therefore the soils of arid regions are typically saline ($EC > 1 \text{ dm/m}$). In these regions ions are released into the soil solution by mineral weathering, or by intrusion of saline surface water or ground water and tend to accumulate in secondary minerals formed as the soil dries. These secondary minerals include clay minerals, carbonates, sulfates and chlorides. The set of metals that contributes most to the salinity of the soil are Na, Ca, K and Mg. These metals are relatively easy brought to solution, either as exchangeable cations displaced from smectite and illite, or as structural cations dissolved from carbonates and sulfate and chlorides. The corresponding set of the ligands then would be CO_3 , SO_4 and Cl. In this case the soil solution of the arid regions is an electrolyte solution which contains chloride, sulfate and carbonate salts of group IA and IIA metals (alkali metals and alkali earth metals) [17].

Table 1: Jackson – Sherman weathering sequence [17]

Characteristic in minerals and soil clay fraction	Characteristic soil chemical and physical conditions	Characteristic soil properties
<p>Early stage Gypsum Carbonates Olivine/ Pyroxene/ amphibole Fe (II)- bearing Micas Feldspars</p>	<p>Low water and humus content Very limited leaching Reducing environment, cold environment Limited amount of time for weathering</p>	<p>Minimally weathered soils: Arid or very cold regions Waterlogging (saturation with water/ high water table), recent deposition</p>
<p>Intermediate stage Quartz Dioctahedral mica/ illite Dioctahedral vermiculite/ chlorite Smectite</p>	<p>Retention of Na, K, Ca, MG, Fe(II), and silica; moderate leaching, alkalinity Parent material rich in Ca, Mg, and Fe(II), but not Fe(II) oxides Silicates easy weathered</p>	<p>Soils in temperate regions; forest or grass cover, Well developed A and B horizons, accumulation of humus and clay minerals</p>
<p>Advanced stage Kaolinite Gibbsite Iron oxides Titanium oxides</p>	<p>Removal of Na, K, Ca, Mg, Fe(II), and silica Intensive leaching by fresh water Oxidation of Fe(II) Low pH and humus content</p>	<p>Soils under forest cover with high temperature and precipitation: accumulation of Fe(II) and Al oxides, absence of alkaline earth metals</p>

2.2 Saudi Arabia and mineralogical properties of its soil:

Saudi Arabia has a desert climate characterized by extreme heat during the day, and abrupt drop in temperature during the night, and slight erratic rainfall. The annual temperature average of the ambient air and soils is 26-27 C, but daily maximum temperature is 32-33 C. and the highest recorded temperature is 46-47 C. The mean annual rainfall is about 89 mm in the east coast and 36 mm in the west coast. Since the precipitation is very intense in the rainfall periods, it rains for a maximum of 98 mm in 24 hour in the east coast and 48 mm/ day in the west coast [21]. The soils types vary from sandy clay loam, sandy loam or only loam, and characterized by high pH values (7.5-8.2) and high CaCO₃ concentrations.

The samples of investigation are from the eastern oasis of Al-Hassa. The oasis of Al-Hassa is situated in the eastern province of Saudi Arabia about 170 Km southeast of Dammam on the Arabian Gulf. The irrigation water is supplied from 32 natural springs

fed from an artesian groundwater reservoir. The climate is continental with a mean annual precipitation of 69 mm and mean annual temperature of 25.2 °C, and 92% of the Al Hassa land is cultivated with date palm [14].

The date palm cultivation caused some changes in the properties of the soils. The variation in depth of the A_P horizons of the pedons could be related to different intensities of date palm cultivation.

The chosen soil samples, in the east coast of Saudi Arabia, are in marine deposit in which illite and smectite predominates, and have high level of salinity. Samples of the study (from Al- Hassa) are dominated by palygorskite (magnesium-aluminum- phyllosilicates) followed by smectite, illite and vermiculite. The abundance of the 2:1 layered clay minerals type like smectite clay minerals in the soil samples is an indication for high water holding capacity of the soil, as well as high nutrient retention against leaching and other losses. The most common impurities are free iron oxide minerals, amorphous silica and alumina, quartz grain, limestone, gypsum and other more soluble salts [13,14]. The soils have high contents of CaCO₃, inherited from their parent materials, which increase the pH and may contribute to the rapid decomposition of organic matter resulting in the formation of mollic epipedons [14].

From the comparison of the soil mineralogical and physical characteristics with the Jackson- Sherman weathering sequence, it appears that the soil of investigation is between the early and intermediate stage.

2.3 The effect of wetting- drying cycles:

During drying of the soil, several processes contribute to crust restructuring. If the soil moisture content is high, the clay particles rearrange themselves and cause age-hardening, that increases the cohesion between mineral soil particles. Age hardening is more noticeable in soils with high clay and organic matter content. Adsorption of organic and inorganic components at contact points between minerals can also produce stable bonds and increase aggregate stability. In addition to enhancing the stability of bonds between crust-forming particles, drying also supports the formation of individual aggregates. The tension caused by introduced water, pulls the primary particles together, promoting closer packing or direct contact. This tensile stress and shrinkage of clay and humus particles causes micro cracks in the crust, and separates the individual aggregates from the coherent crust [6].

The wetting of a clay that previously was exposed to an intensive drying does not restore the same water amount. In this case, the clay particles have experienced rearrangement during the drying period. Drying of water tends to reorganize the crystallites again. Very intense drying of water adsorbed by smectite or vermiculites brings reorganization within those crystallites whose layers are no longer that much disorderly stacked. The stacking order increases as the drying intensity increases or with repetition of the drying-wetting cycle [15].

2.4 Heavy metal retention mechanisms:

The fate of heavy metals on the soil surface is dominated by soil process which depend on the soil constituents. Contents of amorphous oxides, organic matter and clays (aggregates) cause complex interactions between all soil components and influence the

heavy metal distribution [16]. When a solid metal is spilled on to the soil, according to Rikers: ‘three steps are needed for its mobilization and subsequent adsorption. First an oxide coating forms, second the coating dissolves and third the free metal ions form complexes and are adsorbed by organic material and metal oxides’ [16].

As mentioned before heavy metals can retain in the soil by several mechanisms as adsorption to the soil particle and/ or precipitation as low soluble salts, or by fixation, depending on the soil characteristics and conditions. These mechanisms are studied in this section.

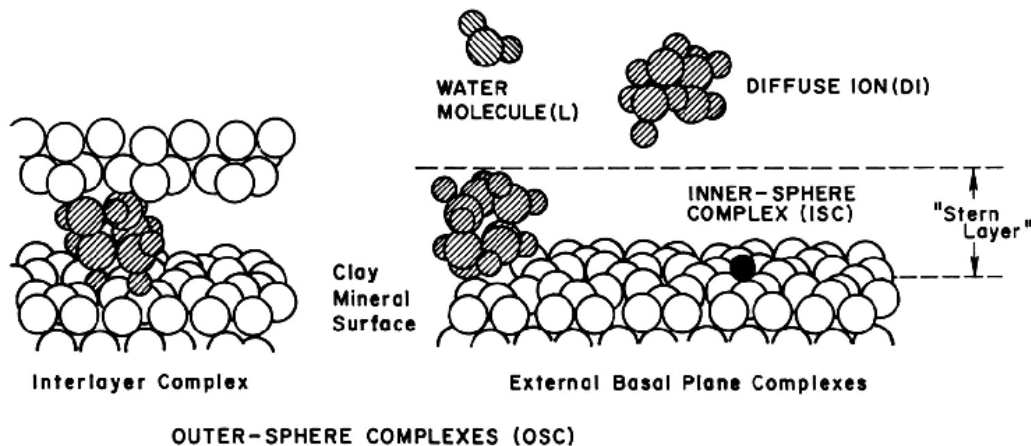
2.4.1 Adsorption mechanism:

Adsorption is the process through which a substance reacts at the boundary of two contiguous phases. In general, coarse- grained soil particles exhibit lower tendency for heavy metal adsorption than fine grained soil particles. The fine grained soil fraction content, soil particles with large surface reactivity, like negative charged clay particles and large surface area constituents, show enhanced adsorption properties [1].

Clays and organic matter have a high bonding capacity and determine the distribution of heavy metal pollution in soil after it has infiltrated into it.

Species adsorbed from the fluid phase on a binding site of the surface of the particle, form a surface complex. Ion adsorption on soil particle surfaces can take place via three mechanisms (figure 2).

Figure 2: the three modes of ion adsorption, illustrated for cations adsorbing on montmorillonite [17]

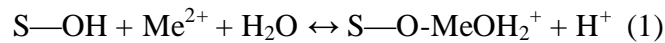


As shown in figure 2, ion inner -sphere surface complexation involves soil functional groups like siloxane cavity, and outer-sphere complex includes the cation release shell. If a released ion does not form a complex with a charged surface functional group, it is said to be adsorbed in the diffuse double ion swarm. These ions are fully dissociated from surface functional group and are accordingly, free to hover nearby in the soil solution. The diffuse ion swarm and the outer-sphere surface complex mechanisms of adsorption are electrostatic bonding, whereas inner -sphere complex mechanisms are likely to involve ionic as well as covalent bonding.

The most important parameters controlling heavy metal adsorption and their distribution in the soils are soil type, dissolved metal speciation, metal concentration, soil pH and contact time. High soil pH cause generally greater metal retention and lower solubility.

Often, heavy metal adsorption is described in terms of two mechanisms, specific adsorption, which is characterized by more selective and less irreversible binding of heavy metal ion with organic matter and metal oxides present in the soil as inner-sphere complexes, and nonspecific adsorption, which involves rather weak and less selective outer-sphere complexes and the diffuse double layer of the charged clay particles [1]. At high pH specific adsorption of heavy metals is likely to take place, because the heavy metals form inner-sphere complexes with functional groups like silanol groups, inorganic hydroxyl groups and organic functional groups, or with an ion in the surrounding solution, which is then a stable unit [1].

Inner-sphere adsorption is based upon adsorption reactions at OH- groups at the soil particle surfaces and edges, which are negatively charged at high pH [1]. In this case the bonded cation influences the surface properties. The adsorption site constituting the metal influence also the adsorption tendency. These reactions depend largely on pH, are equivalent to heavy metal hydrolysis and can be described as follows [1]:



The composition of the solid phases, particularly the content of metals oxides (Fe and Mn oxides) and organic matter, play an important role governing the adsorption of the heavy metals [7]. Fe oxides can act as barrier which delay the spreading of heavy metals and decreases their mobility. An oxidizing environment is an important condition to bind the heavy metal on the Fe- oxides, decreasing the toxicity problem[16]. From geochemical studies it is known that a relationship exists between heavy metals and Fe/Mn oxides. Studies indicate that important amounts of heavy metals in samples are present in the Fe/Mn fraction of sequential extraction tests and show that heavy metals are also adsorbed to the organic matter. These studies also show that Fe complexes strongly with organic matter. Both organic matter and Fe oxides can be mobile as complex ions, and immobile in precipitated form and these ratios depend on the local changes in Eh, pH and moisture content [16]. Studies suggested also that the adsorption capacity in certain soils is largely determined by amorphous Fe- Oxides. These amorphous Fe- oxides are coming from the minerals containing Fe, occurring normally in the soils like Siderite, etc. The Fe (II) diffuses out of the mineral matrix and precipitates as an amorphous Fe(III) – oxide. The Fe-oxides adhere onto quartz grains by irreversible coating reaction, because of Fe-O-Si bonds that are formed. This coating of the quartz grains with colloidal amorphous Fe- oxides is very active and metals are readily adsorbed whit it. The amorphous Fe oxide functional surface hydroxide groups =Fe—OH may act as Lewis basis in deprotonated form (=Fe—O⁻) to bind Lewis acid metal ion Me²⁺ [1], as described by equation 1, where S equals Fe.

Heavy metals have different sorption affinities. The increasing order of adsorption of heavy metals on to soil is Cd < Zn < Cu < Pb ,where Cd and Zn are regarded as very mobile and Cu and Pb of low mobility [16]. Adsorption tendency of components for Pb to Cd decreases in the order: Mn- oxides > Fe- oxides > organic matter.

Affinity of each kind of heavy metals for the same component is very different due to the differences in element behavior [7]. Table 2 shows different affinity found for heavy metal adsorption to the soil compounds:

Table 2: Affinity of heavy metal ions for oxides and OM [16]

Order	Mn-oxides	Amorphous Fe-oxides	Organic matter
High affinity	Cu	Pb	Ni Cu
	Co	Cu	Co Ni
	Mn	Zn	Pb Co
	Zn	Ni	Cu Pb
	Ni	Cd	Zn Ca
	Ba	Co	Mn Zn
Low affinity	Se	Sr	Ca Mn
	Ca	Mg	Mg Mg

Other important groups of minerals in soils that play an important role in adsorption of the heavy metals, are aluminum silicates, clay minerals, and Mn oxides, which are characterized by permanent structural charge. These minerals pose exchangeable ion-bearing sites at the surface in addition to surface protons and can cause inner-sphere and/or outer-sphere adsorption. Soil surfaces exhibit a variety of hydroxyl groups having different reactivities. Aluminum silicates are present in both aluminol ($=Al-OH$) and silanol ($=Si-OH$) edge surface group. The deprotonated aluminol group (i.e. $=Al-O^-$), which occur with decreasing pH, binds metals in the form of more stable surface complexes than the protonated $=Al-OH_2^+$.

As mentioned before variety of soil characteristics influence adsorption of heavy metal ions on soils and soil constituents. The most important parameters are pH, type and dissolved speciation of metal ion involved, heavy metal competition, soil composition and aging. Generally adsorption edge pH is below the pH_{pzc} of pure oxides (e.g. iron and aluminum oxides). Below the pH_{pzc} a mineral or an oxide/hydroxide species has net positive charge and does not adsorb the cations, but adsorption increases with pH (figure 3). The point of zero charge value for silica, organic matter, clay minerals and most of Mn-oxides are less than pH 4. But for Al and Fe oxyhydroxides and calcite is higher than pH7. The point of zero charge of some Fe – minerals and other minerals are listed in table 3 [1,17,30]. The adsorbed metal ion does not desorb easily, and metal adsorption has low dependency on inert background electrolytes, although presence of Ca^{2+} ions suppress adsorption on Fe oxides [1].

Table 3: $pH_{p.z.c}$ of some minerals [30]

Mineral	PZC
Quartz	2-3
Montmorillonite	2-3
Hematite	5-9
Goethite	7.3-7.8
Gibbsite	9.0

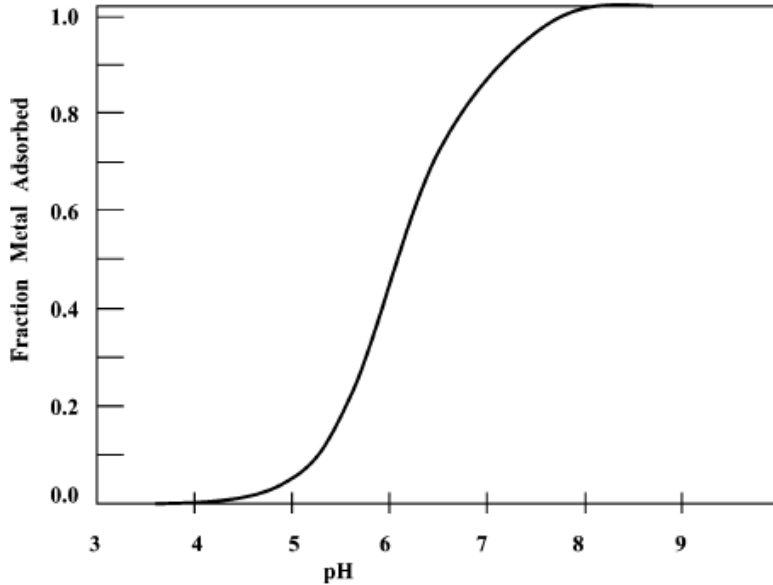
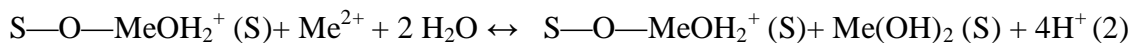


Figure3: Schematic representation of metal- like adsorption [1]

2.4.2 Surface complexation and precipitation:

Surface precipitation is characterized by the growth of a new solid phase. Metals may form salts with the ions in the solution and precipitate as oxides, hydroxides, carbonates, sulfides and phosphates onto soil particle surface [1]. Like adsorption, surface precipitation is also mainly a function of pH and the relative quantities of metals and ions present. In calcareous soils, the carbonates are supposed to be the major factors in time causing the retention of the heavy metals by precipitation. According to Bradl, “the surface precipitation ‘model’ can be described by two reactions: first a surface complex formation of a metal cation Me^{2+} and a surface S and second the precipitation of Me^{2+} at the surface S” [1,2]:



In addition to metal oxides, dissolved organic matter can also act as Lewis bases. After deprotonation the organic acid or other functional group form complexes with the heavy metals. There is often a continuum between surface adsorption and surface precipitation as shown in figure 4 [1].

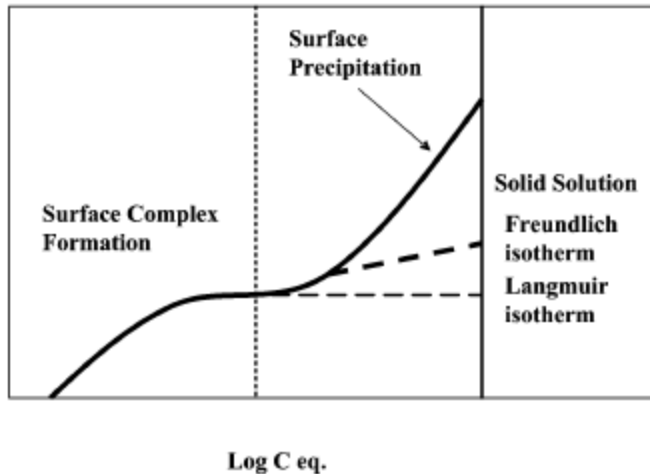


Figure 4: classification of adsorption isotherm by shape[1].

2.4.3 Fixation of heavy metal:

Another principal mechanism of sorption is fixation or absorption. In this case, an aqueous metal species diffuses into the solid phase. The adsorbed heavy metal on the clay minerals or metal oxides may diffuse into the lattice of the structure of these minerals, by solid state diffusion. The retention of heavy metals in the soil increases with ageing time by this mechanism. The metals can diffuse into the oxides and hydroxides of Al and Mn, and into clay minerals [1]. The first rapid reaction is adsorption of the heavy metal on the mineral surface by outer-sphere complexes, driven by the differences in the concentration gradient from the solution phase to the surface of the soil minerals and negatively charged organic matter. The second slow reaction is, shift of heavy metals from its outer-sphere to inner-sphere including the surface of carbonates, Fe- Mn oxides and the edge of soil clay minerals [2].

2.4.4 Heavy metal competitive behavior:

The heavy metals in contaminated soils may compete with each other for sorption sites. This competition among the heavy metals is considered to determine their mobility, and based on this the potential bioavailability, toxicity and leachability of these metals in soils[12].

Different metals may have different selectivity by an adsorbent, depending on the characteristics of the metal ion. The ionic radius and the ionization potential (quantified by Misono softness parameter) determine the tendency of the metals to form covalent bonds. According to this ability the metal cations can form strong complexes, in the following order: $Pb > Cd > Cu > Ni > Zn$ [24].

According to McBride (1994) electronegativity is an important factor in determining which of the trace metals chemisorbs with the highest preference and on this basis, the predicted order of bonding preference would be: $Cu > Ni > Pb > Cd > Zn$ [24].

But if the adsorption is based on electrostatic binding form, the strongest bond should be formed by the greatest charge to radius ratio. This would produce a different order for the same metals: $Ni > Cu > Zn > Cd > Pb$ [24].

Selectivity sequence of heavy- metal cation adsorption on aluminum hydroxides have the order: Cu > Pb > Zn > Ni > Cd and for humic substances: Cu > Pb > Ni > Zn . The ionic radii of the metals are listed in table 4. The competitive adsorption is determined by the soil properties that are most strongly related to heavy metal adsorption. Where pH, CEC for Cd and Cr; organic C, clay, and gibbsite content for Cu; pH and CEC for Ni; and CEC and possibly pH for Pb [24].

Table 4: the electronegativity and radii of the heavy metals [24]

Heavy metal	Electronegativity (pauling scale)	Radius (Å)
Cr	1.6	1.28
Pb	1.9	1.20
Cd	1.8	0.97
Zn	1.7	0.74
Cu	1.6	0.72
Ni	1.8	0.69

2.5 Individual retention behavior of selected heavy metals:

2.5.1 Cd:

Cd is retained in the soil mainly by adsorption mechanism, especially at low concentrations. But at high concentrations, the pH controls the solubility of Cd precipitates. According to studies adsorption behavior of Cd in soils can be described by either the Langmuir or the Freundlich isotherms. Adsorption of Cd by hydrous iron oxide can be described by Langmuir isotherm. Figure 5 shows Cd adsorption isotherms for two soils, a loamy sand and a sandy loam, as function of pH. The sorption capacity of the soils increases with increasing pH. In addition to adsorption, precipitation can play an important role in controlling Cd levels in soils. Cd solubility in soil decreases generally as pH increases with the lowest values for calcareous soils (pH 8.4). The precipitation of CdCO₃ occurs in sandy soils, due to low CEC, and low content of dissolved organic matter. The presence of dissolved organic matter that can act as chelates could prevent metal co-precipitation with CdCO₃ or minimize adsorption of metals onto the solid phases. Cd adsorption is also strongly influenced by the presence of competing cations such as divalent Ca and Zn [1].

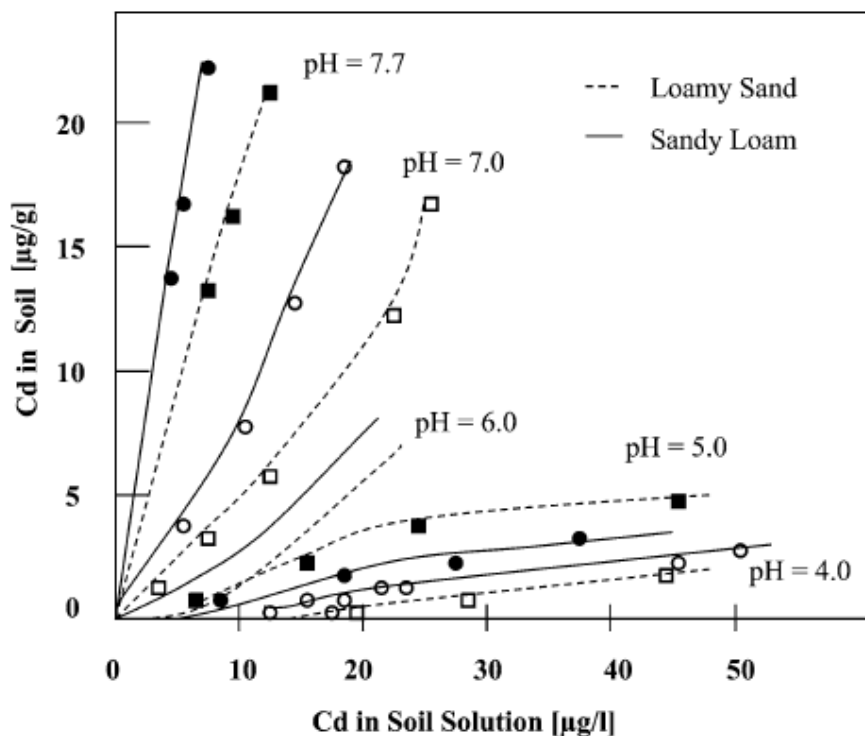


Figure5
Cadmium
adsorption
isotherms in
soils as
influenced by
soil texture
and pH [1].

2.5.2 Cr:

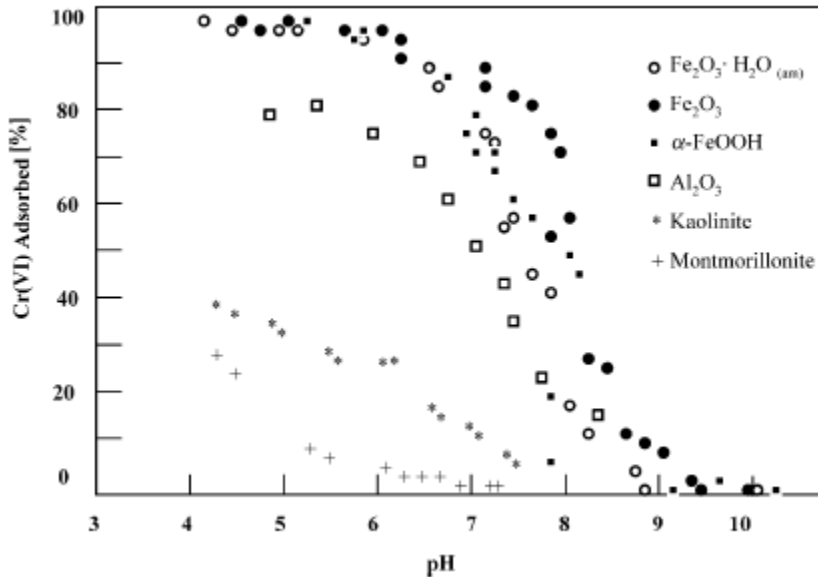
Cr is retained in the soil mostly by adsorption and precipitation and it is controlled by a variety of factors such as redox potential (oxidation state), pH, soil minerals, competing ions, complexing agents, and others [1]. But the most important factors are the hydrolysis of Cr (III) and Cr (VI), redox reactions of Cr (III) and Cr(VI) and adsorption/ desorption and precipitation of Cr (VI) [1].

Hexavalent Cr species occurring at low redox potential can adsorb by a variety of soil phases with hydroxyl and oxide groups on their surfaces such as Fe, Mn, and Al oxide or by clay minerals like kaolinite and montmorillite.

Cr(III) hydroxides are generally quite insoluble in water at physiological pH. Some Cr (VI) compounds (i.e., Cr_2O_3), have higher solubility, whereas calcium chromate and lead chromate are characterized by very low water solubility, and some are intermediate soluble (i.e., zinc chromate) [20].

Figure 6 shows the adsorption of hexavalent Cr as Chromate anion onto various adsorbent as function of pH. The adsorption of Cr (IV) increases as the pH decrease, due to protonation of the hydroxyl group of soil hydrides. Cr (III) is specifically adsorbed by Fe and Mn oxides and clay minerals. Increasing pH and dissolved organic matter content cause increase in adsorption of Cr(III), while this adsorption decreases in the presence of competing cations or dissolved organic ligands in the solution. Both Freundlich and Langmuir isotherms can be used to describe adsorption behavior of Cr(III) on solid phases[1].

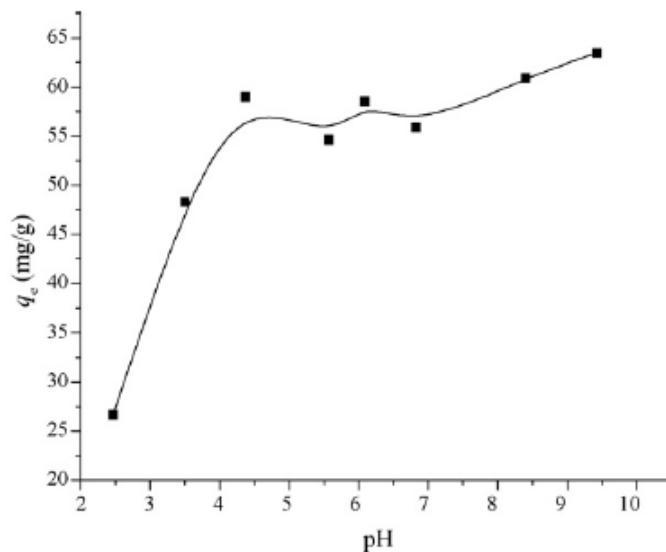
Figure 6: Sorption of Cr (VI) by various absorbent for a fixed adsorption site concentration [1].



2.6.3 Pb

Pb is generally an immobile metal, because it adsorbs on various solid phases by specific adsorption, and it precipitates as moderate soluble or highly stable compounds and it forms complexes or chelates that result from interaction with soil organic matter [1]. Adsorption of Pb onto soils and clay minerals can be described by either the Langmuir or the Freundlich isotherm over a wide range of concentrations. Carbonate content in soils influences the Pb behavior. The formation of PbCO₃ in the calcareous soils occurs as the pH increases. The presence of Mn and Fe oxides and organic matter play an important role on Pb adsorption in soils. The presence of soil organic matter also plays an important role in Pb specific adsorption. An increase in ionic strength results in a decrease in Pb adsorption [1]. Figure 7 shows adsorption of Pb on montmorillonite as function of pH.

Figure7: Influence of initial pH on the adsorption of Pb(II) on montmorillonite (pH 6.0, 25 °C, initial Pb(II) concentration is 250 mg/L) [22].



2.5.5 Cu:

The presence of soil organic matter and Mn and Fe oxides influence mostly the behavior of the Cu in the soils, Mn oxides and soil organic matter are the most likely to bind Cu in a non-exchangeable form [1]. As shown in table 2, Cu has strong affinity for soil organic matter. The adsorption of Cu can be described by either Langmuir or Freundlich isotherms. Sorption isotherms indicate that the adsorption of Cu onto soil organic matter associated with the clay fraction of the soil may occur. Figure 8 shows the adsorption of Cu onto various soil constituents. Specific adsorption seems to play a more important role than nonspecific adsorption [1].

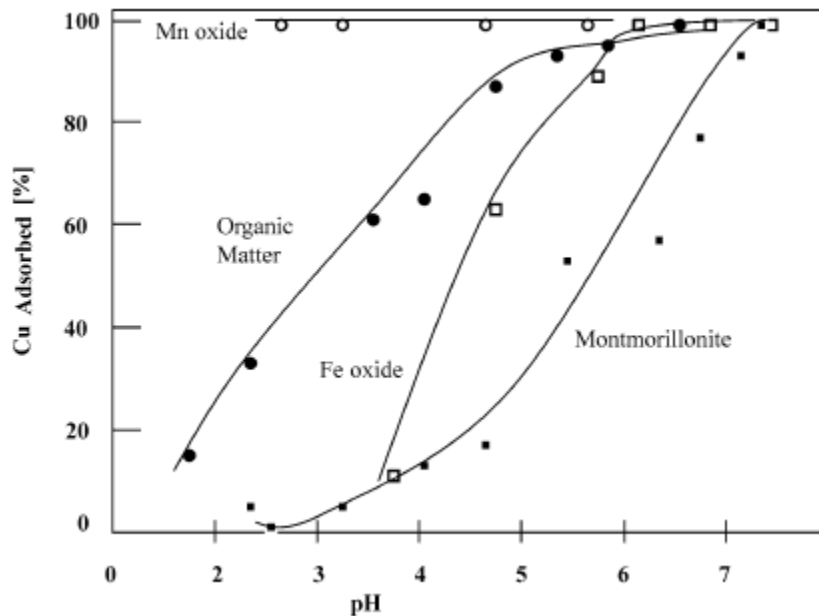


Figure 8: adsorption of Cu by different soil constituents as function of pH [1]

2.5.5 Zn:

The Zn retention behavior in the soils is influenced by several factors, such as pH, clay minerals content, CEC, soil dissolved organic matter and soil type. Different types of clay minerals show variability in their adsorption capacity due to their different CEC, specific surface area and basic structural design. Zinc binds to organic material at pH larger than 6.5, and it adsorbs to kaolinite and illite clay as hydroxyl species in increasing amount up to pH 10.5 [20].

The 2:1 type clay minerals like as montmorillonite and illite exhibit greater fixing capacities for Zn than the 1:1 clay mineral types such as kaolinite. This is due to the fact that the Zn^{2+} can entrap to the interlattice wedge zones of the clay when the zones are expanded due to wetting and contracted upon drying. The Zn can be sorbed by carbonates, or precipitate as stable Zn hydroxides or carbonates in calcareous and alkaline soils. Zn can also form insoluble calcium zincate in soils. The presence of oxide surfaces in the soil influences Zn retention at high pH. However Zn forms also dissolved complexes with Cl^- , PO_4^- , NO_3^- and SO_4^{2-} [1]. Zinc co-precipitates with Fe and Mn oxides, and franklinite, $ZnFe_2O_4$ and with $CaCO_3$ [20].

Zinc adsorbed on particles with low radius and density can be transported in air over great distances, atmospheric Zn is mostly in aerosols in oxidized form [20].

2.5.6 Ni:

Nickel retention in soils is usually controlled by competitive adsorption (exchange) behavior and surface precipitation. Competitive adsorption is non-specific, so it is affected by changes in ionic strength, concentration of Ca^{2+} and other competing metals, pH, and complexation reactions with inorganic and organic ligands in the solution phase. Since the Ni shows high affinity to dissolved organic matter as shown in table 2, organic matter content and pH are assumed to be the most significant factors affecting Ni binding. The pH influences complexation of Ni in solution, precipitation of Ni hydroxide, due to the protonation of soil constituents like the Al hydroxides. Nickel retention in soils dramatically increased above pH 7.0 due to the deprotonation of the soil constituents, and the increase in the net negative surface charge of the soil, which may enhance adsorption [18].

3. *Materials and methods:*

To investigate the upward movement of the heavy metals by evaporation, it is necessary to analyze the soil characteristics. In this research the properties as pH, CEC (cation exchange capacity), EC (electrical conductivity), particle size distribution, organic matter and soil moisture content of the two soil types are determined. The soil samples are one clayey soil and one sandy soil. To study the upward movement, the samples were contaminated by introducing a solution with different concentration of heavy metals (Cd, Cr, Cu, pb, Ni and Zn) into the soil sample reactors. This solution was flushed into the samples until water saturation. After saturation, the soils samples were left for aging during three weeks. Two samples of each soil type (in duplicate) were subsequently dried during three weeks. Two samples were dried for five weeks and other two samples were dried for seven weeks. The samples were dried in different stages by blowing air above the sample surface in closed reactor. The dust of the samples was captured in tubes with water. After drying, the soil samples were divided into several slices and incubated with Aqua-regia to determine the concentrations with the ICP-OES (Inductive Coupled Plasma Optical Emission Spectroscopy) technique. The speciation of some slices was estimated with Micro XRF (X-ray fluorescence) and XRD (X-ray powder diffraction) techniques.

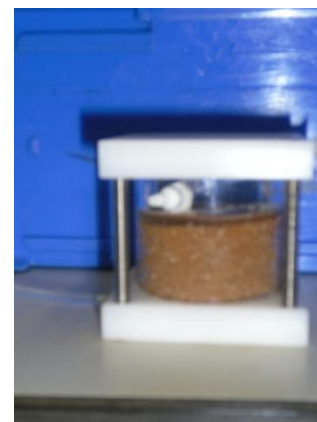
3.1 *Soil characterization:*

The soil pH, and EC were measured by dissolving 1 gram of soil with 2.5 ml of water, using pH and EC electrodes.

The particle size distribution is estimated with the Malvern technique. The soil sample is treated with TGA (thermo Gravimetric analysis). TGA is a semi- quantitative method to measure the moisture content, organic matter content and carbonate content. The measurement is based on loss of weight by increasing temperature: 105, 450, 550, 800 and 1000 °C. This is done with thermogravimetric analyzer (LECO- TGA 701). The instrument contains a well conditioned room and an intern scaling unit. The conditioned room is filled with O₂ or N₂ gas. The sample is heated in this room to the mentioned temperatures and weighted after each heating step. The lost weight at each temperature quantifies the amount of evaporated content at that temperature [25].

TGA heating procedure:

105 °C	water content,
450 °C	Organic matter content
550 °C	Iron carbonate content
800°C	calcium carbonate content
1000°C	the rest of carbonates



Furthermore the cation exchange capacity of the sample is estimated. In this analysis, 1 gram of the sample is dissolved in AgTu solution (0.01M Ag and 0,1M Thiourea) and centrifuged. The extract is acidified with 50µl of HNO₃ 65% [26].

The concentration of the alkali metals (Ca, Mg, K, and Na) which occupy the CEC of the soils, are measured with the ICP-OES technique [26]. These metals are released due to the replacement with Ag⁺ ions in the diffuse double layer. The determined CEC, is calculated according to Sposito 2008.

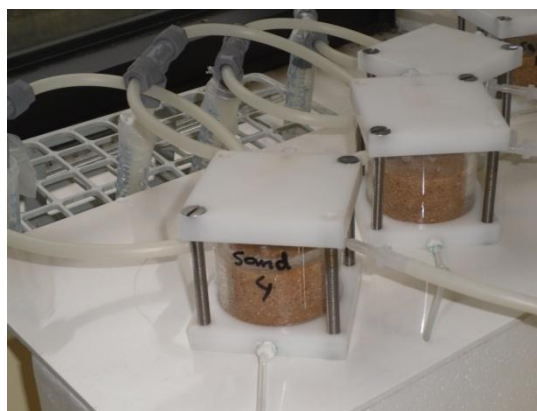
3.2 Experimental setup:

The soil samples were put in closed reactors of 4.2 cm diameters and 3 cm length. The weight of the dry soil was about 55 grams for sand sample and about 40 grams for clay samples (table 9). These reactors contain openings in the wall to introduce the tubes for blowing air. The heavy metal solution was introduced by flushing flow of 1cm/day to the bottom of the sample. The sand samples were saturated in about one day of flushing the solution, but the clay samples were saturated during a week. The concentrations of the heavy metals and the used metal salts are listed in table 5. After saturation the samples were left to age during three weeks. The sample weight and added water weight are listed in table 9.

Table 5: concentration of the metals in the contamination solution

Metal	Concentration mg/l	Used complex
Cr	69.609	Chromium (III) chloride
Ni	643	Nickel (II) chloride hex hydrate
Zn	1248.34	Zinc acetate
Pb	843.87	Lead (II)nitrate
Cu	537.43	Copper (II)chloride
Cd	46.94	Cadmium chloride

The evaporation of the pore water in the contaminated soil samples was accomplished in different stages. These stages are three, five and seven weeks. The air was blowing at the surface of the sample from the openings in one side of the wall and it was coming out in the other side going into a tube filled with water, to capture the dust particles. Argon gas was used in this evaporation experiment. The samples were weighted before and after saturation to determine the added water amount by saturation, and the lost water amount after drying.



The sandy soil sample was divided into 3 slices after the three week evaporation stage, and into five slices after five weeks of evaporation and into 6 slices after seven weeks of evaporation. But the clayey soil samples were divided into 8 slices in all stages, because the clayey soil has more sorption properties than the sandy soil. The surface layers of the samples were also separated. All the slices and the surface layers, were incubated with

aqua regia and the heavy metal concentrations were measured with ICP-OES technique. Some of the slices, bottom, middle and the surface, were analyzed with Micro XRF to study the heavy metal distribution patterns in the samples. The bottom and the surface slices were also analyzed with XRD to get more information about the speciation and complexation during the upward movement of the metal. The dust particles were captured, by introducing the out coming air tube into a water bottle.

The inside of the reactors cover were also rinsed with 2% HNO₃ acid to dissolve any dust adhered on the cover wall. This dust solution and the captured dust in the water tubes were also acidified with 67% HNO₃ and measured by ICP-OES technique to determine the heavy metal concentrations in the captured dust particles.

After finishing the contamination and evaporation treatments, the pH and EC of the soil samples were measured. The soil samples were also analyzed with TGA for soil moisture to make a mass balance for lost moisture during the evaporation. The samples were weighted before flushing the solution, after saturation and after drying to measure the water mass balance and the amount of added heavy metals in each sample.

3.3 XRF analysis:

Three slices of each sample (surface, middle, bottom), were analyzed with the Micro XRF technique, to predict the possible speciation and/ or binding mechanism of the heavy metals during their migration through the soil columns. In this analysis the alkali and earth- alkali metals and other possible elements present in the soil samples are also qualitatively estimated to compare the heavy metal distribution patterns with these naturally present elements in the sample. From this comparison will be predicted whether the metals are adsorbed or precipitated on the soil particle surfaces. In the case of similarities between the heavy metal pattern, and the pattern of any other element, the form in which the heavy metal is present can possibly be predicted. For instance if a metal pattern show similarity with the pattern of Ca²⁺ or Na⁺, Me-CO₃, Me-SO₄ or Me-Cl₂ species might be formed, or the metal might be scavenged by the salts. But in the case of similarities with the Fe or Mn patterns, the heavy metal might be adsorbed to the Fe and Mn oxides. If the heavy metal distribution pattern does not correlate with other elements patterns, Me-hydroxide or Me-oxide species might be formed, or the heavy metal might also be complexed with organic matter or adsorbed on clay minerals, which are not detectable with this analysis. The Micro-XRF data are presented in appendix C. The solubility products of some possibly formed species are listed in table 6.

Table 6: solubility products of possibly formed salts [28,29]

Salt/ complex	Solubility product
CaCO ₃	4.96 * 10 ⁻⁹
CaSO ₄	7.5 * 10 ⁻⁵
CdCO ₃	6.18 * 10 ⁻¹²
Cd (OH) ₂	5.27 * 10 ⁻¹⁵
CuCl ₂	1.72 * 10 ⁻⁷
Cu ₃ (PO ₄) ₂	1.39 * 10 ⁻³⁷
CuBr	6.27 * 10 ⁻⁹
CuC ₂ O ₂ (copper(II)oxalate)	4.43 * 10 ⁻¹⁰
CuSO ₄	water soluble
CuCO ₃	1,4 * 10 ⁻¹⁰
PbCO ₃	1.46 * 10 ⁻¹³
PbCl ₂	1.7 * 10 ⁻⁵
Pb(OH) ₂	1.42 * 10 ⁻²⁰
PbC ₂ O ₄ (lead(II)oxalate)	8.51 * 10 ⁻¹⁰
PbSO ₄	1.82 * 10 ⁻⁸
NiCO ₃	1.42 * 10 ⁻⁷
Ni(OH) ₂	5.47 * 10 ⁻¹⁶
Ni ₃ (PO ₄) ₂	4.73 * 10 ⁻³²
ZnCO ₃	1.19 * 10 ⁻¹⁰
Zn(OH) ₂	6.86 * 10 ⁻¹⁷
ZnC ₂ O ₄ 2H ₂ O (zinc oxalate 2-hydrate)	1.37 * 10 ⁻⁹
ZnSO ₄	Water soluble
CuCrO ₄	3.6 * 10 ⁻⁶
Cr(OH) ₃	6.3 * 10 ⁻³¹
CrPO ₄ 4H ₂ O green color	2.4 * 10 ⁻²³
H ₂₄ Cr ₂ S ₃ O ₂₄	Anhydrous: insoluble in water (20 °C) hydrous: water soluble
CaCrO ₄	1 * 10 ⁻⁸

3.4 XRD analysis:

The three slices (surface, middle, bottom) of the sand sample were also analyzed by XRD to gain additional information about the speciation of the heavy metals during their migration through the soil column. This analysis was not useful for the clay samples, because the clay minerals are dominating the heavy metals precipitates in the clay sample. In this case detection of the heavy metals with this technique was not possible. Although heavy metal concentrations in the sand samples were also low to be detected, some of the metal precipitates were identified with this analysis. But not all of the metal species are detected, and the detected metal species are also missing some peaks of their complete patterns. This is because the highest concentrated metal concentration was about 0.5%, while to be detected with XRD, it has to be present at 5%. The data of XRD measurements are presented in appendix D.

4. Results and discussion:

4.1 Soil characteristics:

The soil properties, pH and EC (electrical conductivity) of the both soil samples were measured before and after the experiment.

The clay sample has a pH of 8.0 and the sand sample pH is 8.2 before any preparation. After introduction of the heavy metals solution which has a pH of 4.7, the pH of the clay and the sand samples is decreased to pH 7 and pH 7.2 respectively.

They have high carbonate and gypsum contents and low water and humus content which are characteristics for soils in arid regions, and the early stages of the weathering sequence, but they contain also quartz, illite and smectite and high amounts of soluble salts (Na, K, Ca, Mg, Fe), silica and also iron oxides that are more characteristics for the intermediate stage of weathering (table 1).

After three weeks of evaporation the pH of the samples increases again, but this higher pH decreases again during the evaporation stages of five weeks and seven weeks. This might be due to the migration of the carbonate salts upward with the water and water vapor and their accumulation at the surface. In this case the clay minerals, organic matter and Mn- oxides are negatively charged, because these pH values are above the point of zero charge of this soil constituents. The Al and Fe oxides/hydroxides might have negative or positive charge, because their point of zero charge is above pH 7. The pH measurements are summarized in table 7.

The EC does not show this trend. The EC of the clay sample is 0.174 ms/cm and the sand sample has an EC of 0.168 ms/cm before any preparation. The EC of each of the soil type changes differently after introduction of the heavy metal solution through it. In the clay soil sample the EC increases, which indicate the increase of the ions in the soil solution after introducing the heavy metal solution. The EC decreases after the evaporation step in the clay sample, indicating the precipitation of salts in clay sample.

In the sand sample the EC decreases after introducing the heavy metal solution. The EC of the sand samples increases again after drying for three weeks and decreases during the evaporation of five weeks and seven weeks, like the pH does. This increase in the EC might be due salt precipitations. The EC results are also summarized in table 7.

Table 7: pH and EC measurements

Clay	Original clay	After saturation	3 weeks	5 weeks	7 weeks
pH1	8.0	7.0	7.9	7.3	7.1
pH2	8.0		7.8	7.3	7.1
EC1(ms/cm)	0.173	0.292	0.165	0.112	0.130
EC2 (ms/cm)	0.175		0.120	0.124	0.113
Sand	Original sand	Contamination only	3 weeks	5 weeks	7 weeks
pH1	8.2	7.2	8.4	7.8	7.5
pH2	8.1		8.4	7.6	7.5
EC1(ms/cm)	0.155(*)	0.149	0.159	0.137	0.064
EC2 (ms/cm)	0.168		0.192	0.139	0.045

* unreliable measurement

Furthermore the soil moisture, organic matter and the carbonate contents were measured before the experiment and after the experiment as well.

The soil moisture and organic matter contents of the sand samples did not change after the evaporation step, which means that the added water by the contamination solution of the heavy metals was almost evaporated already after three weeks of drying. Since the moisture content of the sand sample was relatively low before saturation, no significant losses of moisture are measured after five weeks, only a loss of 0.075% is measured after seven weeks of drying.

The FeCO_3 and the CaCO_3 contents show some fluctuation during the different evaporation stages. The CaCO_3 content is decreased in most of the sand samples, but the FeCO_3 is increased.

The case is different in the clay sample, the soil moisture is decreased about 0.5% in all of the evaporation steps, but the organic matter contents are increased about 0.5% in all of the steps. The FeCO_3 and CaCO_3 contents are also increased about 0.2-0.4 % after each evaporation step. This increase in the organic matter and carbonate contents might be due to presence of acetate in the contamination solution, since the used Zn in the contamination solution was in Zn-acetate form.

The results of the TGA analyses are summarized in table 8 (Next page).

The grain size distribution of the both soil types was very different:

Clay sample:

- About 7.2 % is between 0.06 μm and 2.28 μm (clay size).
- About 42 % has a particle size between 3.09 μm and 754.23 μm (silt and fine sand size).
- A big portion of about 51% has a size between 56.23 μm and 878.67 μm (medium sand size).

Sand sample:

- About 2.22 % is between 35µm and 88µm (silt size)
- About 7.4 % is between 103µm and 190µm (very fine sand size)
- About 7.4 % is between 222.2 µm and 259 µm (fine sand size)
- About 83 % is between 301 µm and 878.7µm (medium to coarse sand size)

The cation exchange capacities of the both soil type were also determined:

- Clay sample CEC: 0.03 mol/Kg
- Sand sample CEC: 0.07 mol/Kg

The CEC value of the sand sample is relatively high, this could be due to the CaCO₃ content of the sand soil. Minerals like Calcite are dissolved or partially dissolved during the course of CEC experiment. In this case, non exchangeable cations are added to the extracted exchangeable cations resulting in a significant overestimating of exchangeable cations. During the experiment, calcite could be partially dissolved, and released Ca²⁺ will lead to high overestimated CEC results [27].

Table 8: TGA results:

Sample	Water content (%)	Dissolved organic matter content (%)	FeCO ₃ content (%)	CaCO ₃ Content (%)	Rest of carbonates (%)
Original sand	0.268	0.3377	0.07266	1.9606	0.007262
3 weeks					
Sand 3	0,205	0,325	0,094	1,67	0,034
Sand 4	0,268	0,351	0,089	1,745	0,021
5 weeks					
Sand 5	0,274	0,277	0,091	1,822	0,008
Sand 7	0,242	0,303	0,072	1,591	0,008
7 weeks					
Sand 1	0,266	0,348	0,11	2,371	0,02
Sand 2	0,193	0,276	0,075	1,771	0,02
Original clay	3.022	1.979	1.298	12.02	0.120
3 weeks					
Clay 5	2,474	2,358	1,495	13,09	0,107
Clay 7	2,515	2,369	1,61	12,84	0,117
5 weeks					
Clay 3	2,628	2,458	1,654	12,9	0,114
Clay 4	2,599	2,47	1,585	13,08	0,122
7 weeks					
Clay 1	2,543	2,46	1,61	12,56	0,102
Clay 2	2,538	2,48	1,672	12,63	0,124

4.2 Experimental results:

The contaminated clay and sand samples showed different behavior during saturation with the contamination solution and also during the ageing period. They were saturated during different periods, as mentioned before. The sand samples did not adsorb much water after ageing period. This might be due to the coarse particle size of the sand. But the clay samples adsorbed more water during the ageing period.

After three weeks of evaporation, salts had migrated to the top of the sample reactor, a white layer was developed on the surface of the samples and on the wall of the reactor. This salt on the surface was clear in the sand sample. The pictures of the samples are in appendix A.

After five weeks of evaporation even more salts had migrated to the top of the sandy soil, the developed salt layer was thicker compared to the three weeks evaporation stage. This is also the case in the clay sample. The soil became also harder coming closer to the top. This might be due to the wetting and drying effect. Since drying and the precipitated salts enhances the stability of the bonds and increase the cohesion between mineral soil particles. [6]

After seven weeks of evaporation a green colored mineral was developed on the surface of the sand samples. This is an indication of the formation of CuCO_3 and/ or NiCO_3 species in the salt, since they have a light green color. This was not clear in the clay sample. The clay sample developed a fracture at the surface, because of tension by forming aggregates and shrinkage of the clay and humus particles cause micro cracks in the crust separating the individual aggregate from the coherent crust [6]. The dust particles at the reactor ceiling of the seven weeks dried samples were substantially more than in the previous evaporation steps.

As mentioned before, the samples were weighted before and after saturation and also after each drying step. As shown in table 9, almost the same amount (grams) of the added water during the saturation was evaporated after drying.

Table 9: water mass balances in grams

Sand samples	After saturation	3 weeks (duplicates)		5 weeks (duplicates)		7 weeks (duplicates)	
Dry sample weight	57.82	53.49	54.11	56.65	56.98	55.35	55.80
Added water (solution)	12.9	11.34	11.08	10.99	12.71	10.90	13.57
Lost water		11.08	10.53	10.70	12.28	10.80	13.09
Clay samples							
Sample weight	40.77	40.91	40.65	40.56	40.26	40.49	42.32
Added water (solution)	22.12	21.54	20.51	19.74	19.10	18.52	21.28
Lost water		20.98	20.54	19.51	19.13	18.59	21.26

The amounts of the metals that are retained in the soil column, after drying, are calculated by multiplying the added solution amount with the heavy metals concentrations in the solution. Since the retained water content is very low, this is not included in the calculations. These amounts and the calculated amounts from the ICP-OES measurements are shown in tables 10 and 11.

Table 10: calculated amounts of the heavy metals (mg) from initial input water quantities:

<i>Metals (duplicate)</i>	<i>3 weeks evaporation</i>		<i>5 weeks evaporation</i>		<i>7 weeks evaporation</i>	
	Sand	Clay	Sand	Clay	Sand	Clay
Cr-1	0.79	1.50	0.77	1.37	0.75	1.29
Cr-2	0.77	1.43	0.88	1.32	0.94	1.48
Cu-1	6.09	11.57	5.91	10.61	5.86	9.95
Cu-2	5.95	11.02	6.83	10.26	7.29	11.44
Cd-1	0.53	1.01	0.52	0.92	0.511	0.87
Cd-2	0.52	0.96	0.57	0.89	0.64	0.99
Ni-1	7.29	13.85	7.07	12.69	7.01	11.91
Ni-2	7.12	13.19	6.88	12.28	8.73	13.68
Pb-1	9.57	18.17	9.27	16.66	9.19	15.63
Pb-2	9.35	17.31	10.73	16.12	11.45	17.96
Zn-1	14.16	26.89	13.72	24.64	13.61	23.12
Zn-2	13.83	25.60	15.87	23.84	16.94	26.58

Table 11: calculated amounts (mg) of the heavy metals from the ICP-OEC measured concentrations:

<i>Metals (duplicate)</i>	<i>3 weeks evaporation</i>		<i>5 weeks evaporation</i>		<i>7 weeks evaporation</i>	
	Sand	Clay	Sand	Clay	Sand	Clay
Cr-1	2.81	4.49	2.04	6.72	3.39	5.83
Cr-2	1.71	5.01	1.40	4.85	4.09	5.26
Cu-1	16.83	12.41	5.87	14.41	17.27	24.03
Cu-2	6.65	14.96	5.06	15.09	15.74	16.204
Cd-1	1.03	1.19	0.68	0.97	0.88	1.06
Cd-2	1.10	0.98	0.86	0.93	0.87	1.10
Ni-1	8.59	10.70	5.0	9.79	7.32	12.96
Ni-2	6.40	9.09	6.52	9.50	8.66	9.80
Pb-1	86.87	17.76	10.88	16.41	96.88	27.30
Pb-2	5.52	15.30	5.55	15.63	93.97	21.75
Zn-1	52.87	45.14	21.41	42.97	33.82	39.36
Zn-2	27.62	36.53	28.88	40.94	42.94	40.04

The calculated amounts of the heavy metals added in solution, are not similar to those, calculated from measurements data. There is a general increase in the amounts of the heavy metals after the evaporation experiment. There is no clear explanation for this effect.

Beside the soil slices, there were dust particles adhered on the reactor ceiling and captured in the water tube. This dust was extracted with 67% HNO₃, and subsequently, the measured concentrations are much lower than in their actual concentrations. The dust amount was not sufficient for weighting and the dilution factor with this extraction could not be calculated.

The heavy metal concentrations of one sample of both soil types were measured directly after saturation and ageing, to compare how the concentration profile and the amount of each metal changes after each drying step. Heavy metals masses were calculated by dividing of the end amount (after drying) of the metal by the initial amount added to the sample (in the water saturated sample) in milligrams of metal.

These results are shown in table 12. The relative distribution of the metals in each slice, are shown in the graphs of appendix B.

As shown in the table 12, the Pb amounts are fluctuating dramatically in all of the drying steps, in both soil types especially in the sand sample. The reason for the high amounts of Pb after drying is unknown. The remaining metals have higher amount in the seven weeks dried samples in both clay and sand sample. The discrepancy in these samples might be due to initial higher concentrations, caused during flushing the heavy metals solution through the soil columns. The duplicates of most of the metal concentrations differ significantly; Cd, Ni and Zn have relatively better duplicates. This difference in the duplicates might be due to the slightly different experimental conditions, like the shade / sun position of the sample duplicate, during the saturation and/ or evaporation periods. The flow of the blowing air in each sample might also be slightly different, which can cause differences in migration behavior of the heavy metals. This could influence the concentration profiles, and cause significant differences between duplicates.

Table 12: mass balance of the heavy metals after each evaporation stage

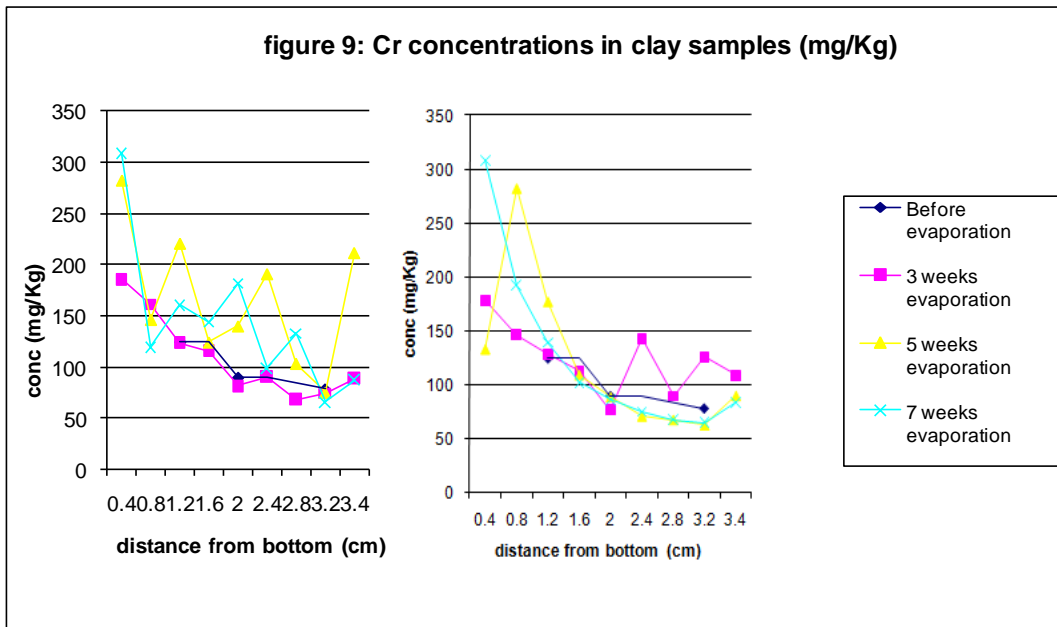
<i>Metals (duplicate)</i>	<i>3 weeks evaporation</i>		<i>5 weeks evaporation</i>		<i>7 weeks evaporation</i>	
	Sand	Clay	Sand	Clay	Sand	Clay
Cr-1	183%	113%	133%	169%	221%	147%
Cr-2	112%	123%	91%	122%	267%	132%
Cu-1	262%	231%	92%	268%	269%	447%
Cu-2	104%	278%	79%	281%	245%	302%
Cd-1	185%	137%	122%	111%	159%	122%
Cd-2	198%	113%	155%	106%	157%	126%
Ni-1	177%	110%	103%	100%	151%	133%
Ni-2	131%	93%	134%	97%	175%	100%
Pb-1	1084%	311%	136%	287%	1209%	472%
Pb-2	69%	368%	69%	273%	1173%	381%
Zn-1	249%	124%	101%	118%	160%	108%
Zn-2	130%	100%	136%	112%	203%	110%

4.3 Cr:

4.3.1 The Cr migration and speciation behavior in the clay soil samples:

The concentration profile of the Cr is shown in figure 9. Each of the slices of the clay samples contains some Cr content, it means that the Cr migrates upward through the soil column, but the concentrations in the bottom slices are higher than the middle and the top of the soil columns in all of the three evaporation steps. This indicates that the Cr bind stronger in the bottom slices. The retention of the Cr in the soil is controlled by adsorption and precipitation (section 2.5.2). If the Cr is adsorbed to the clay particles it migrates slower than the dissolved Cr species that can precipitate as the pore water evaporates. If the Cr is in cationic form, adsorption on the clay minerals is electrostatic and it can be exchanged by other ions and migrate upward. In addition the Cr could bond on the Fe and Mn oxides by inner-sphere adsorption of chromate, in oxidized conditions and cannot migrate, so it is retained in the soil.

The Cr concentrations in the dust particles are shown in figure 10. As it is clear in the graph, the particles of the seven week evaporation have the highest concentration, although the bottom soil slices of this sample has generally the highest concentrations.



As mentioned in the literature, adsorption and precipitation behavior of Cr in the soils is controlled by a variety of factors such as redox potential, pH, soil minerals, competing ions, complexing agents, and others [1]. Since the samples have high pH (even after drying) and are in oxidizing conditions, mediated by the presence of Mn and Fe minerals and/ or oxides, the Cr³⁺ might be oxidized to the more toxic and stable Cr⁶⁺. The Micro XRF data of the Cr (appendix C) in the three weeks drying step, indicate the presence of Cr as Cr- hydroxides species, like Cr(OH)₃ precipitated in the middle and surface slice of this sample, because the Cr pattern does not show any correlation with other elements pattern.

But the Cr in the bottom slice of this sample might be retained by adsorption on the Mn and Fe oxides, or precipitated as salt species formed with Ca (calcium chromate). In this case the Cr is possibly in hexavalent oxidation state, as indicated by the correlation with the Fe and Mn (oxides).

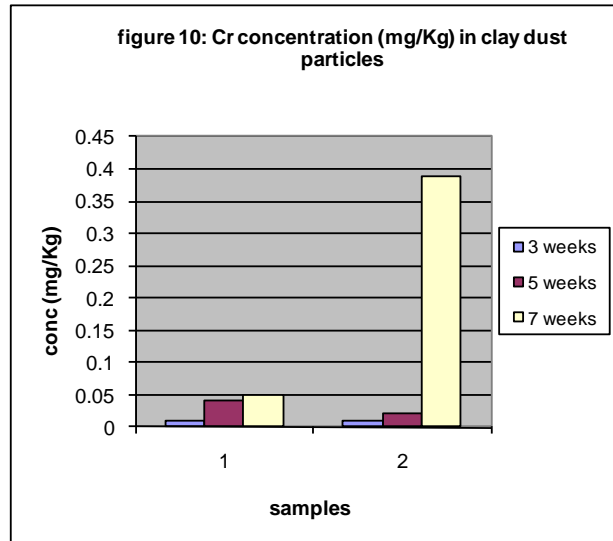


Cr behaves differently after five weeks of drying, in this case the Cr is correlated with Mn and Fe in the surface and also in the middle slices of this sample. The Cr might be adsorbed on the Fe and Mn oxides present at the surface sample due to the dehydration effect by intense drying . The Cr might also be precipitated as stable species, since some correlation with Na is observed. In the bottom slice of this sample, the Cr shows also correlation with Na, which can be NaCl and/ or Na₂SO₄, which also indicate the precipitation of the Cr in salt complexes.

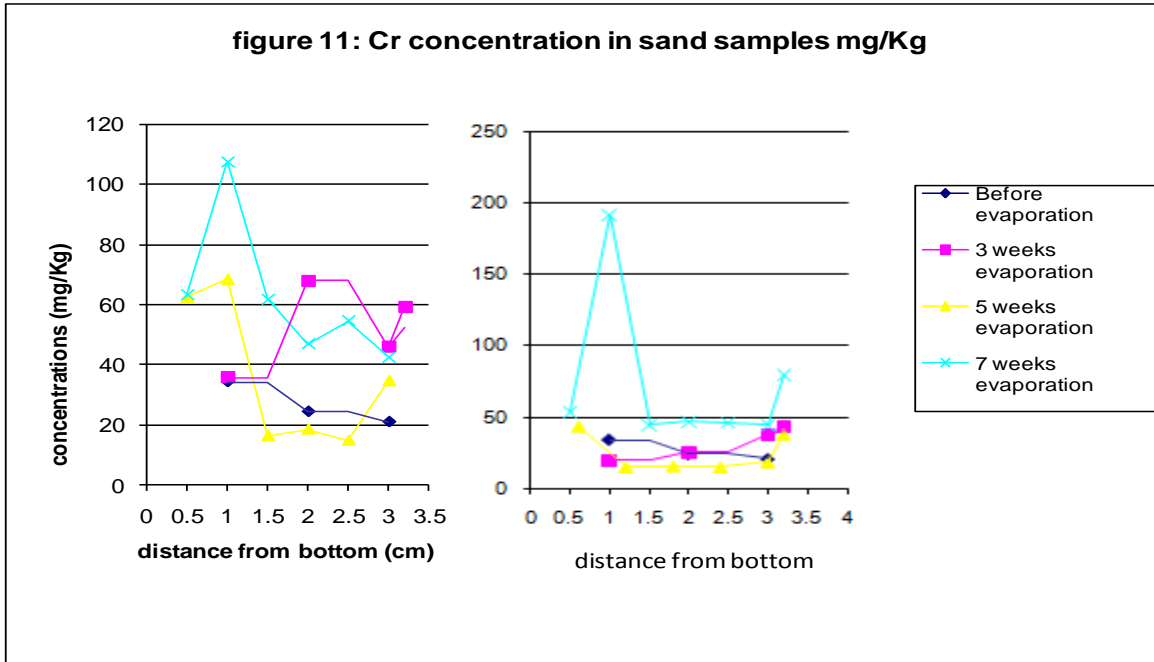
As it is clear from ICP- OES results, there is more force to move the Cr from the middle of the column to the surface, but the stable Cr in the bottom does not move upward. After seven weeks of drying, the Cr might be either precipitated as calcium chromate and other salt species, or adsorbed on the Mn and Al oxides and hydroxides in the surface slice of this sample. But in the middle and the bottom slices the Cr might be retained mostly by adsorption of the Cr⁶⁺ or Cr³⁺ on the Mn- oxides.

4.3.2 The Cr migration and speciation behavior in the sand soil samples:

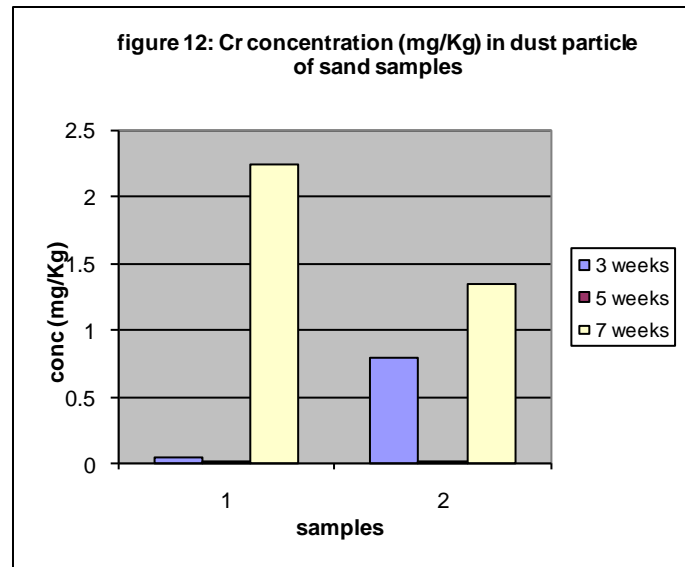
The concentration profile of the Cr in the sand sample is shown in figure 11. Although the concentration in the top soil and the surface is lower than the concentration in bottom slices, there is upward movement. The Cr retained in the bottom slices might be adsorbed to the Fe-oxides by inner-sphere adsorption and retained in the soil sample, since the sand particles do not adsorb the metals.



The concentrations of the Cr in the blown dust particles are shown in figure 12. In this case the samples dried until seven weeks also have the highest concentrations, but that is also the case in the soil slices concentrations of the seven weeks soil samples.



The Cr behaves differently in the sand sample compared to the clay samples. The Cr present in the surface slice of the three weeks dried sample, is possibly migrated upward in dissolved salt species like the calcium chromate or $\text{Cr}(\text{SO}_4)_3$ salts (table 6). The Cr at the surface might also be adsorbed on the Mn oxides present at the surface, since the correlation of the Cr with Mn in Micro- XRF data. The Cr in the middle and bottom slice of this sample might also be retained by either precipitation as stable salts or adsorbed on the Mn and Fe oxides present in the sandy soil. In sandy soil sample, the oxidation of the Cr^{3+} to the Cr^{6+} is also possible, because of the oxidizing conditions and the mediation of the Fe and Mn oxides [9].



The main Cr in the surface slice of the five weeks dried sample, is accumulated in the salt spots that are present at the surface of the sample, which indicates that the Cr is dissolved as low solubility salts and is possibly moved upward with the evaporating pore water, although it does not correlate with other elements, some Cr-hydroxide or Cr-oxide species might be precipitated at the surface.

In the middle and bottom slices of this sample, the Cr might be adsorbed on the Mn and Fe oxides and did not moved upward. Since this adsorption is inner-sphere.

The predicted speciation of the Cr is not significantly changed after seven weeks drying, but the distribution of Cr species through the soil column is different in this case.

In the surface slice, the most of the Cr is possibly adsorbed to the Mn oxides present at the surface due to intense drying. There might be also some calcium chromate or $\text{Cr}(\text{SO})_3$ salt precipitation at the surface (see table 6 for solubility products). The Cr in the middle and bottom slices of this sample might also be adsorbed on the metal oxides, since it is associated with Al, Mg, Mn and Fe. The low carbonate content in the sand samples, make it quite sure that these metals are present in oxides species rather than carbonate species, which might be present in the clay sample.

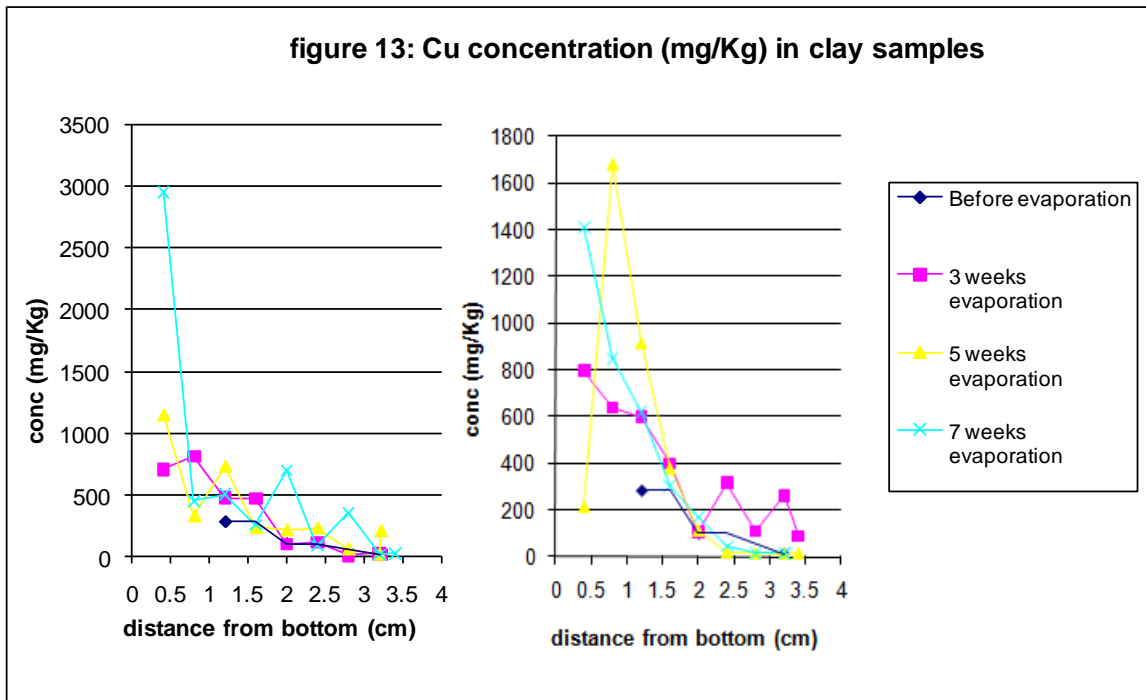
In the bottom slice some Cr might be in $\text{Cr}(\text{SO}_4)_3$ species, which is insoluble in anhydrous form (table 6). In addition to this, the Cr might also be precipitated in Lead Chromium Oxide and Copper Chromium Chloride hydrate complexes, which are partially detected by XRD.

4.4 Cu:

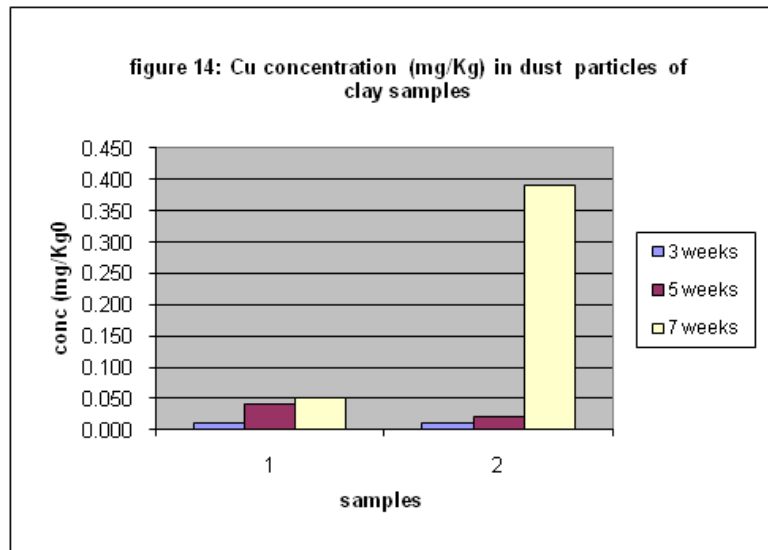
4.4.1 The Cu migration and speciation behavior in the clay soil samples:

The concentration profile of the Cu in the clay soil samples is shown in figure 13. The Cu does not migrate upward very well. As is clear in the graph, most of the Cu is accumulated at the bottom slices. Since adsorption to soil constituents, is the mechanism mostly influencing the distribution of the Cu, it might be adsorbed to the organic matter, or Fe and Mn oxides present in the clay sample. In this case the Cu is strongly adsorbed possibly to organic matter, causing the accumulation of the Cu at the bottom slices and preventing the upward movement. The Cu can also be adsorbed to the clay particles, which are negatively charged, but if it was the case, Cu would migrate slowly upward because adsorption to the clay particles is electrostatic and can be exchangeable.

There is an amount of Cu found in the dust particles of the clay samples, as shown in figure 14. Although the concentrations are very low, it indicates that, some of the Cu reached the surface. This Cu might be adsorbed to the clay particles, and wind blown away with them, especially in the seven weeks evaporation step.



The Micro XRF analysis of the Cu indicates the migration of the Cu as dissolved CuCO_3 species. The Cu at the surface slice of three weeks dried sample might be in CuCO_3 species. In the middle and bottom slices of this sample, the Cu has higher intensity and it is more distributed on the sample, some of the Cu might be also present in CuCO_3 species, as indicated by correlation with Ca. Some of Cu, might be adsorbed on Mn oxides, Fe and Al hydroxides by non-exchangeable adsorption.



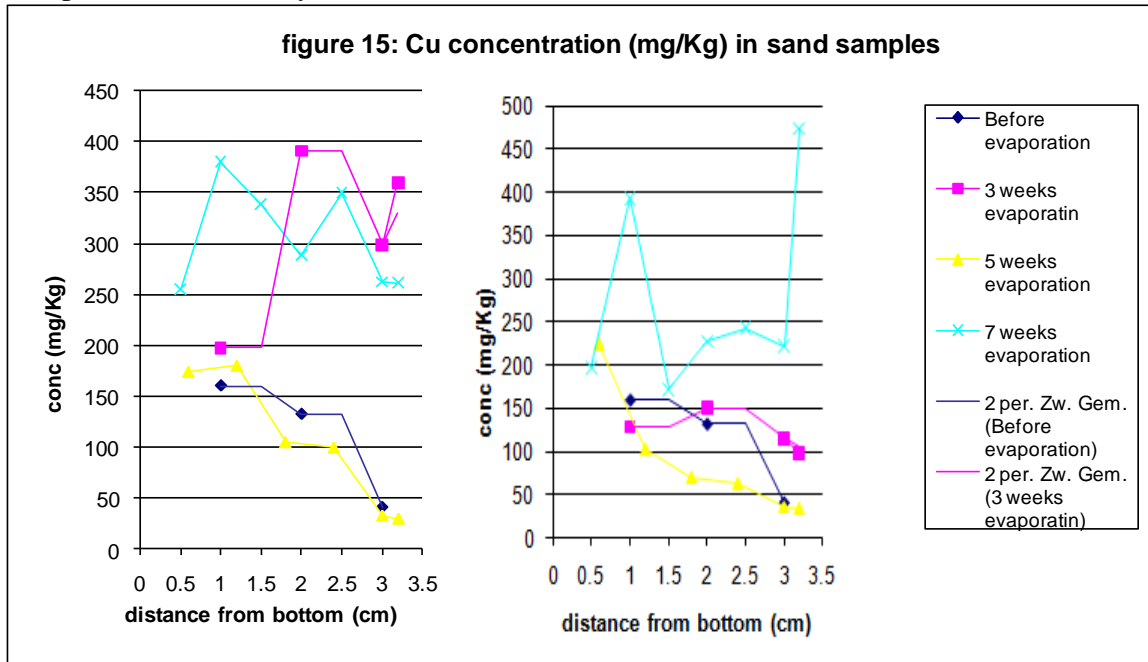
The surface sample of the five weeks evaporation step shows also the accumulation of the Cu at several spots, with the Micro XRF analysis. The Cu might be forming some CuCO_3 , CuSO_4 or CuCl_2 species in addition to adsorption to the Fe and Mn oxides. In the middle slice of this sample the Cu might be CuSO_4 salt precipitated at the clay particle surface (table 6). In the bottom sample the Cu might be retained by precipitation as CuSO_4 or adsorbed on the Fe oxides/hydroxides.

In the surface sample of the seven weeks, the very low intensity Cu is distributed over the whole sample, that might be adsorbed on Fe and Al oxide/hydroxides in addition to adsorption on clay particles. The Cu might also be migrated upward in precipitated CuCl_2

species (table 6). In the middle and bottom slice of the sample the Cu might also be retained by adsorption onto the soil constituents like the Fe and Al oxides, dissolved organic matter and clay particles. In addition, the Cu might be present in CuSO_4 species, in the bottom slice and some CuCO_3 and CuSO_4 in the middle slice of this sample.

4.4.2 The Cu migration and speciation behavior in the sand soil samples:

The Cu behaves totally different in the sand soil samples, as shown in figure 15. The Cu migrates upwards through the sand soil sample faster than in the clay sample, especially after seven weeks of evaporation. In this case precipitation might be controlling the Cu migration, since the adsorption capacity of the sand particles is low. The Cu might be retained by adsorption on to the Fe and Mn oxides in this case. Because the sand soil contains amounts of Fe and Mn oxides, inner-sphere adsorption of the Cu could take place, which can cause accumulation of the Cu at different slices and slightly prevent the migration. The Cu concentrations in the dust particle are shown in figure 16. The Cu concentrations in sand dust particle are significantly higher than the concentrations in the dust particles of the clay.

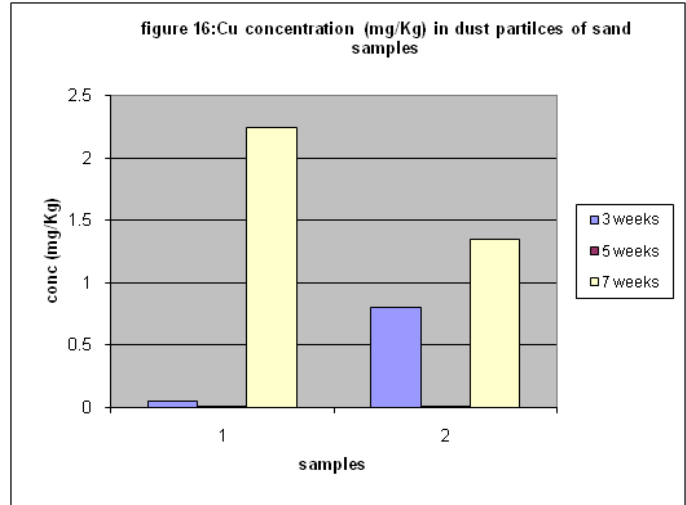


The Micro XRF analysis of the Cu in the sand samples shows also that the Cu speciation and distribution in the sand sample is different from the clay sample. The Cu in the surface sample of the three weeks evaporation, might be in dissolved salt species like CuSO_4 and CuCl_2 migrated upward by evaporating pore water.

In the middle slice of this sample the Cu is more distributed, in this slice the Cu might be precipitated in CuBr or $\text{Cu}_3(\text{PO}_4)_2$ (table 6) species, since the dissolved organic matter content of the sand is negligibly low. In the bottom slice the Cu might be adsorbed to the Mn and Fe oxides by inner-sphere adsorption, which prevent the upward movement of the Cu. Some CuSO_4 might also be formed which is not migrated upward, this might be due force demand as the pore water is evaporated totally.

In the surface and middle sample of five weeks evaporation, the Cu might be migrated upward as dissolved CuSO_4 and CuCl_2 species respectively and precipitated as the water dried (table 6). In addition to this, Cu might also be adsorbed to the Mn and Fe oxides present in these slices. In the bottom slice of this sample the Cu might be retained by inner-sphere adsorption on the Fe and Mn oxides.

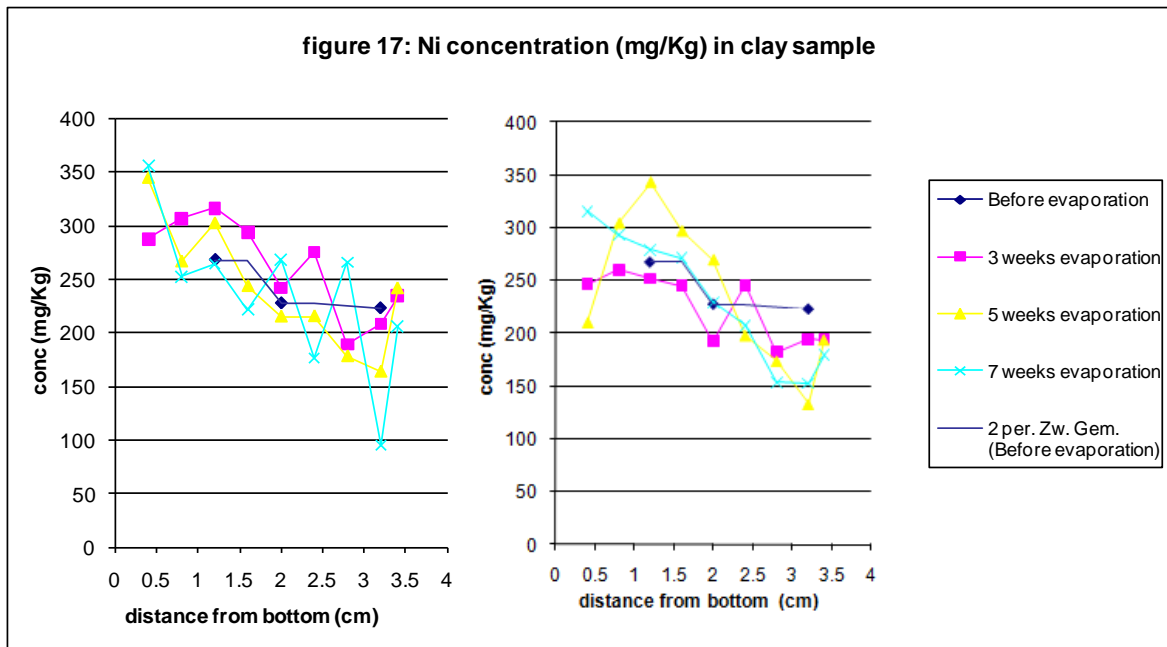
The Micro XRF data of the Cu in the seven weeks evaporation stage does not differ much from the previous steps. The migrated Cu might be in CuSO_4 and CuCl_2 precipitates, and the retained Cu might be adsorbed on the Mn and Fe oxides like the previous evaporation steps. In the surface and middle slices of this sample copper chromium chloride hydrate complexes are partially detected by XRD measurement.



4.5 Ni:

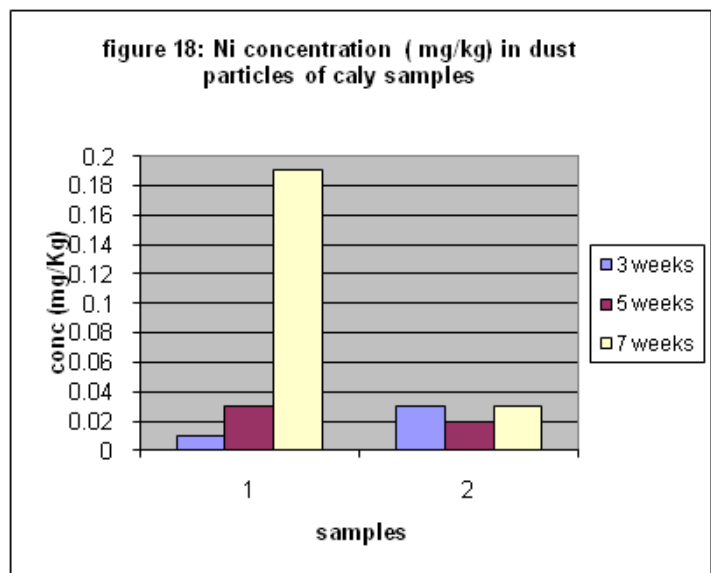
4.5.1 The Ni migration and speciation behavior in the clay soil samples:

The Ni is moved upward through the clay soil column faster than the Cr and the Cu, as is shown in figure 17. The Ni concentrations at the surface samples of each evaporation step are significantly higher. Although the bottom concentrations are also higher, the Ni is distributed quite well through the soil column. Ni is mainly retained in the soil by exchangeable adsorption to the clay particles (2.5.6). In the presence of stronger binding metals, like Cu or Pb (see table 2), it will be exchanged and migrate upward. The Ni has high affinity to dissolved organic matter, that might cause the retention of the Ni in the bottom slices. The Ni might also precipitate in stable salts, and migrate upward by evaporation of the pore water. The Ni concentrations in the dust particles are shown in figure 18. Although the surface concentrations of the three evaporation stages are relatively high, the Ni concentrations of the dust particles are very low, compared with the Cr and the Cu concentrations in the clay dust particle. This indicates that the most of the migrated Ni to the surface of the samples is in salt forms which do not erode easily with the flowing air.



The Micro XRF analysis of Ni in the surface slice of three weeks dried samples shows distribution of the Ni over the clay particles, which indicates the adsorption of Ni on the clay particles. The Ni might be distributed in the soil column by dissolution and precipitation, competitive adsorption and complexation with inorganic and organic ligands, since all of these retention mechanisms might play a role, influencing the distribution of the Ni in the soil [18]. In the middle slice of this sample the Ni might be in NiSO_4 or NiCO_3 species. In the bottom slice the retained Ni might be adsorbed on organic matter (inner-sphere) or clay particles (outer-sphere). But the general intensity of the Ni is lower at the bottom compared to the middle and surface slices of these samples, which confirms the upward movement of the Ni.

After five weeks drying the Ni behavior does not differ much from the three weeks sample. The Ni might be complex with organic matter present in the clay sample or it might be adsorbed on clay particles. In addition the Ni might be migrated in dissolved NiSO_4 species and precipitated as the pore water dried (table 6). In the surface sample of the seven weeks drying, the Ni might be in NiCO_3 precipitates. The Ni might also adsorbed on the clay particle in this slice. These particles could be blown away with the flowing air and contain the adsorbed Ni.

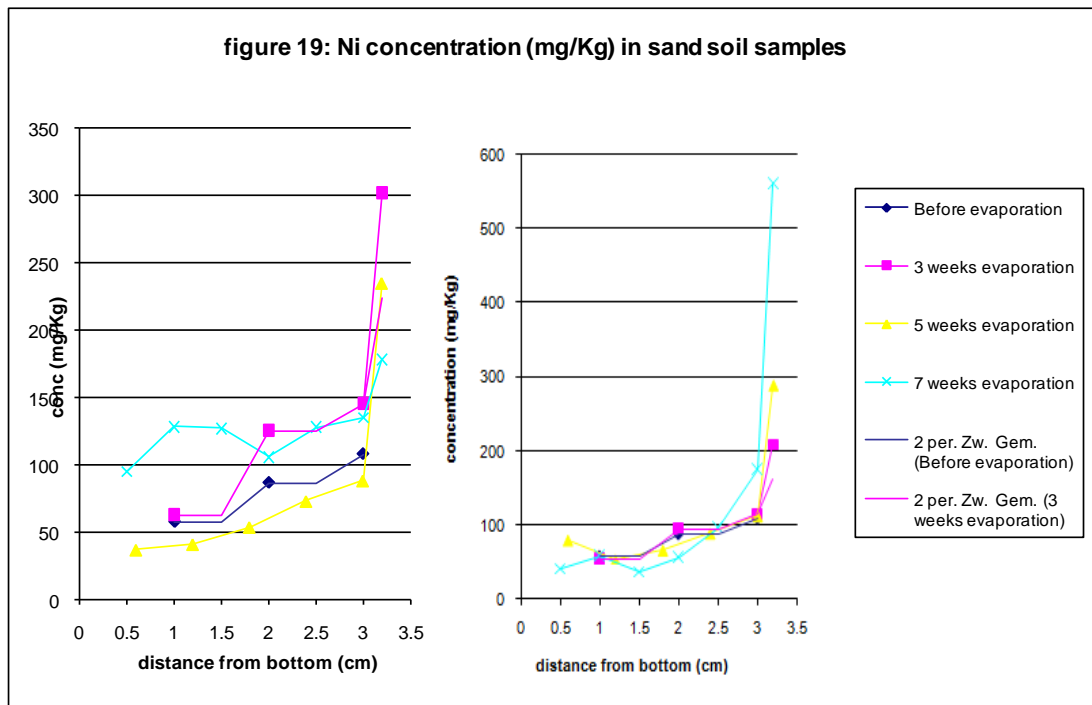


In the bottom slice the most retained Ni might be adsorbed, or complexed with organic matter, some NiSO₄ species might also be formed and retained in the bottom slice after evaporation of the pore water.

4.5.2 The Ni migration and speciation behavior in the sand soil samples:

The concentration profiles of the Ni in the sand samples are shown in figure 19. The Ni, like the other metals is more mobile in the sand soil rather than clay soil. The ICP-OES measurements of the Ni in the sand samples shows that the Ni is migrated upward dramatically with the evaporation of the pore water. There is also an upward migration after saturation, because the Ni concentrations are significantly high in the surface slices after each evaporation step. In this case the precipitation of the Ni as stable salts is more likely, since the organic matter content of the sand is very low.

The Ni concentrations in the dust particles are also much higher, compared to the clay dust particles. The Ni concentrations in the dust particles are shown in figure 20.

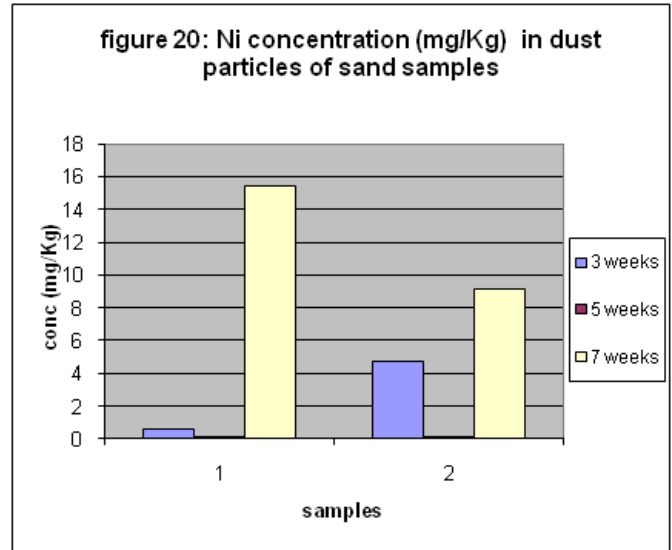


The Micro XRF data of the Ni in the surface and middle slices of the three weeks dried sand samples shows that the Ni is distributed well over the sand particles. The Ni might be migrated upward by forming NiSO₄ and or the NiCO₃ species that are precipitated at the surface as the pore water is evaporated. The Ni might also be precipitated in hydroxide or oxide species, since the system is under oxidizing conditions.

In the bottom slice of this sample the Ni might also be in NiSO₄ specie, but it might also be retained by adsorption onto the Mn and Fe oxides. The Ni in the surface slice of the five weeks evaporation step does not differ much in the sense of speciation. But it is much more intense than the surface slices of the three weeks evaporation step.

In the surface and middle sample of the seven weeks drying, the Ni might be precipitated also in NiSO_4 and NiCl_2 . But in the middle slice, in addition to precipitation, the Ni might also be adsorbed to the Fe, Al, and Mn oxides present in the sand sample.

In the bottom slice of this sample the Ni speciation behaves differently, in this slice the Ni, is not adsorbed to the Fe oxides, it is also not precipitates as the low soluble salt like in the previous slices, so it might be present as Ni- oxides or hydroxide complexes distributed at the surface of the sand particles. In the XRD analysis, nickel chloride and cadmium nickel chloride complexes are detected in the all sample slices.

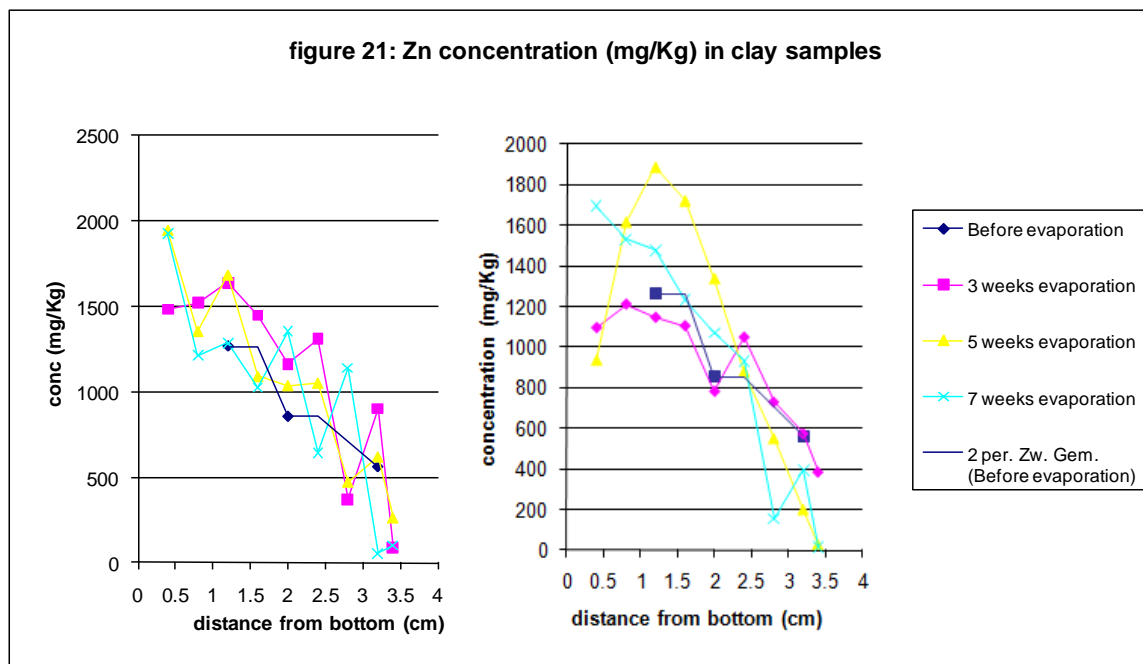


4.6 Zn:

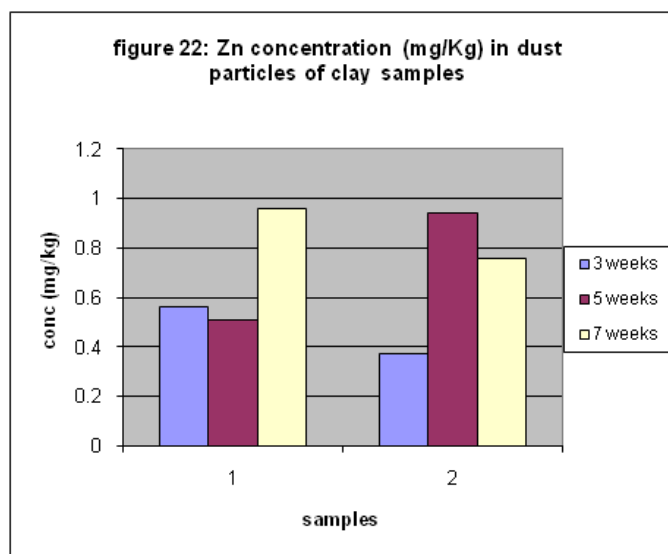
4.6.1 The Zn migration and speciation behavior in the clay soil samples:

The concentration profile of the Zn through the soil sample is shown in figure 21. Zn has migrated through the soil column by flushing the solution and by evaporation of the pore water. Zn concentration is higher at the bottom and decreases toward the top, which means that some of the migrated Zn is retained at each slice. It might be sorption mechanisms that cause retention of Zn in each slice, since Zn binds to the organic material by inner-sphere complexation and adsorbs to the clay minerals as hydroxyl species, which is an outer-sphere adsorption mechanism and it can exchange and migrate. Zn might also be precipitated and migrated as stable salts and is more likely to migrate than the “exchangeable” adsorbed Zn.

But although the Zn concentrations of the surface slices are not very high relative to the middle and bottom slices of the samples, Zn concentrations in the dust particles are relatively high compared to earlier discussed metals, except Ni, even after three weeks of evaporation as shown in figure 22.



The Micro XRF analysis of the Zn in the surface slice of the three weeks sample shows that Zn is distributed on the clay particles, this indicates the adsorption of the Zn onto the clay particles for instance as hydroxyl species. Zn might also migrate as dissolved $ZnSO_4$ species and precipitated at the surface by evaporating the pore water. In the middle slice of this sample the Zn might be adsorbed to the clay minerals as montmorillonite and illite, since they exhibit high capacity to absorb Zn. This is also the case in the bottom slice of this sample. In addition to adsorption on the clay minerals the Zn might be retained by sorption, or scavenged onto carbonates or bind with dissolved organic matter.



The Zn in the surface slice of the five weeks dried sample correlates also with Ca and Fe. This indicates Zn precipitation by carbonate species like $ZnCO_3$ or the Zn might be scavenged by the carbonates or co-precipitated with Fe oxides [20]. In the middle and the bottom slices of this sample the Zn might be retained by outer-sphere adsorption on the clay particles, since it is distributed very well on the clay particles, sorption and scavenge on the carbonates might be occurred. The Zn distribution pattern in the surface slice of the seven weeks dried sample is slightly different from the previous evaporation steps. In this case the Zn is associated with Al and Fe, which indicates the sorption or complexation of the Zn on these oxides and

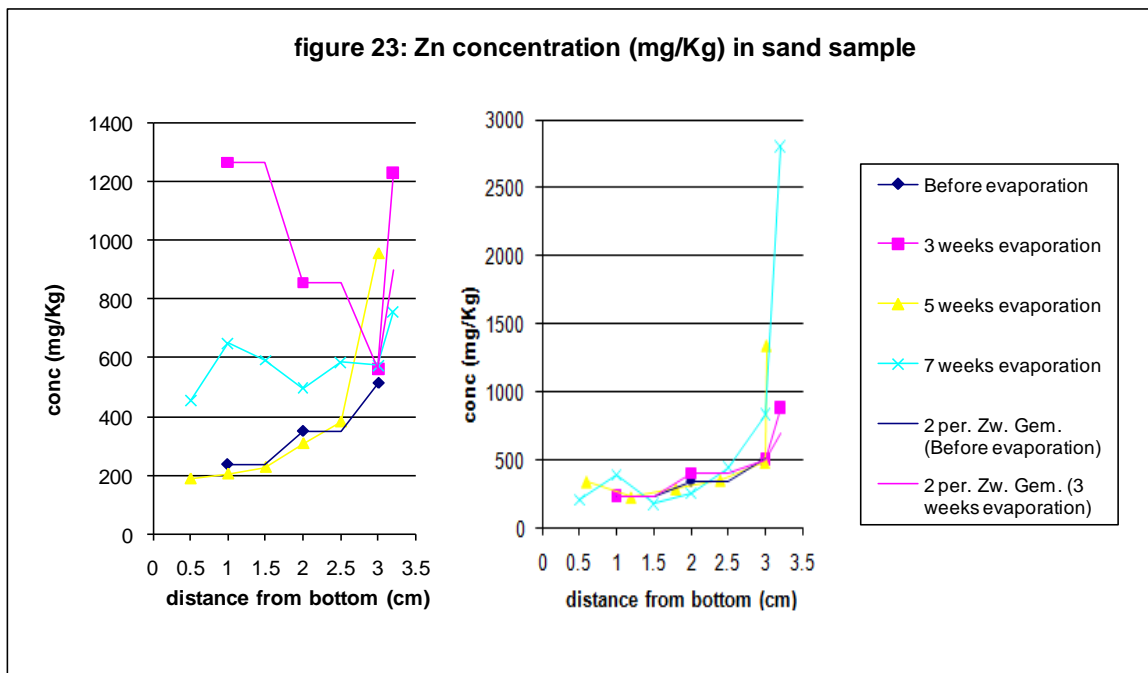
hydroxides. Adsorption onto the clay particles might also cause the retention of the Zn at the surface of the sample. In this case the Zn may be transported with the clay dust particles due to air flow above it.

The Zn in the middle and bottom slices of this sample, the Zn might be precipitated in calcium zincate as mentioned in the literature, or in ZnSO₄ salt species, as indicated by correlation with Ca and S.

The ZnSO₄ is more likely to be retained at the bottom slice. In addition to this, the Zn might also be co-precipitated with the Fe, Al and Mn oxides or scavenged into the carbonates.

4.6.2 The Zn migration and speciation behavior in the sand soil samples:

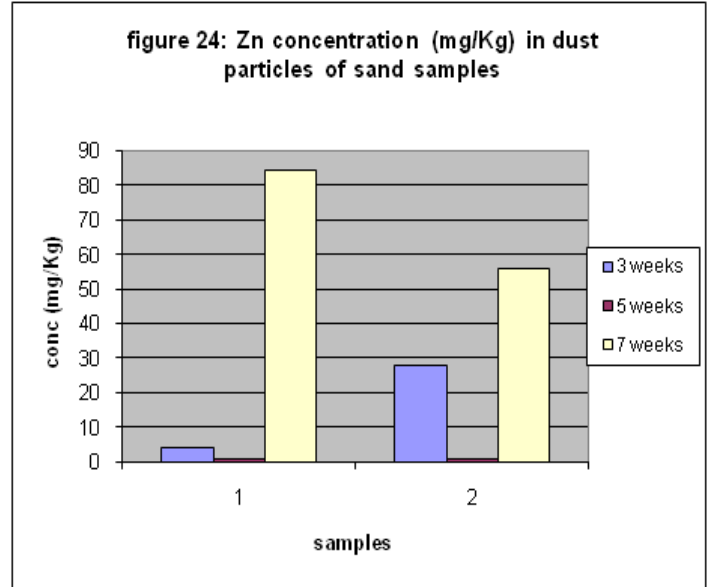
The upward migration of the Zn in the sand soil differs significantly from that in the clay soil. The concentration profile of the Zn in the sand soil is shown in figure 23. The Zn migrates well through the soil column, and reaches the surface. In this case precipitation might be controlling the migration of the Zn. The Zn is transported to the sand dust particle after reaching the surface, as it is shown in figure 24. The Zn concentrations in the dust particles are relatively high.



The Micro XRF analyses of Zn in the surface and middle slices of the three weeks dried sample shows that Zn might migrate as dissolved ZnSO₄ and transported by the evaporating pore water. It might also be adsorbed on the Fe- oxides in this sample. In addition to this, Zn might also be in hydroxide species, since the role of the organic matter content of the sand is negligible. In the bottom slice of this sample Zn might be retained by sorption on Al, Fe and oxides. Some ZnCl₂ species are also detected in this slice.

Zn in the surface and middle slices of the five weeks evaporated sample does not differ in the sense of speciation. The upward migration of the Zn in $ZnSO_4$ species and retention by sorption of Zn by the Fe, Al, and Mn oxides might have occurred. In the bottom slice of this sample the Zn is distributed well on the surface of the sand particles, some $ZnCl_2$ might be formed in this slice which is not migrated.

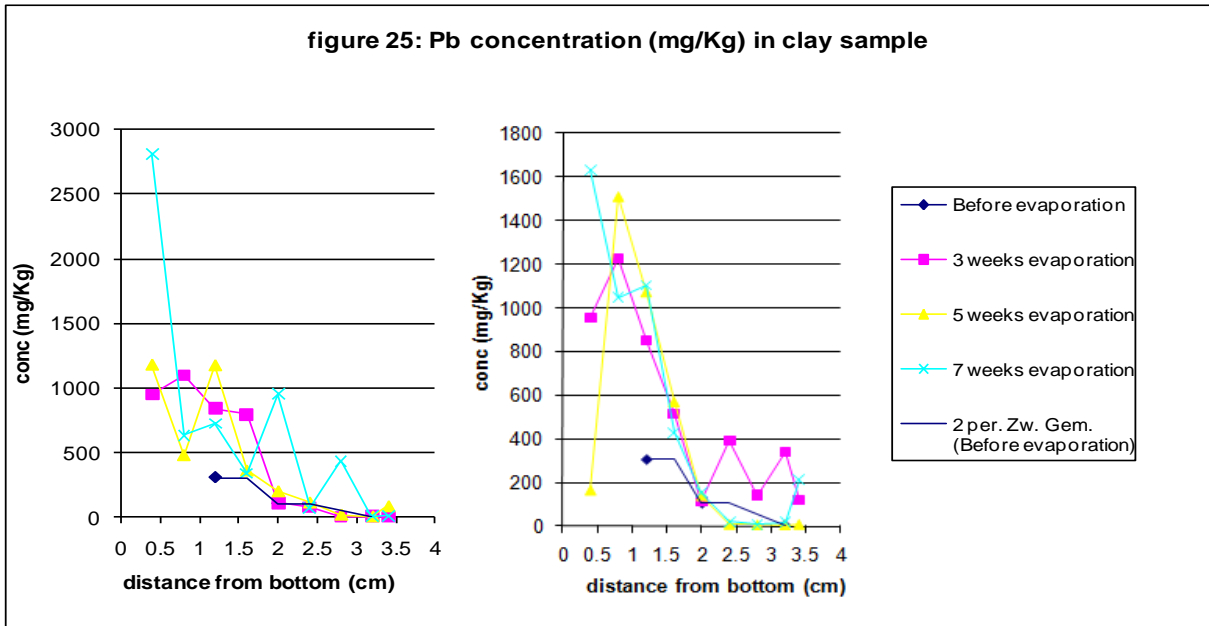
The Zn in the surface slice of the seven weeks dried sample, might also be dissolved in $ZnSO_4$ or $ZnCl_2$ species and precipitated at the surface as the pore water dried. In the middle slice of this sample the most of the present Zn might be in $ZnSO_4$ species. In addition to this the Zn might also be sorbed on the Al, Fe and Mn oxides in this slice. The Zn in the bottom slice of this sample is different. The Zn is distributed over the sand particles, in this case the Zn might be present as Zn-hydroxide species.



4.7 Pb:

4.7.1 The Pb migration and speciation behavior in the clay soil samples:

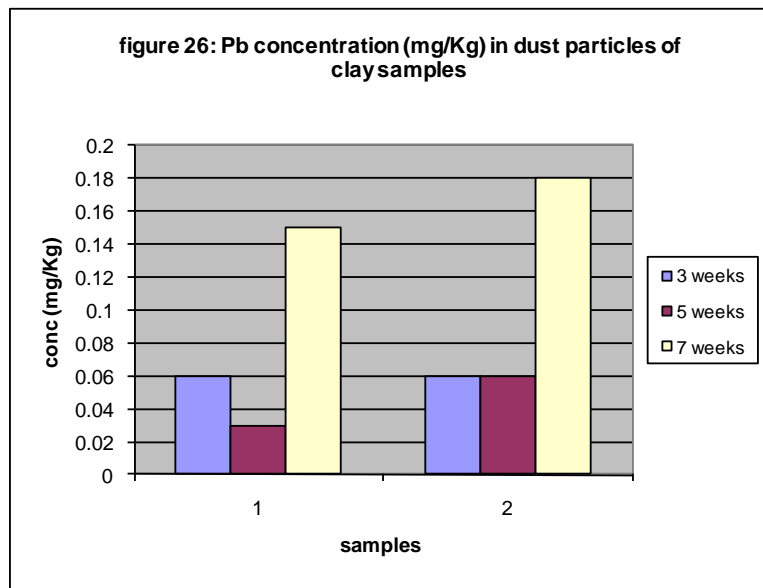
The concentration profile of the Pb is shown in figure 25. It is clear in the graph, that Pb, like Cu, does not migrate upward very well. The concentrations in the bottom slices of the three evaporation steps are higher than the middle and the surface slice, the surface slices show the lowest Pb concentrations in all of the evaporation steps. Therefore, the concentrations in the dust particles of the clay sample are relatively low. These concentrations are shown in figure 26. Since the clay soil sample is rich in clay minerals and other soil constituents like organic matter and Fe and Mn oxides, the retention of the Pb might be caused by adsorption. Pb shows high affinity to Fe oxide as shown in table 2. The Pb can also be precipitated in stable salts. In this case the Pb could also be dissolve in $PbCO_3$ and precipitated as the water dried since the soil has high carbonate content and high pH.



In the Micro XRF analysis the Pb in the surface sample of the three weeks drying step shows a distribution over the whole sample. An amount of $PbCO_3$ might be precipitated at the surface after upward migration with the evaporating pore water (table 6).

In the middle slice of this sample the Pb shows a different pattern. In this case the Pb might be adsorbed on the Fe and Mn species, since the presence of Mn and Fe oxides may exert a predominant role on adsorption in soils. In contrast to the ICP-OES results, the Pb has low intensity in the bottom slice of this sample. But this might be due to the heterogeneity of the sample. The Pb in this sample is also distributed well over the clay particles like in the surface slice. This indicates the retention of Pb by adsorption on the clay particles or Al- hydroxides.

In the surface slice of the five weeks drying sample Pb is also distributed very well on the clay particles. Adsorption on clay particles or complexation with organic matter might have occurred. In the middle slice of this sample the Pb is distributed as well, but there are some more intense spots recognizable. In this case precipitation of the $PbSO_4$ or adsorption of Pb on Fe and Mn oxides might be possible. In the bottom slice of this sample the intensity of the Pb is higher than the previous slices which fits with the ICP-OES results.

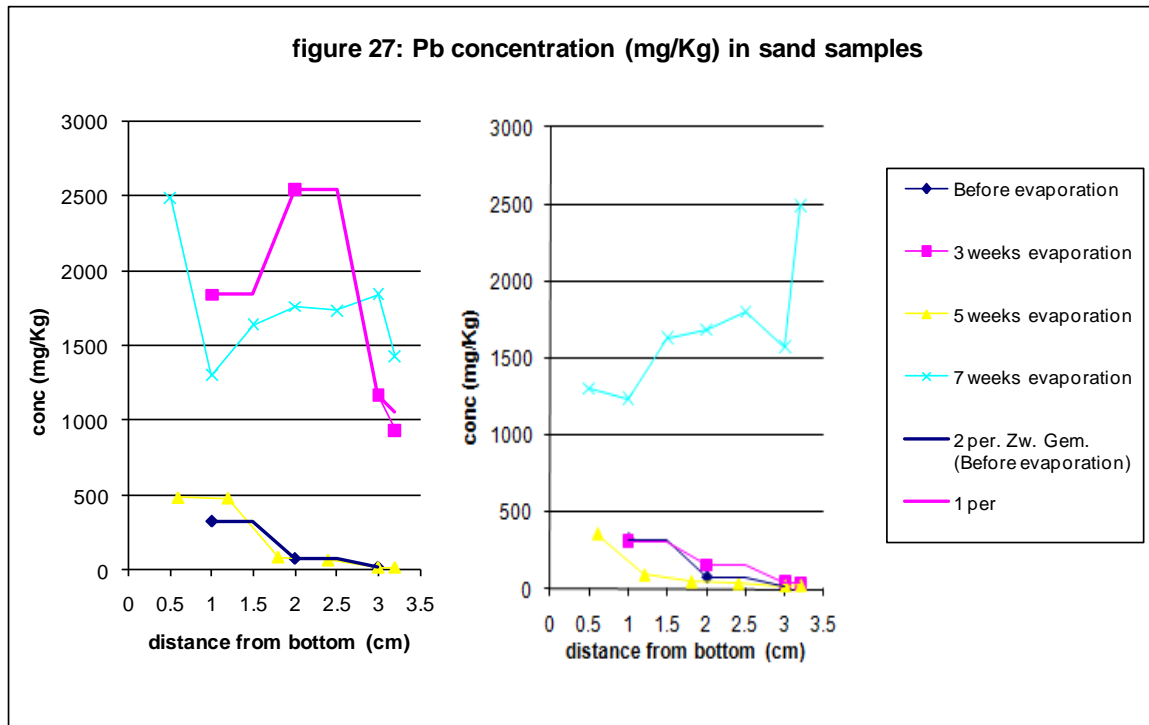


The Pb is also well distributed in this slice, and might be retained by adsorption on the Fe oxides or Fe-minerals.

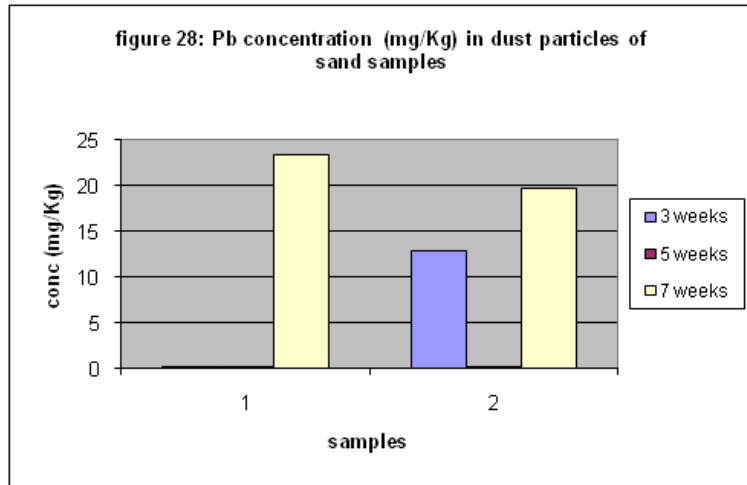
In the surface sample of the seven weeks drying the Pb is distributed on the clay particles as well. But migration of the Pb as $PbCO_3$ and its precipitation at the surface is probable. This is also the case in the middle slice of this sample, but in addition to precipitation the Pb might be also retained by adsorption to the clay particles and other soil constituents. The distribution pattern of the Pb in the bottom slice of this sample is different. In this case, some $PbSO_4$ precipitation might be occurred. But generally after seven weeks of drying the Pb looks more adsorbed to the clay particles, as the Micro XRF analysis shows.

4.7.2 The Pb migration and speciation behavior in the sand soil samples:

The concentration profile of the Pb in the sand samples is shown figure 27. Although the upward movement of the Pb is faster in the sand soil rather than in the clay soil, like for other metals, the Pb is retained in the sand soil as well. This retention might be due to the inner-sphere adsorption of the Pb to the Fe and Mn oxides present in the sand soil [1]. The Pb results in the sand sample are actually not trustable, due to the large overestimations, that are found in the mass balance of Pb (see table 12). The concentrations of the Pb in the dust particles are relatively high, especially after seven weeks of evaporation as shown in figure 28, and depending on the form in which this Pb is present in the dust particle, it might be important toxicologically.



In the Micro XRF analysis of the sand sample, the Pb is distributed well, in the surface slice of the three weeks drying. The distribution pattern of the Pb in this sample shows that the lead might be adsorbed on the Fe oxides. The Pb is also distributed like a cover on the sand particles surface, in this case Pb might also be precipitated as PbCO_3 or PbSO_4 on the sand particle surface. In the bottom slice of this sample the Pb might also be retained by adsorption on the Fe and Mn oxides. The Pb might also be precipitated as some PbCO_3 and PbSO_4 species when the pore water is dried. In the middle and bottom slices of this sample, lead iron chloride hydrate is detected with XRD analysis.

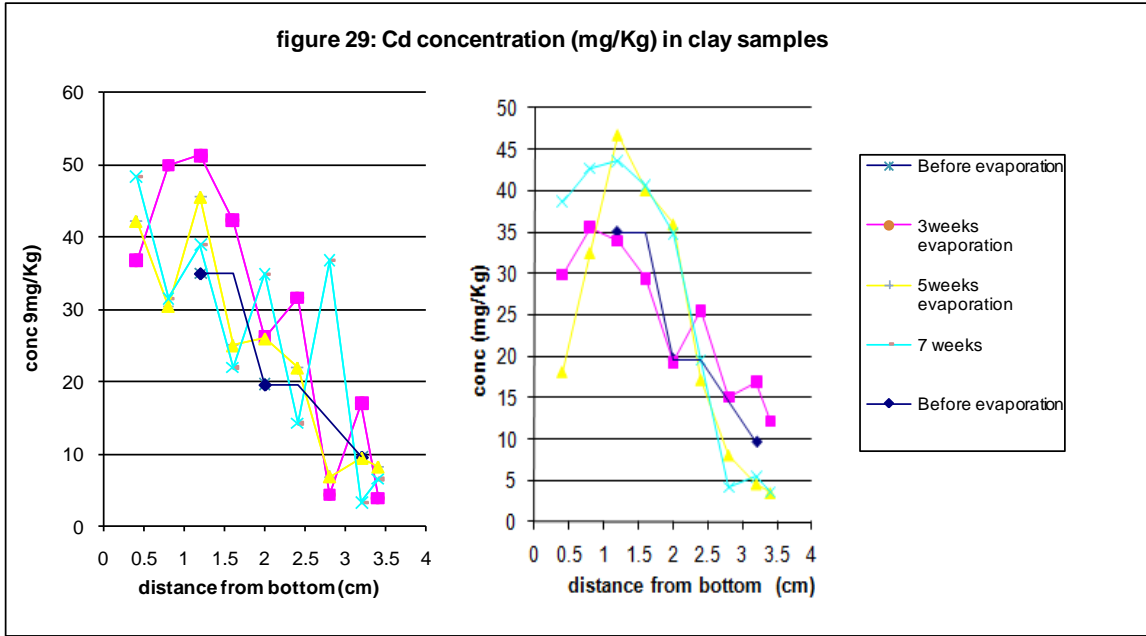


The Pb is distributed in the surface slice of the five weeks dried sample as well. In this slice the Pb might be precipitated as PbCO_3 and or adsorbed on the Mn-oxides present in the sand sample. In the middle and bottom slices of this sample the Pb is also distributed as a cover on the sand particles. In this case some Pb hydroxide species might be precipitated at the sand particle surface by evaporating the pore water (table 6). In the surface slice of the seven weeks dried sample, the Pb distribution pattern is different from the previous samples, in this case the Pb might be dissolved as PbSO_4 and migrated upward with the evaporating pore water. In the middle slice of this sample the Pb might be retained by adsorption on the Al, Fe, Mn oxides. In the bottom slice of this sample, the Pb is distributed well on the sand particles. In this slice in addition to retention by adsorption on Mn oxides, the Pb is probably also retained by precipitation of PbSO_4 .

4.8 Cd:

4.8.1 The Cd migration and speciation behavior in the clay soil samples:

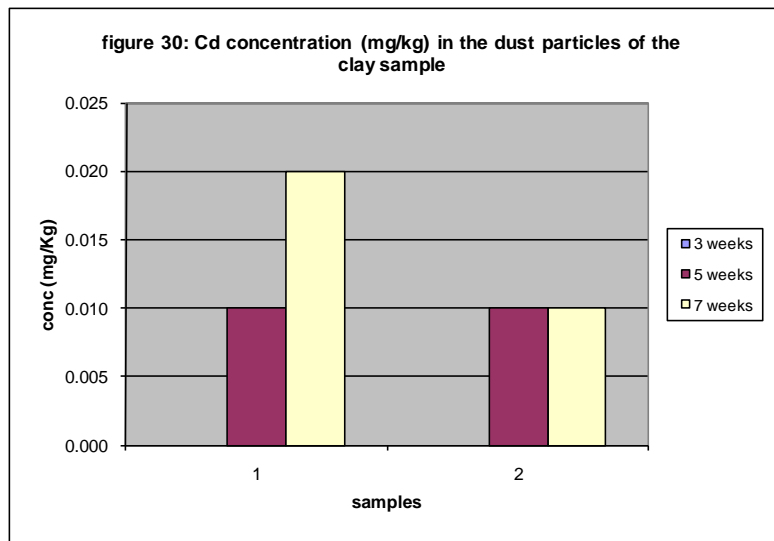
The concentration profile of the Cd is shown figure 29. The Cd concentration is higher at the bottom and decreases toward the top, which means that some of the migrated Cd is retained at each slice. In this case an amount of the Cd that is retained might be adsorbed to the soil constituents like Fe- hydroxides and oxides, and /or to the clay particles. The Cd might also be precipitated as stable salt species, since precipitation and adsorption are the main retention mechanisms controlling the Cd behavior in the soils [1]. But the adsorbed Cd on the clay particles migrates slower than the precipitated Cd species, because it is exchangeable adsorption, which make it slower to migrate upward. The Cd concentrations in the dust particles are low compared with the other metals. These results are shown in figure 30. The binding form of the Cd on the clay dust particles make it more important toxically.



The Micro XRF analysis of the surface slice of the three weeks dried samples shows that the Cd is distributed well over the clay particles. In this case the Cd might be precipitated as CdCO_3 or it might also be adsorbed on the Al, Fe and Mn oxides and the clay particles. In the middle slice of this sample the Cd might also be precipitated as CdCO_3 or CdSO_4 species. The Cd is also distributed very well in the bottom slice. CdCO_3 species are probably also present in this slice.

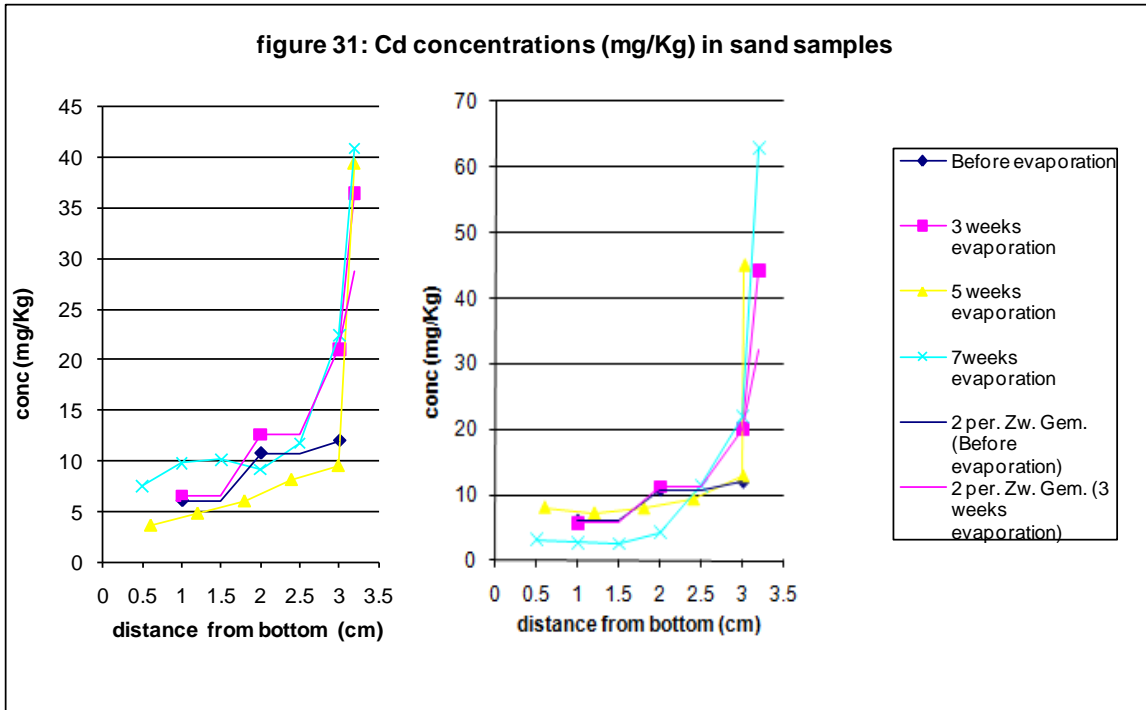
In the surface and middle slices of the five weeks dried sample, the Cd is distributed over the clay particles as well. Cd might be present as CdCO_3 and CdSO_4 species, as well as adsorbed on the Al-hydroxides, Fe and Mn oxides. In the middle slice some CdCl_2 might also be formed. The Cd is also distributed on the clay particle in the bottom slice of this sample, but in this case, in addition to adsorption, the Cd is probably in CdCl_2 species that might be precipitated on the clay particle surface.

In the surface slice of the seven weeks dried sample the Cd is also distributed over the clay particles, in this slice the Cd adsorption to the Fe oxides or precipitation as CdCO_3 species might have occurred. The Cd behavior in the middle slice of this sample is not very different, but in this case some Cd-hydroxides species might be precipitated.



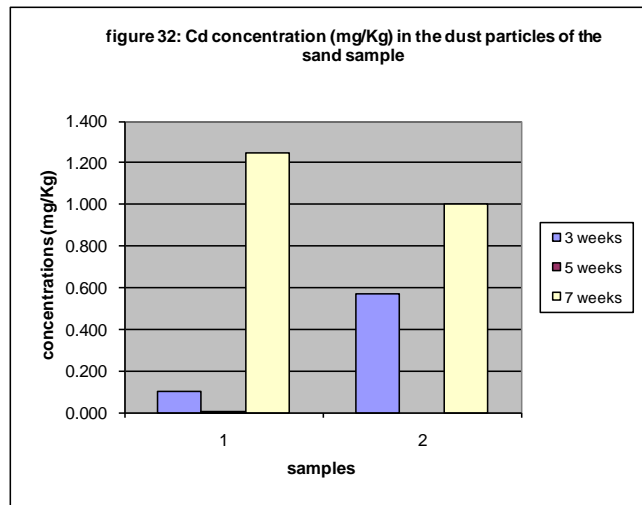
4.8.2 The Cd migration and speciation behavior in the sand soil samples:

Like other metals do, the Cd behaves differently in the sand soil. The concentration profile of the Cd in the sand soil is shown figure 31. The surface slices of all the three evaporation steps have the highest concentrations. It means that the Cd is migrated upward in the sand sample, in this case, the migrated Cd might be precipitated as carbonate, chloride or sulfate species, since the soil characteristics and the conditions are suitable for formation and precipitation of the Cd- carbonates or Cd- clorides rather than adsorption. The Cd in the bottom and middle slices of the sand sample, might also be adsorbed to the Fe- or Mn oxides, since they are present in the sand sample, but in lesser extent than in the clay sample. The Cd concentrations in the dust particles of the sand samples are also significantly higher than in the clay dust particles (figure 32).



The Micro XRF analysis of the surface slice of the three weeks evaporation sample shows that the Cd is accumulated on some places in this sample. The Cd might be migrated upward in CdCO_3 , CdSO_4 and/or CdCl_2 species and precipitated at the surface.

In the middle slice of this sample the Cd might also be in these species, but in this slice some Cd- hydroxide species might also be formed and precipitated as the pore water is evaporated.



This is also the case in the bottom slice of this sample, but in this case the Cd might be retained by inner-sphere adsorption on the Al and Fe oxides. In all three slice of this sample some cadmium nickel chloride hydrate complexes are detected by XRD analysis.

In the surface and middle slices of the five weeks evaporation sample, the Cd might also be migrated as CdCO_3 or Cd- hydroxide species and precipitated as the pore water is evaporated (table 6). The Cd in the bottom slice of this sample might be retained by precipitation CdCO_3 and/ or CdSO_4 . Cadmium nickel chloride species are also detected in all slices of this sample as well.

In the surface slice of the seven weeks evaporation sample, the Cd is also accumulated in some places. Some of these spots might be CdSO_4 species. But the most intense spots might be Cd- hydroxide species. In the middle slice of this sample, in addition to precipitation of CdSO_4 , the Cd is probably complexed with Al hydroxide and/or adsorbed on Fe oxides. This is also the case in the bottom slice of this sample, in addition to possible complexation with Al hydroxides, the Cd might be retained by precipitation of the CdCl_2 , Cd- hydroxides and /or CdCO_3 species. Because some cadmium aluminum chloride complexes are also detected in the bottom slices of the five and seven weeks evaporation steps by XRD analysis.

4.9 The change in alkali metals and other elements present in the soils:

The concentration of the other elements and earth alkali metals present in the soil samples originally were also measured by the ICP-OES analysis. The concentration profiles of these elements are in appendix E.

The measured elements are: Ca, Mn, Mg, Na, K, P, Fe, Al and S. In addition to S all of these elements have relatively the same concentration profile in the samples before drying. In the clay sample they are distributed relatively equally in all slices. But in the sand sample, most of them were higher concentrated in the middle slice of the sample. S was higher in the top slices of the sand and clay samples after saturation and ageing, the S might be migrated already during the saturation stage, since the flow of the contamination solution was from the bottom upward.

The migration behavior of these elements is not significantly different during the three evaporation steps. After drying, Na, S and Ca were higher in the surface slices of both soil samples. Na and S were much higher in the surface slice of the clay sample than the middle and bottom slices, this indicates the upward movements of these salts. Since the Ca and the Na are probably in carbonate and sulfate salt complexes, the formed metal carbonates and metal -sulfates, or carbonates scavenged metals could also be migrated with these salts, to the surface of the samples.

The concentration profile of the rest of the elements, K, Mg, Mn, Fe and Al, is slightly different. After drying, these elements are higher in the middle and bottom slices of the sand sample. The higher concentrations of Mn Fe and Al in the middle and bottom slices of the sand sample adsorbed probably the heavy metals in this slices and prevented the upward movement of the metals. Fe and Mn are probably in oxide forms, because of the oxidizing condition in the samples. The carbonate content in the sand sample is low, which indicate that the most Fe might be in oxide or hydroxide form.

These oxides could bind the metals by adsorption and prevented some of the metals, like Cu, Cr and Pb to migrate more upward. But in clay sample they are distributed through the soil column, and they are slightly higher at the surface of the sample, so the heavy metals could be adsorbed to oxides of these metals in each slice. These alkali-metals might be also in carbonate species, because of the substantial carbonate content of the clay sample, the heavy metals might be precipitated as carbonate species by the interaction with these alkali metal- carbonates, due to the competitive behavior of the heavy metals.

The P has also a different concentration profile, this is higher in the middle and bottom slices of the sand sample, but in the clay sample it is quite equally distributed through the soil column.

5. *Final considerations and conclusions*

Most of the soil properties and characteristics of the two soil types differ significantly. Only the pH and the EC are relatively similar. The differences in soil properties cause differences in the behavior of the heavy metals in both soils. The heavy metals migrate differently in both soil types because their metal adsorption capacity is different. The clay soil is in general finer grained, and it contains more clay minerals, organic matter content and higher contents of carbonates, so it has a higher capacity to adsorb the metals, compared to the sand soil, which is coarser grained, it has higher porosity and very low organic matter and carbonate content and so lower adsorption capacity. However the heavy metals can also be retained in the sand soil by specific adsorption on the Fe, Mn oxides and Al hydroxide, since the sand soil is rich in these oxides. The high pH, that is due to relatively high CaCO_3 of the sand support the adsorption of the heavy metals as well.

In general all of the retention mechanisms discussed played a role in the migration behavior of the heavy metals. Inner-sphere and outer-sphere adsorption, complexation and precipitation are the mechanisms mostly controlling their behavior. The behavior of the heavy metals is distinguished in the phenomena, retention and migration.

In both soils most of the heavy metals of the study like, Cr, Cu, Pb, are retained and accumulated in the bottom and middle slices by specific, non-exchangeable adsorption on the Fe, Mn and Al oxides, depending on their affinity to these oxides (table 2), or by complexation with organic matter in clay soil in the case of Cu and Ni. Other metals e.g. Cd and Zn are retained and accumulated in the bottom soil slices mostly by outer-sphere adsorption on the negatively charged clay particles. These adsorbed metals can exchange and migrate upward after occupying the adsorption site by stronger binding metals (table 4). The retention of the metals might also be influenced by solid solution, since they are left to age during three weeks and further ageing occurs in the evaporation stages. The heavy metals might be complexed with carbonates and other salts or scavenged into the carbonates and precipitated in these complexes as the pore water dried. As mentioned in the literature [2], solid solution of metals takes place by the slow diffusion of metals into Fe-oxides, hydrous oxides of Al and Mn, clay minerals and by diffusion or precipitation in carbonates. In calcareous soils, the presence of carbonates is supposed to be a major factor controlling the heavy metals availability because the carbonates control the pH. All of the heavy metals are adsorbed on the clay particle by outer-sphere adsorption in higher or lower extent. The heavy metals are mobile under this adsorption mechanism, due to their exchangeability. This is more likely in the clay soil, but does not really occur in the sand soil. As mentioned in the literature [1] the fast retention is initiated by the rapid adsorption to soil surfaces via formation of outer-sphere complexes driven by the differences in the concentration gradient from the solution phase to the surface of the soil minerals and negatively charged organic matter. Following the rapid adsorption, a secondary (slow) shift of heavy metals from outer-sphere to inner-sphere surface complexation including the surface of carbonates, Fe- Mn oxides and the edge of soil minerals may occur, by fixation mechanism, but it is not clear if this mechanism has taken place during this research.

The migration of the heavy metals is influenced mostly by dissolved complexation and precipitation. The heavy metals could form dissolved carbonate, sulfate and chloride complexes or stable salt species like Cadmium Nickel Chloride, Zinc chloride hydrate etc, that are dissolved and subsequently precipitated during the upward movement of the evaporating pore water.

The electrostatically adsorbed metals on the clay particles could migrate upward as well, due to the exchange with other ions present in the soil solution. In this case the selectivity exchange of the metals plays an important role in the migration of the metals. The more electronegative metals with larger radius will exchange the lesser electronegative and smaller radius metal. This might cause the faster migration of Ni, and in lesser extent Zn, Cr and Cd compared to the stronger binding, and slower migrating Cu and Pb. But the migration of the metals, in this case is slower than the dissolved fraction of the metal. These dissolved metal complexes can precipitate if the pore water is totally evaporated in, for instance, middle slice and do not migrate upward.

Generally it is difficult to distinguish between adsorption and precipitation of the heavy metals, because as mentioned in the literature, there is a continuum between these mechanisms [1].

In addition to the migration of these toxic metals, another issue that might be of great importance, is the oxidation of Cr^{3+} to Cr^{6+} which is the most toxic form of the Cr. This oxidation may have occurred, since the soils samples of the experiment are in oxidizing conditions, given the high concentrations of Fe and Mn oxides in both soil samples. This is also the case in the soils of the arid and semi arid environment, since these soils are calcareous and contain high amounts of Fe and Mn oxides, that support the oxidation of the Cr.

The other elements and alkali metals present in the soils are also changed during the experiment. Minerals like calcite and gypsum may have dissolved by introducing the contamination solution through the soil columns, due to the low pH of this solution. As mentioned section 4.9, the Na^+ , Ca^{2+} and the S were migrated upward in both samples. This confirms the possibility for the heavy metals to form the carbonate and sulfate species, like for instance ZnSO_4 , CdSO_2 or NiCO_3 and PbCO_3 .

Conclusion:

The migration behavior of heavy metals, in soils of arid and semiarid environments, is mostly controlled by evaporation and depends on the type of the soil and soil constituents. The soil characteristics like pH, carbonate and organic matter contents, amount and type of clay mineral, presence of Fe and Mn oxides and hydroxides govern the heavy metals retention and migration behavior. Since the soils in the arid and semiarid climates are mostly calcareous, and contain high amounts of the Fe, Mn and Al oxides and hydroxides, their retention capacity for the heavy metals is high, especially in the case of clayey soils. In the sandy soils, the upward migration of the metals with the evaporation flux is faster, due to the fact that the sand particles are coarser and their adsorption capacity is generally lower. However the metals that have high affinity to the Fe and /or Al oxides and hydroxides may be retained and accumulated by inner-sphere adsorption on these metal oxides in the sandy soils. In the clay soils both outer-sphere

and inner-sphere adsorption play important role in the retention of the metals in the soil and their migration with the evaporation flux.

The metals migrated to the soil surface could also be adsorbed on the clay particles, by exchange during their migration. They stay at the surface, adsorbed on the clay particles. This indicates that the heavy metals may be windblown with the clay dust particles by adsorption on them.

The heavy metals may migrate upward with the evaporation flux, and precipitate as carbonate, sulfate and chloride salts. These species dissolve and precipitate again by wetting and drying, and migrate upward as they are dissolved and precipitate as the water evaporates. In this case the metals can accumulate at the top soil and the surface of the soil as salts after a period of evaporation.

In this study it became clear that the heavy metals migrate upward differently by evaporation. However, whether they are precipitated or electrostatically adsorbed on the soil particles, determines their migration rate. They cause an important hazard for men, by inhalation of dust particles or by other contact with the soil.

Acknowledgement:

I would like to especially thank the supervisors Dr. Ana Teresa Lima and Dr. J.P. Gustav Loch.

I would like to thank Pieter Kleingeld and Dienne van de Meent for the technical help.

I would like to especially thank M.J.C Tilly Bouten for her effort, to teach me work with the Micro XRF technique, and her supervising by the measurements.

I also would like to thank A.W.E Anita van Leeuwen- Tolboom and Ton Zalm for the XRD and the ICP OES measurements.

This work was supported by the University of Utrecht, department of Earth Sciences, division of Geochemistry.

References:

1. Bradl, H.B, Adsorption of heavy metals ions on soils and soil constituents, *Journal of Colloid and Interface Science*. 2004; 277: 1-18
2. Jalali, M. Khanlari Z. V, effect of ageing process on the fractionation of heavy metals in some calcareous soils of Iran. *Geoderma* 2008; 143; 26- 40
3. Quan –Ying Cai, Ce Hui Mo, concentration and speciation of the heavy metals in six different sewage sludge- composts. *Journal of hazardous materials*. 2007; 148: 1063-1072
4. Rawat, M. Ramanathan, AL. Subramanian, V. Quantification and distribution of heavy metals from small- scale industrial areas of Kanpur city, India. *Journal of Hazardous materials*. 172, 2009; 1145-1149
5. Aydin, M. A model for evaporation and drainage investigations at ground and ordinary rain fed areas. *Ecological modeling*. 2008; 217: 148-156
6. Kuhn, N.J. Bryan, R. B. Drying soil surface condition and interrill erosion on two Ontario soils. *Catena* 5224, 57: 113-133
7. Deming Dong, Liang Liu, Comparison of Lead, Cadmium, copper and Cobalt adsorption onto metal oxides and organic metals in natural surface coatings, *Microchemical Journal* 2007; 85:0270-275
8. Novak, M. D. Dynamics of the near-surface evaporation zone and corresponding effects on the surface energy balance of a drying bare soil. *Agriculture and forest meteorology*. 2010; 150: 1358-1365
9. Cave, K. Talens- Alesson, F.I. Comparative effects of Mn(II) and Fe(III) as activators and inhibitors of the adsorption of other heavy metals on Calcite. *Colloids and surface*. 2005; 268: 19-23
10. Walton, J.C. Effects of evaporation and solute concentration on presence and composition of water in and around the Yucca mountain. *Waste Management*. 1993; 13: 293-301
11. Grifoll, J. Gsto, J.M. Non- isothermal soil water transport and evaporation. *Advanced in water Resources* 2005; 28: 1254- 1266
12. Rabi, A. Usman, A. The relative selectivities of Pb, Cu, Zn, Cd and Cdby soil developed on shale in New Vally, Egypt. *Geoderma*. 2008; 144: 334-343
13. Sheta, A.S. Al- Omran, A. M. Characteristics of natural clay deposits in Saudi Arabia and their potential use for nutrients and water conservation. *J. King Saud University* 2006 vol 19: 25- 38
14. Al-Barrak, S.A. Characteristics of some soils under Date palm in AL-Hassa eastern oasis, Saudi Arabia. *J. King Saud University* 1990 vol 2: 115-130
15. Meunier, A. *Clays* 2005. Publisher: Springer ISBN: 3-540-21667-7
16. Rikers, R. Characterization of heavy metals in soils, using magnetic separation 1999, Proefschrift technische universiteit Delft. Publisher: [S.I]: [S.N]. ISBN: 90-6464-809-3
17. Spósito, G. *The Chemistry of Soils* 2nd edition 2008 ISBN:978-0-19-531369-7
18. Ponizovsky, A.A Thakali, S. Nickel partitioning in acid soils at low moisture content. *Geoderma* 2008; 145: 69-75

19. . Elrick, D.E. Mermout, A. An analysis of solute accumulation during steady states evaporation in an initially contaminated soil. *Journal of hydrology*, 1994; 155: 27- 38
20. Handbook on the toxicology of metals, 2007
21. Saudi Arabia's National Industrial Cluster Development Program (internet site: www.saudiclusters.com/faq.html)
22. Zhang, S.Q. Hou, W.G. Adsorption behavior of the Pb(II) on montmorillonite. *Colloids and surfaces*, 2008; 320: 92-97.
23. Lafuente, A. L Gonzalez, C. Mobility of heavy metals in poorly developed carbonate soils in the Mediterranean region. *Geoderma* 2008, 145; 238-244
24. Gomes, P. C. P. F. Fontes Mauricio, Selectivity sequence and competitive adsorption of heavy metals by Brazilian soils. *Soil SCI. SOC. AM. J* 2001, 65
25. Werkvoorschrift, Geowetenschappen, TNO-NITG geïntegreerd laboratorium
26. Reeuwijk, L.P van, Procedures for soil analysis. sixth edition 2002. Publisher: ISRIC (International Soil Reference and Information Center) ISBN: 90-6672-044-1
27. Dohrmann, R. Cation exchange capacity methodology III: correct exchangeable calcium determination of calcareous clay using new silver- thiourea method. *Applied clay science* 2006, 34; 47-57
28. Speight, S.G. Lange's Handbook of chemistry 16th edition 2005, Publisher: McGraw-Hill ISBN: 0-070143220-5
29. Lide, D.R. Handbook of physics and chemistry 71th edition 1990-1991, publisher: CRC press ISBN: 0-8493-0471-7
30. Konrad B. Krauskopf, Introduction to geochemistry, third addition, 1995. Publisher: New York [etc]: McGraw- Hill ISBN: 0-07-035820-6

Appendix A: pictures of the samples after evaporation

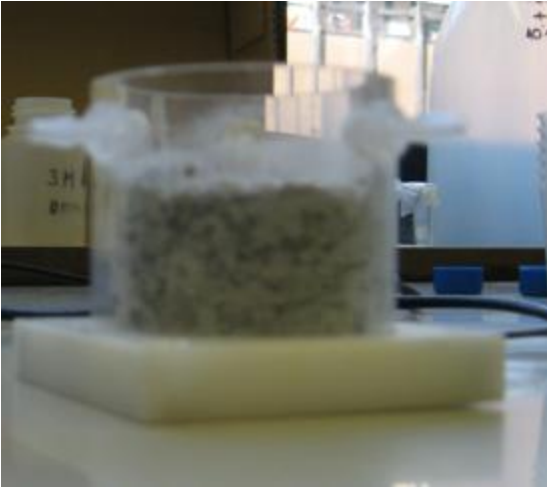
3 weeks evaporation sand sample



3 weeks evaporation clay sample



3 weeks evaporation clay sample (shrinkage)



5 weeks evaporation clay sample



5 weeks evaporation sand sample



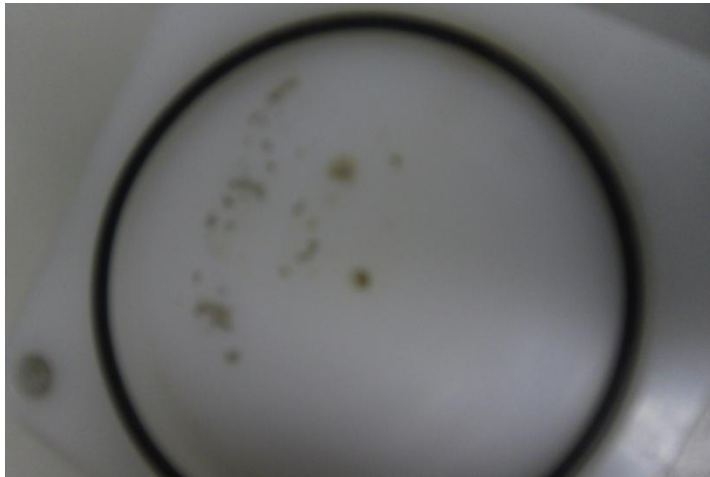
7 weeks evaporation
Sand sample



clay sample

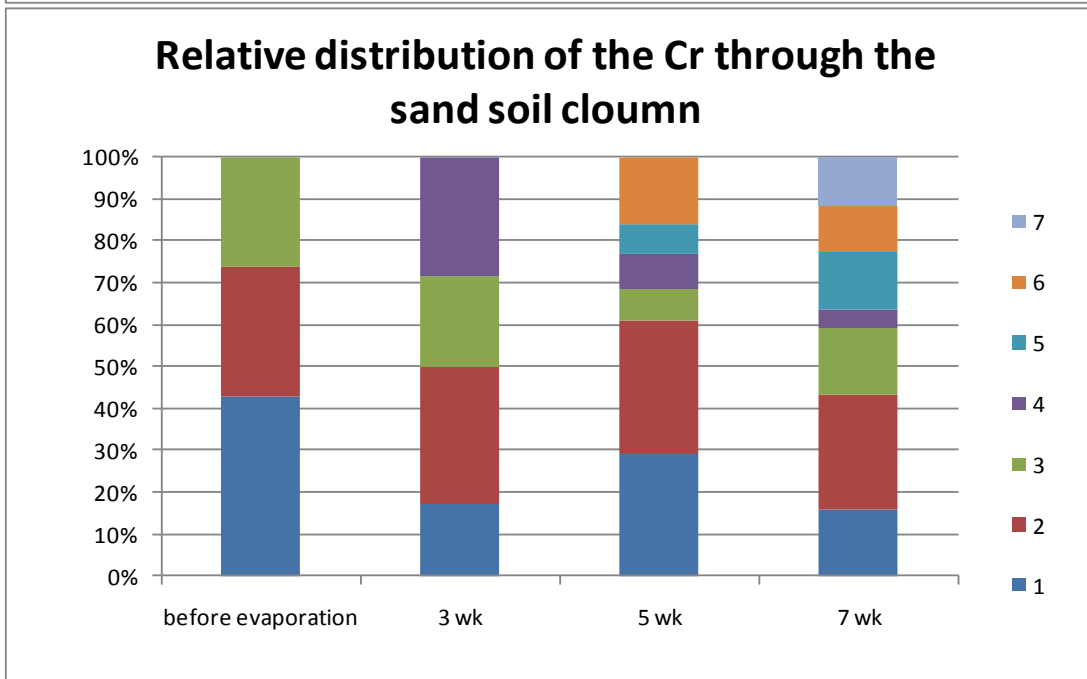
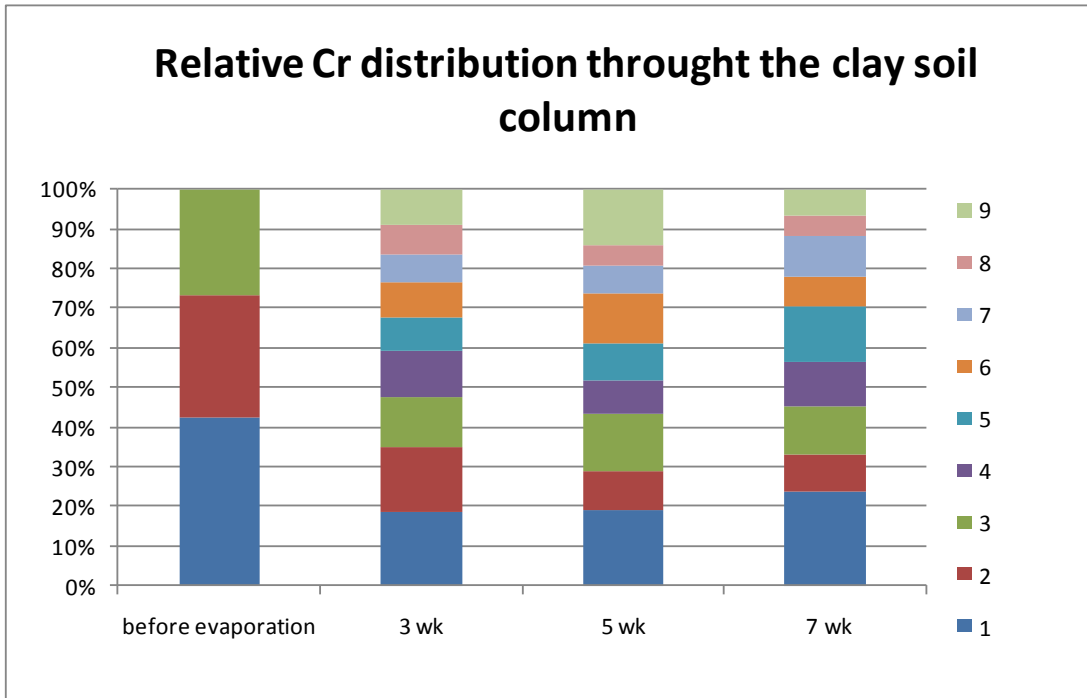


Clay dust particles after seven weeks evaporation

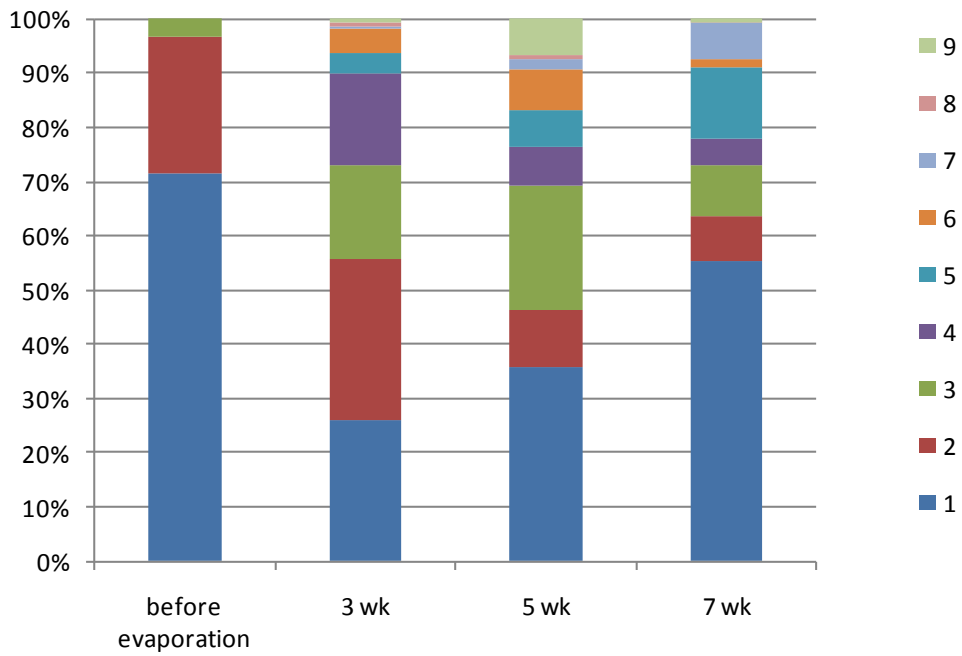


***Appendix B: graph of relative distribution of the heavy metals
through the soil columns***

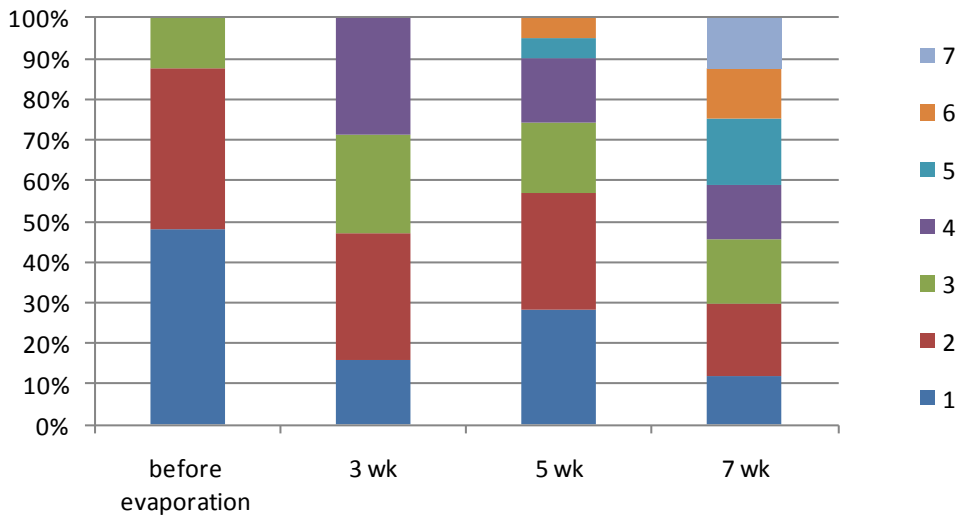
1 is the bottom and #7 and #9 are surface



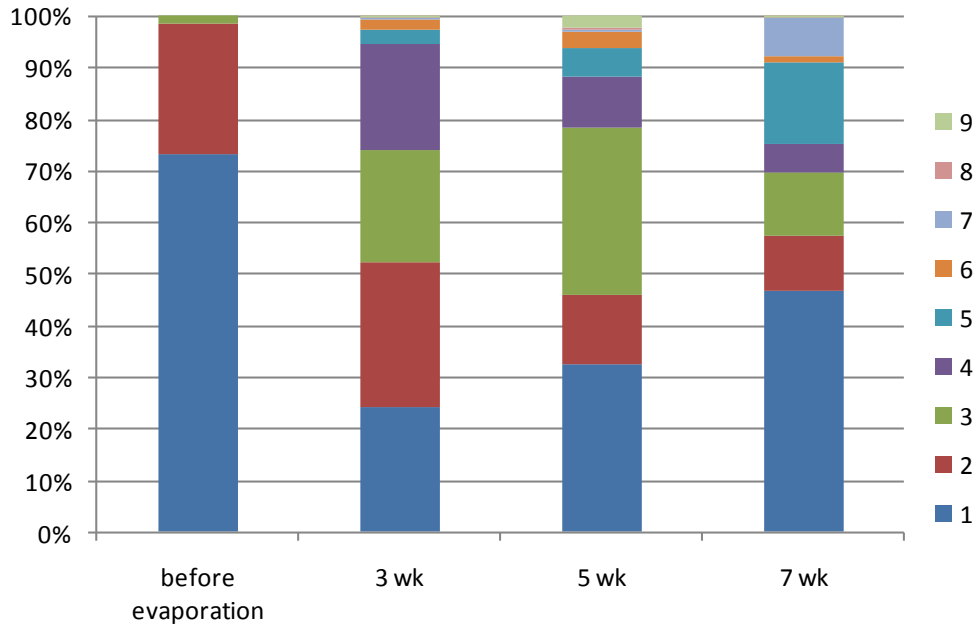
Relative Cu distribution through the clay soil column



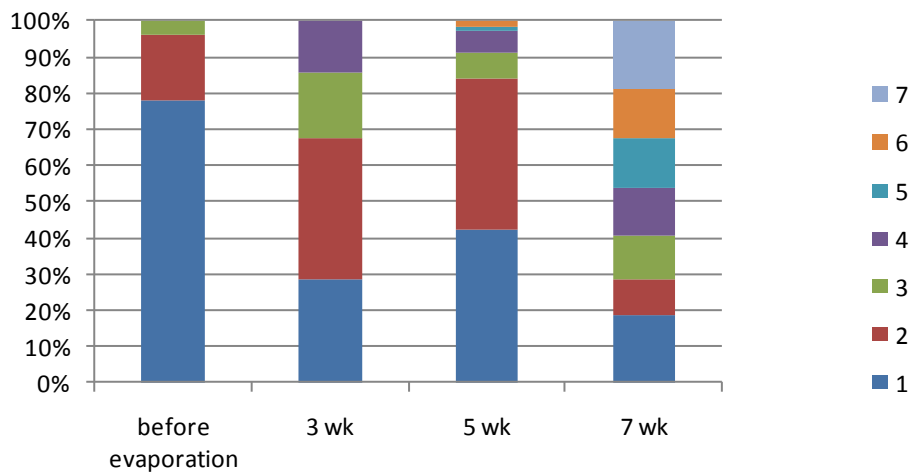
Relative distribution of the Cu through the sand soil column



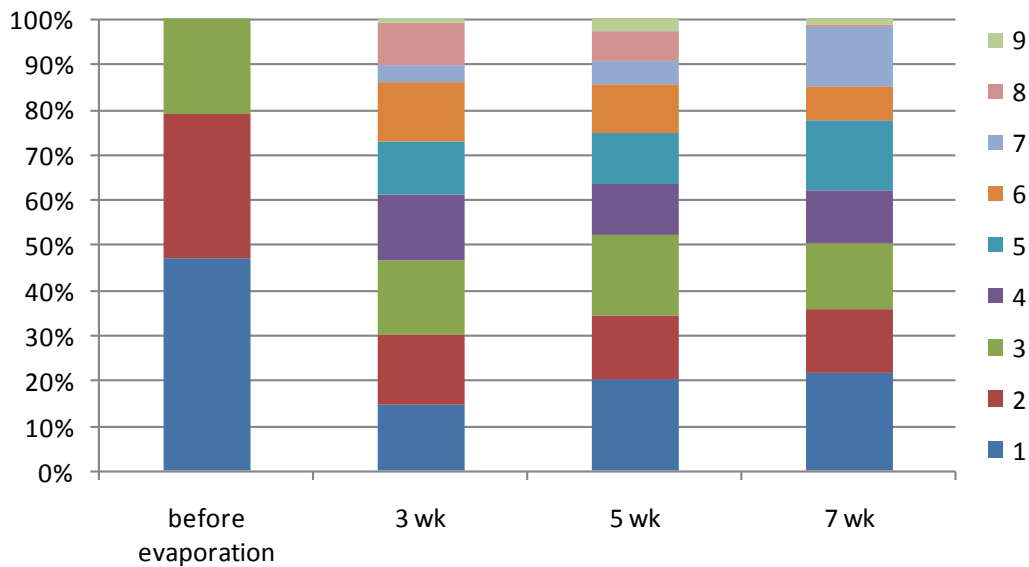
Relative Pb distribution through the clay soil column



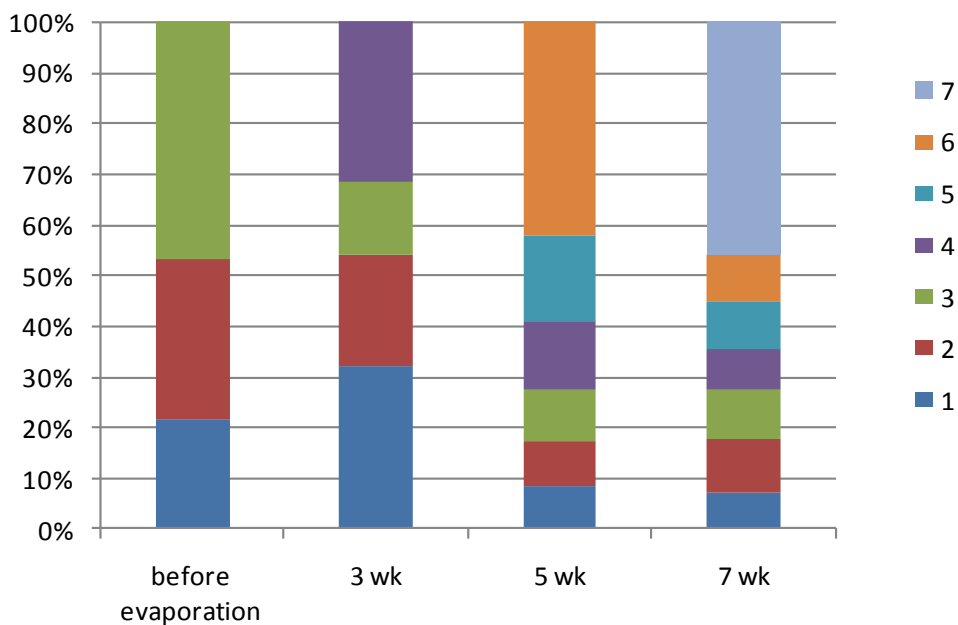
Relative Pb distribution through the sand soil column



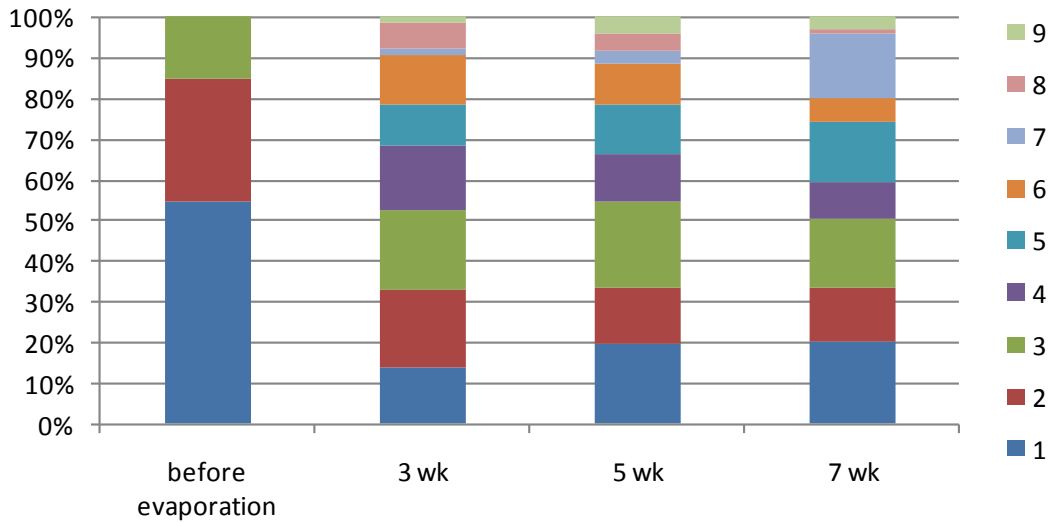
Relative Zn distribution through the clay soil column



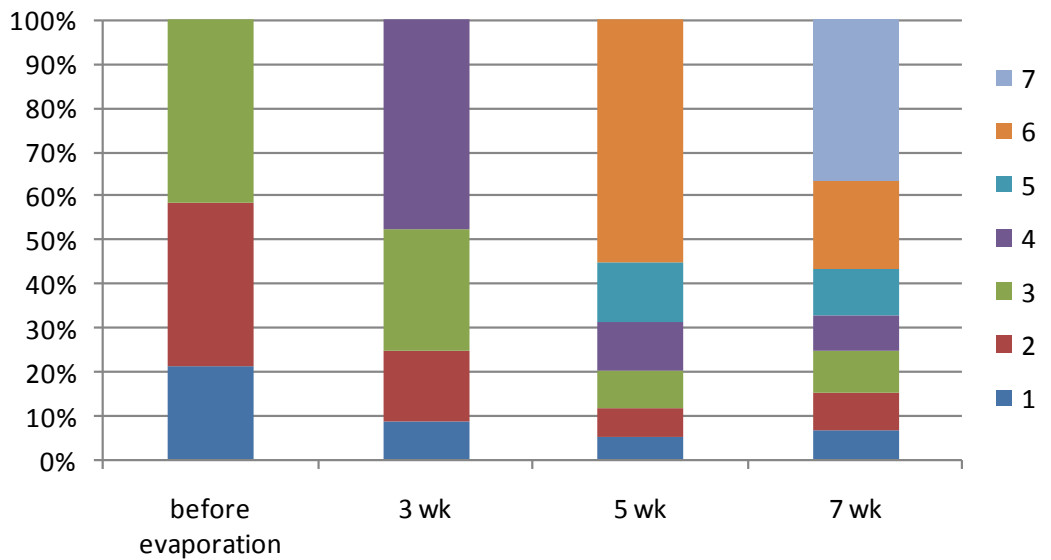
Relative Zn distribution through the sand soil column



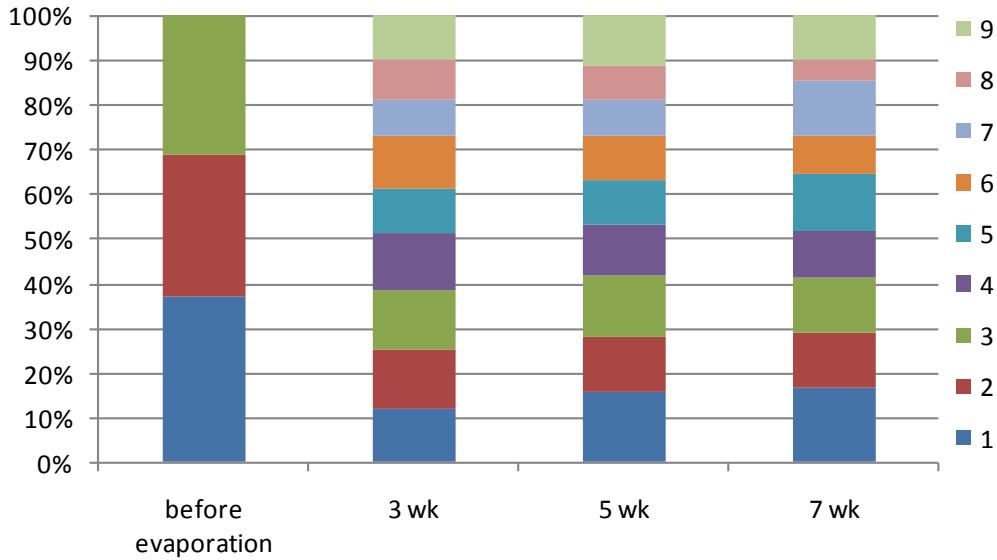
Relative distribution of Cd through the caly soil column



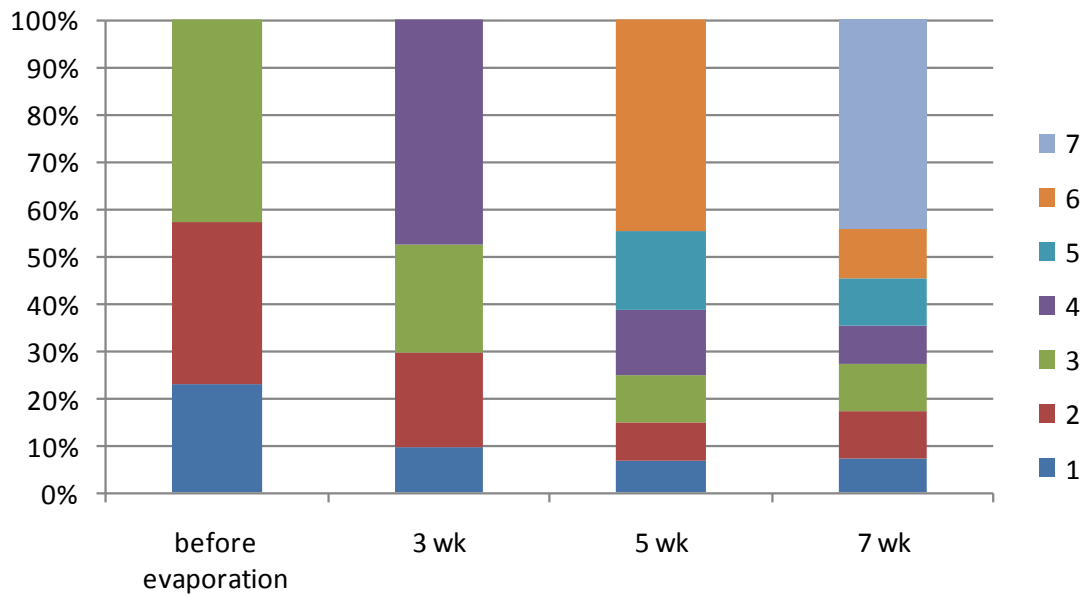
Relative Cd distribution through the sand soil column



Relative Ni distribution through the clay soil column



Relative Ni distribution through the sand soil column

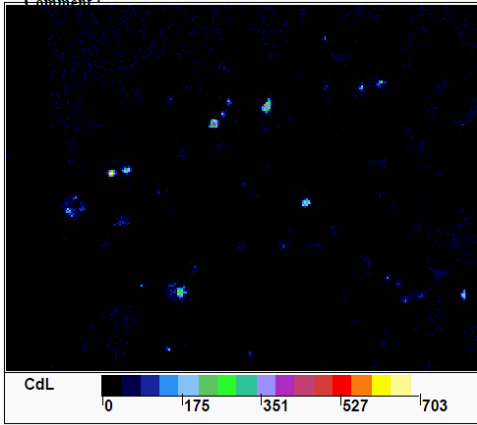


Appendix C-1 : Micro XRF data of the sand

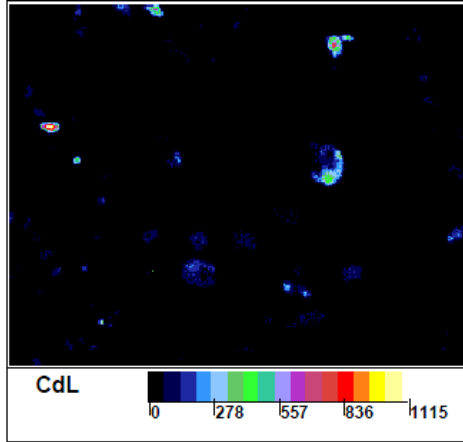
Micro XRF data sand samples Cd:

3 weeks

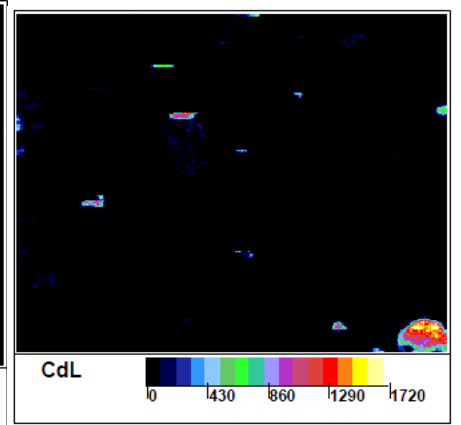
Surface



middle

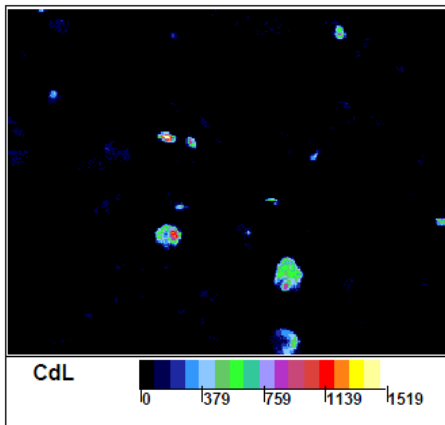


bottom

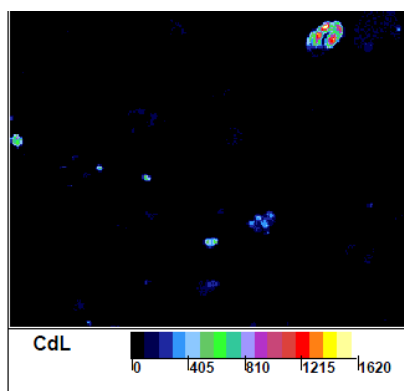


5 weeks

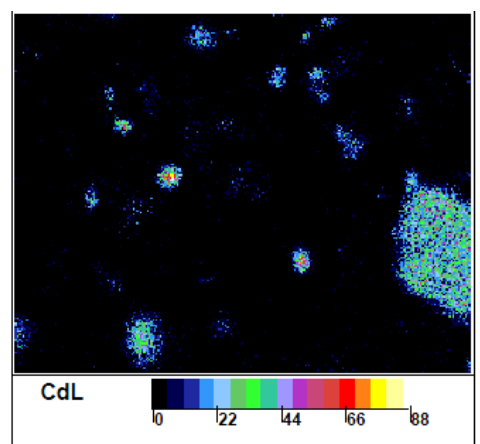
Surface



middle

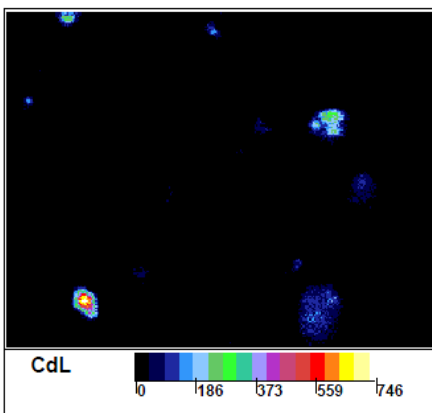


bottom

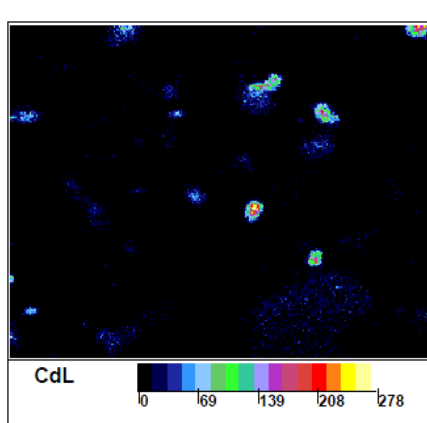


7 weeks

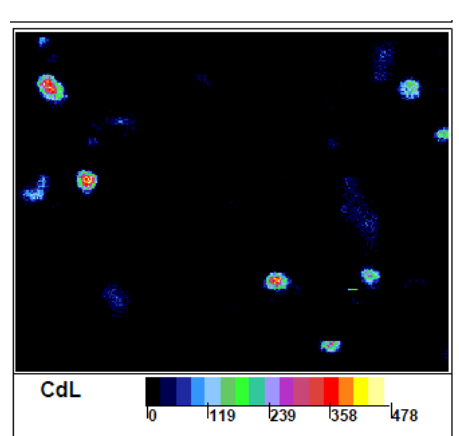
Surface



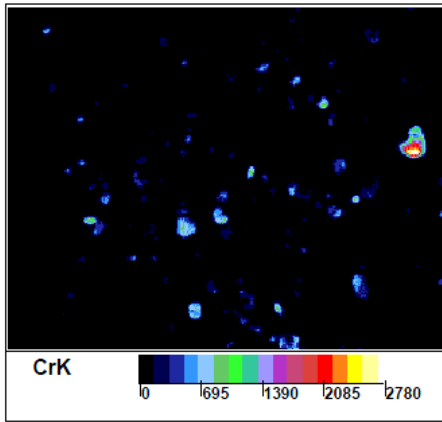
middle



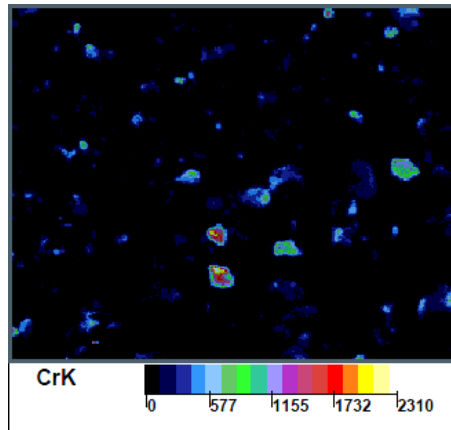
bottom



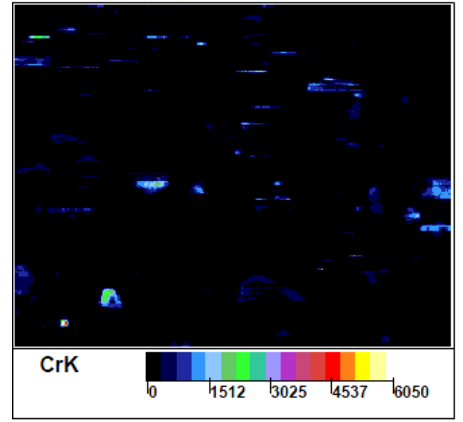
Micro XRF data sand samples Cr
3 weeks
Surface



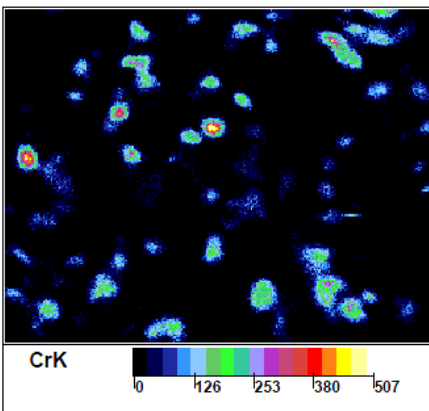
middle



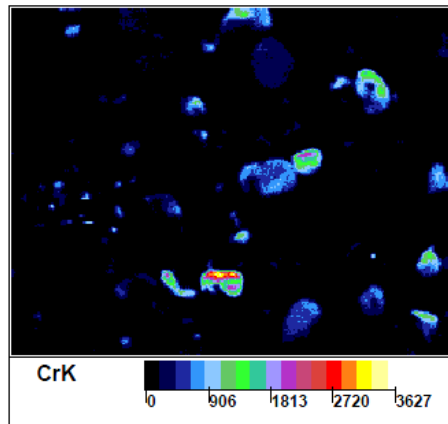
bottom



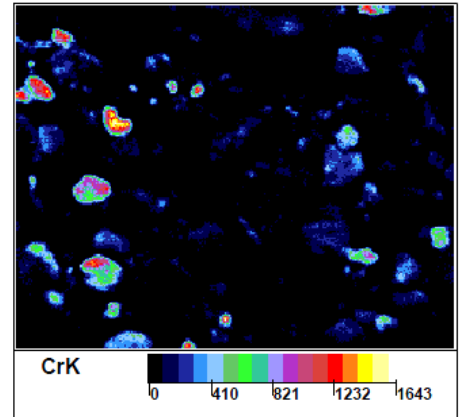
5 weeks
Surface



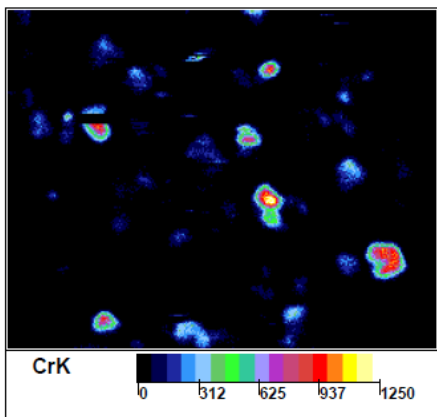
middle



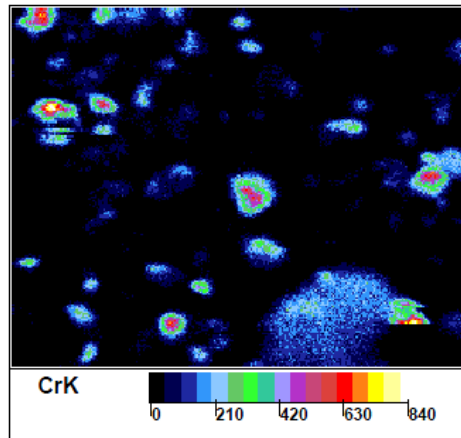
bottom



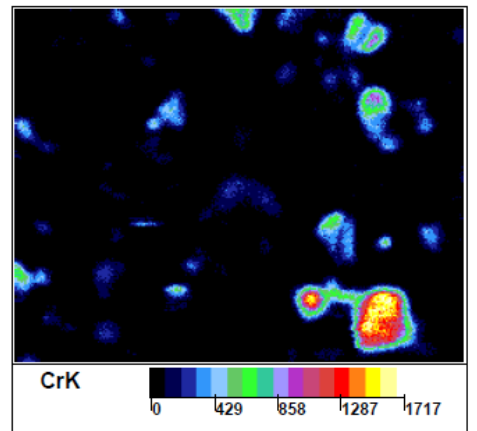
7 weeks
Surface



middle



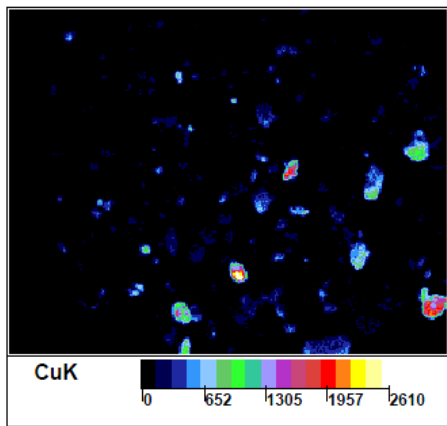
bottom



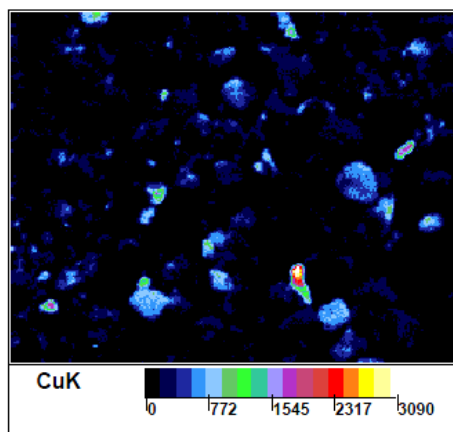
Micro XRF data sand samples Cu:

3 weeks

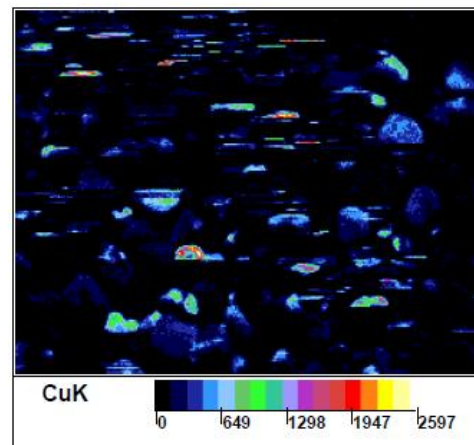
Surface



middle

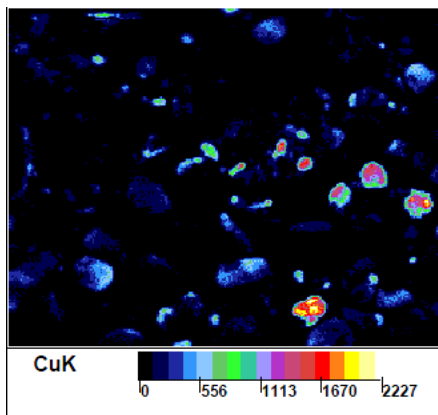


bottom

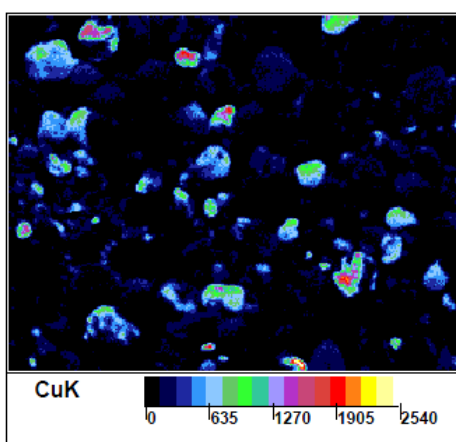


5 weeks

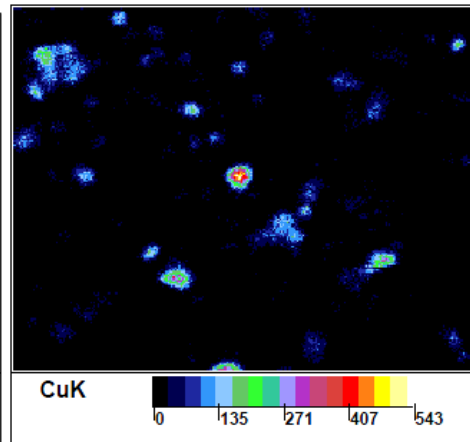
Surface



middle

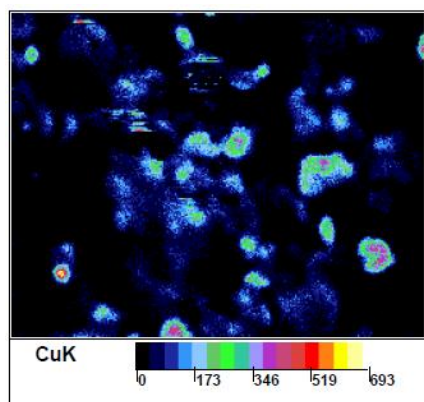


bottom

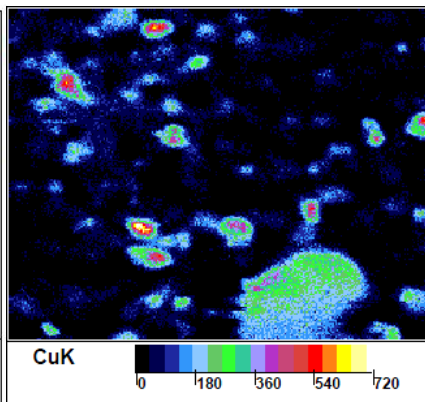


7 weeks

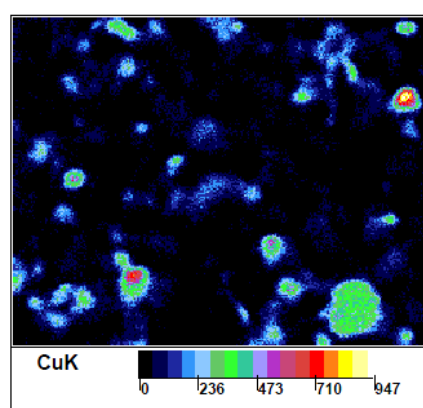
Surface



middle



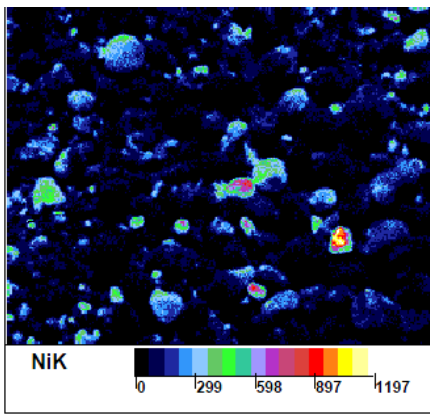
bottom



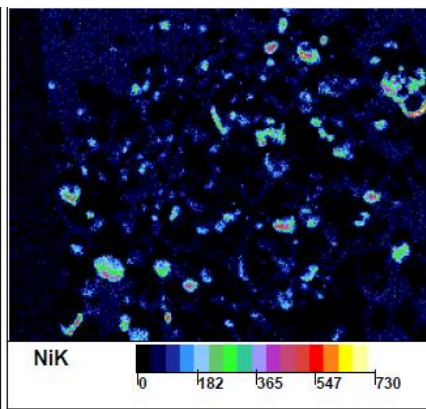
Micro XRF data sand samples Ni:

3 weeks

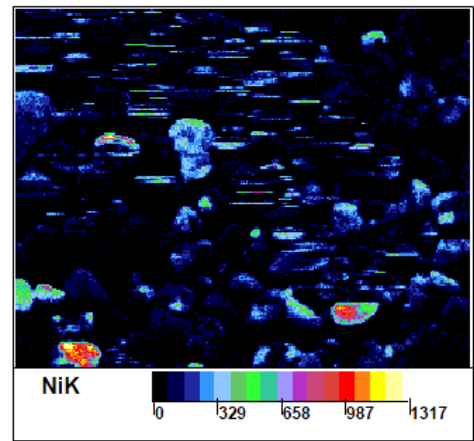
Surface



middle

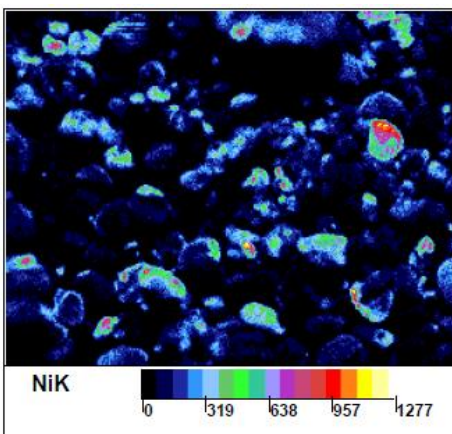


bottom

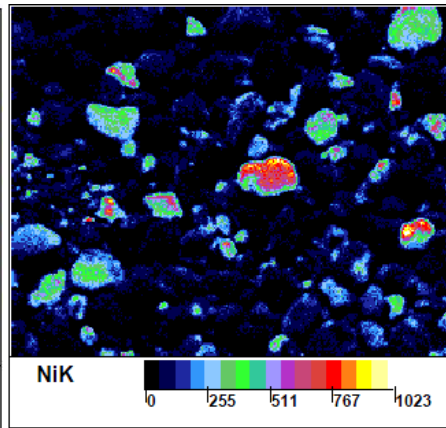


5 weeks

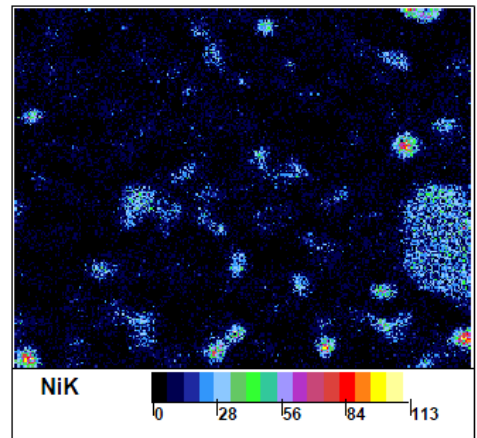
Surface



middle

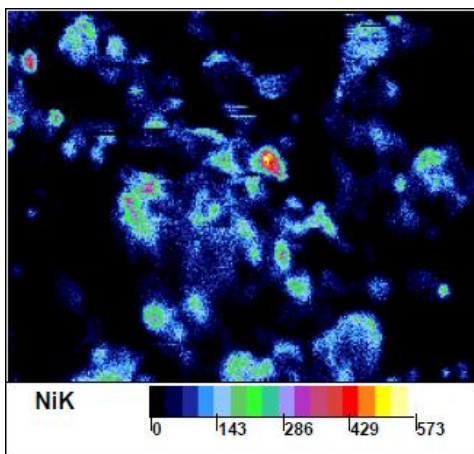


bottom

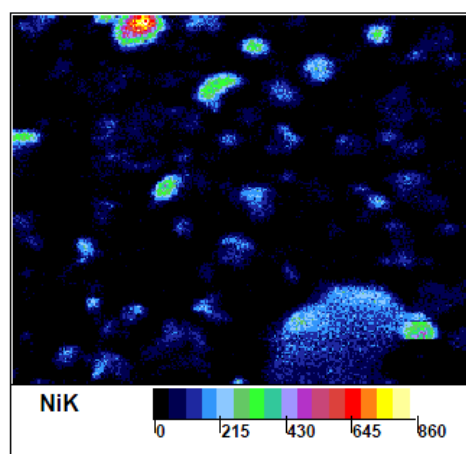


7 weeks

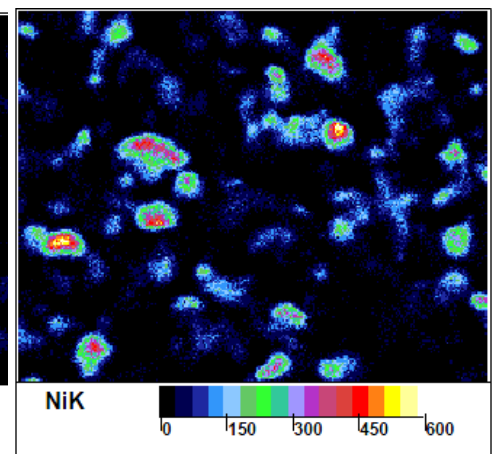
Surface



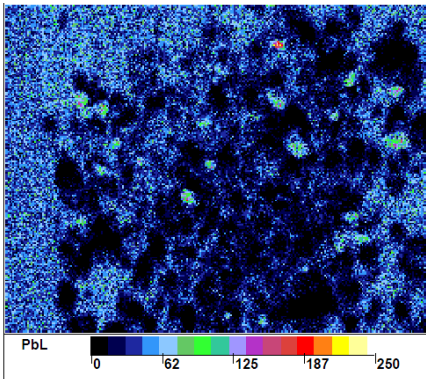
middle



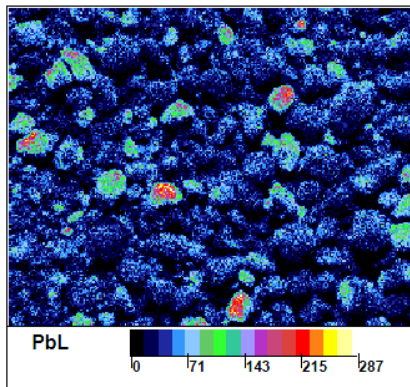
bottom



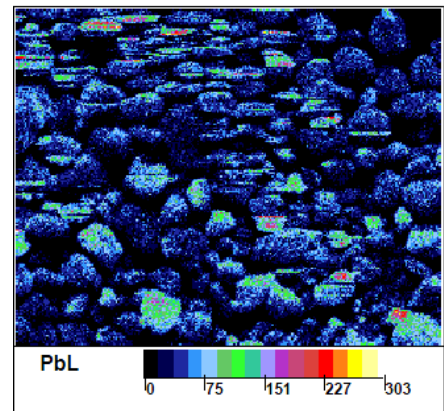
Micro XRF sand sample Pb:
3 weeks
Surface



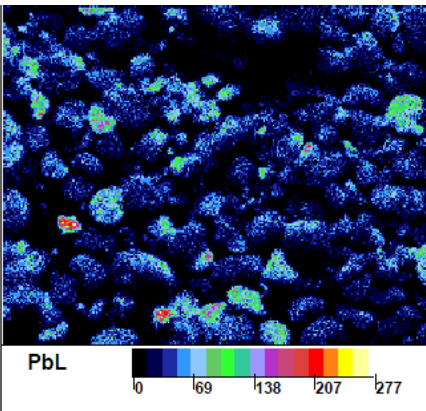
middle



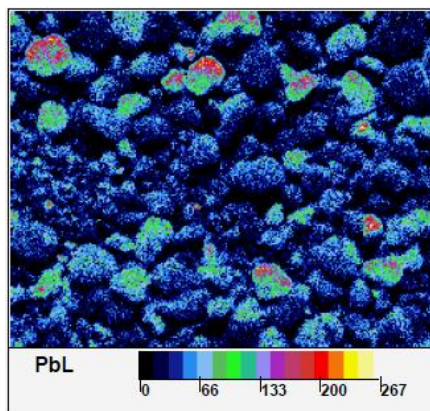
bottom



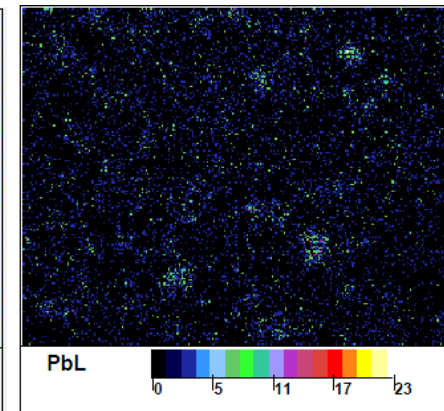
5 weeks
Surface



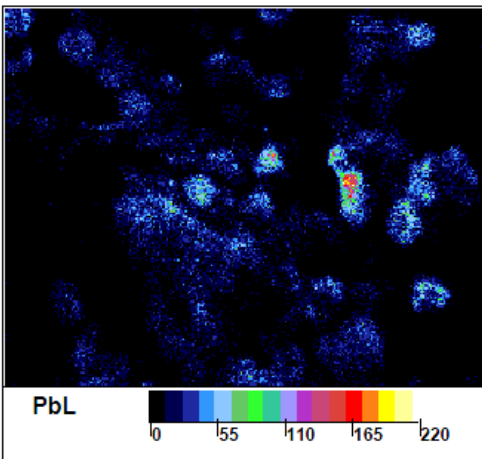
middle



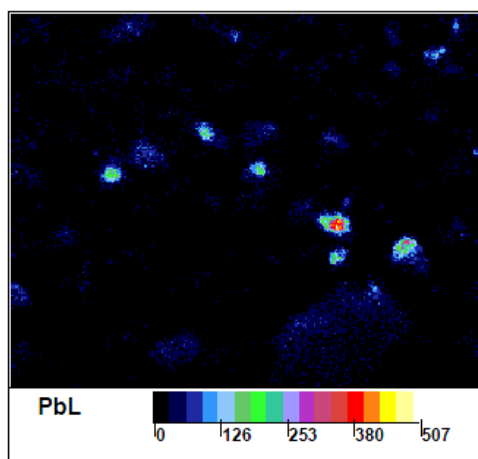
bottom



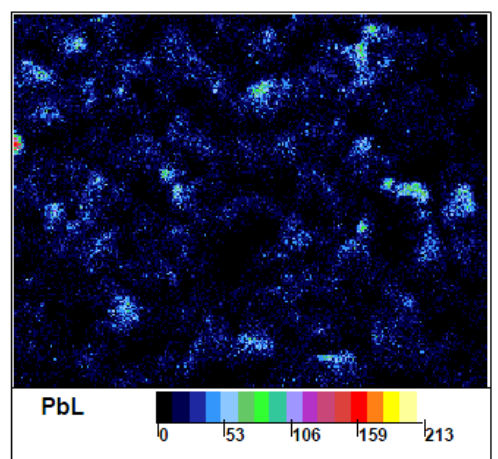
7 weeks
Surface



middle



bottom



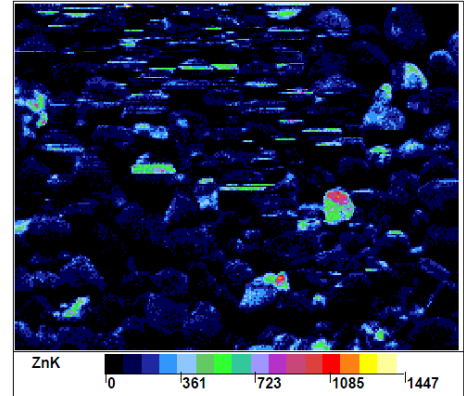
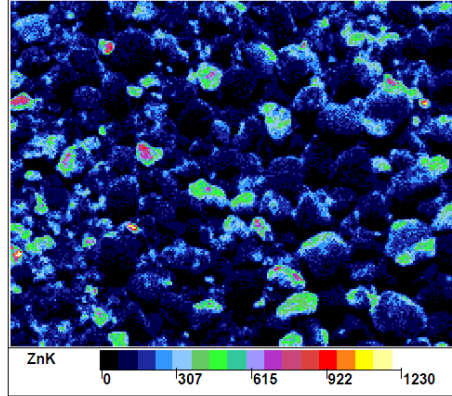
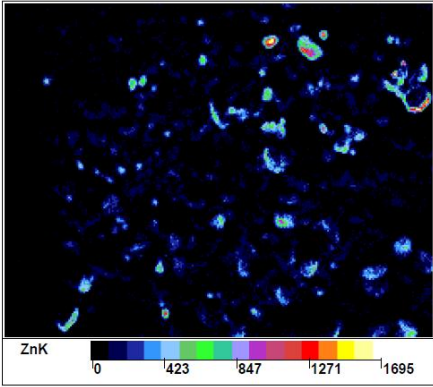
Micro XRF data sand samples Zn:

3 weeks

Surface

middle

bottom

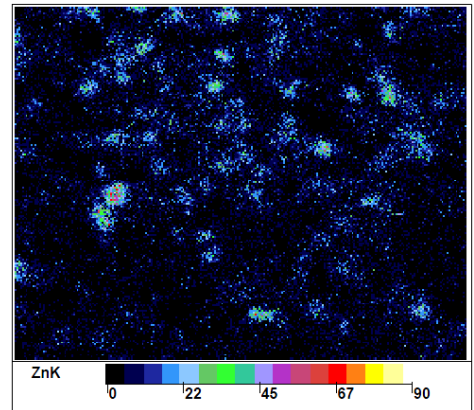
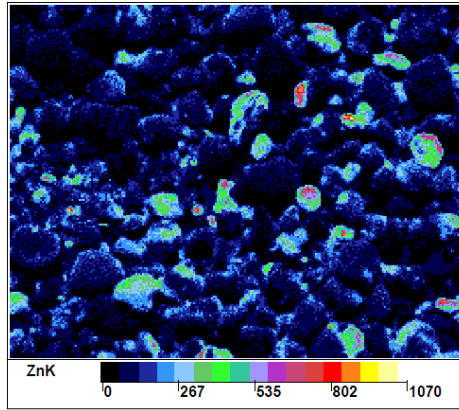
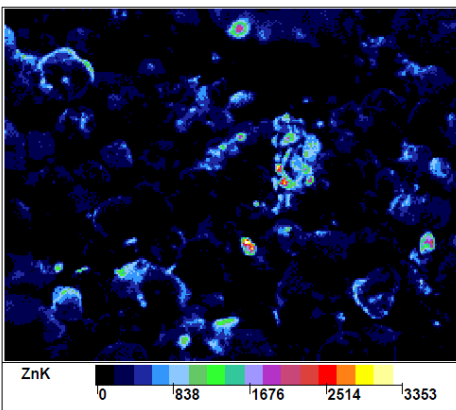


5 weeks

Surface

middle

bottom

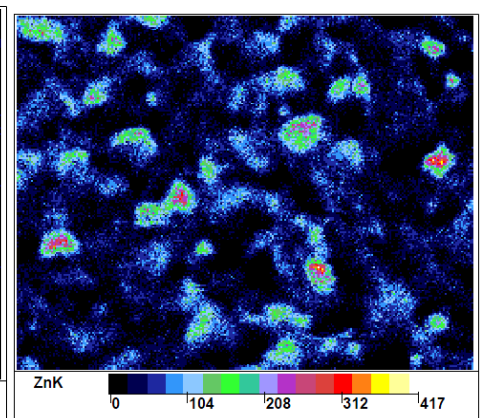
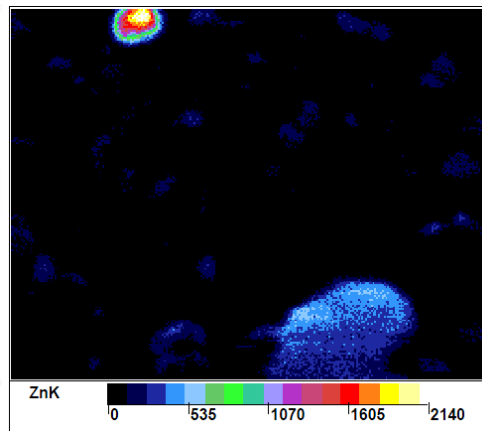
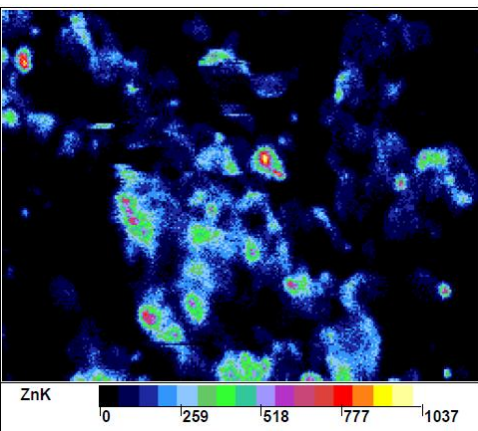


7 weeks

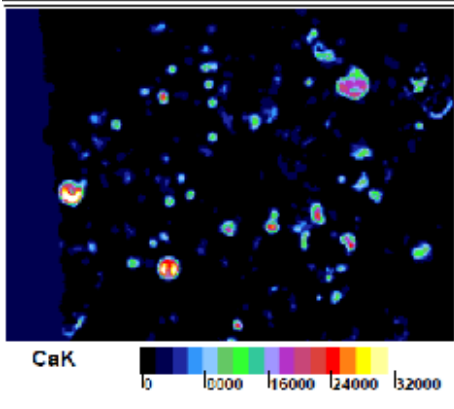
Surface

middle

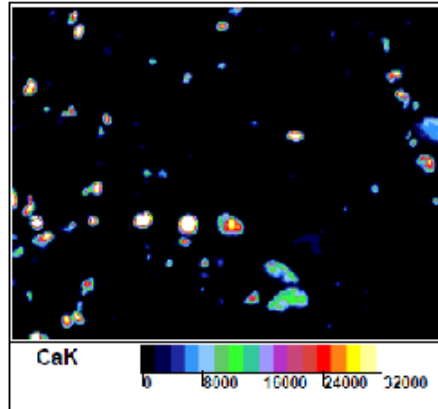
bottom



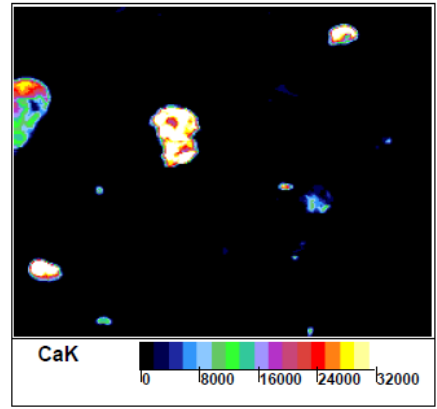
Micro XRF data sand samples Ca:
3 weeks
surface



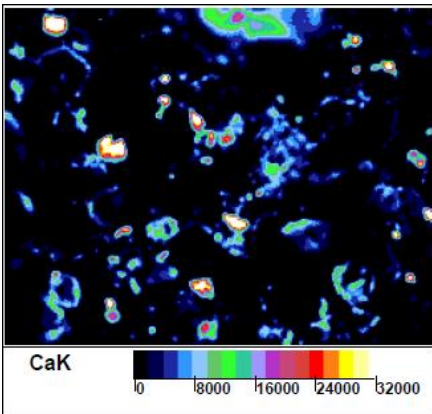
middle



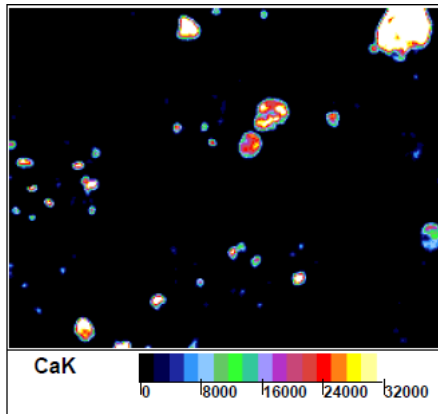
bottom



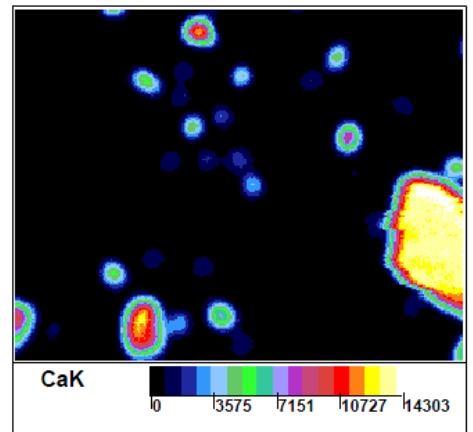
5 weeks
surface



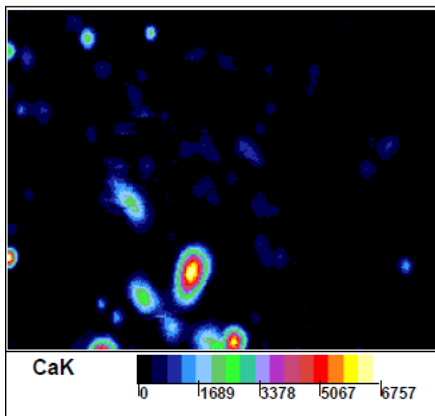
middle



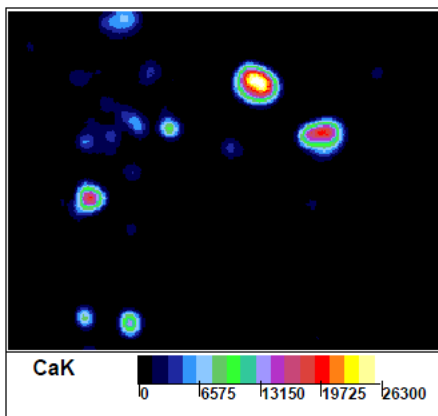
bottom



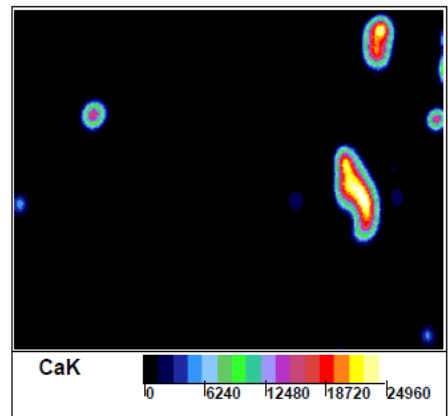
7 weeks
Surface



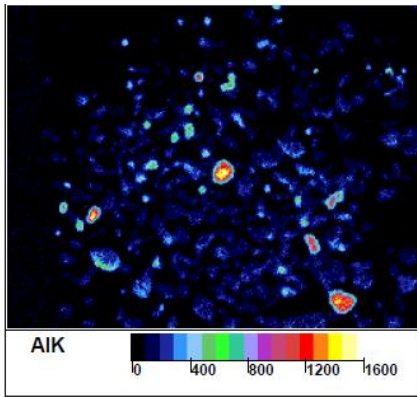
middle



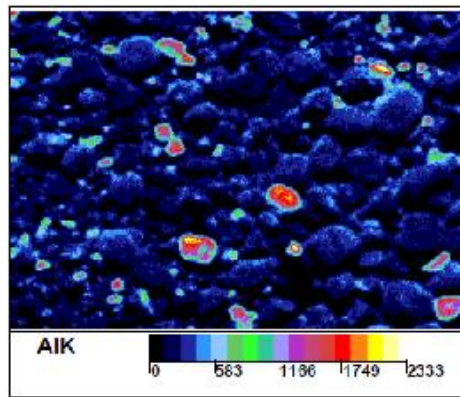
bottom



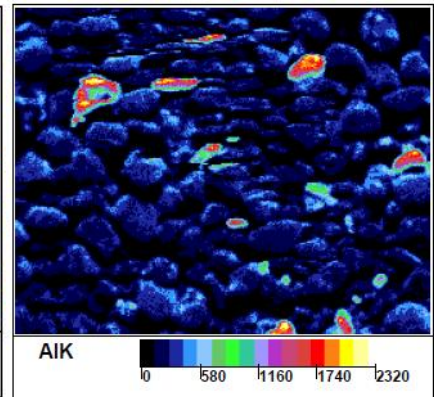
Micro XRF data sand samples A1:
3 weeks
surface



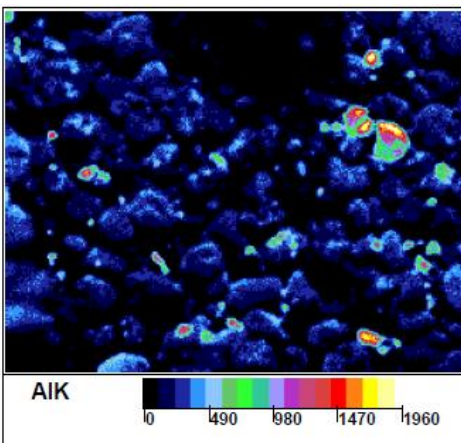
middle



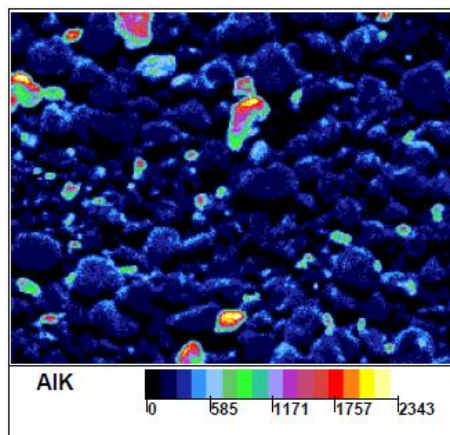
bottom



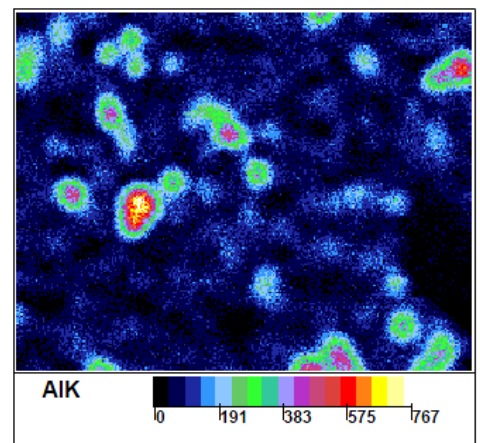
5 weeks
surface



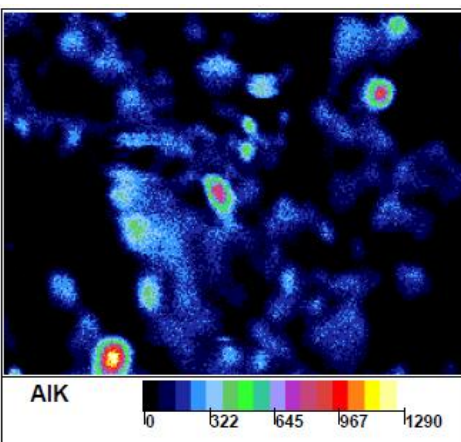
middle



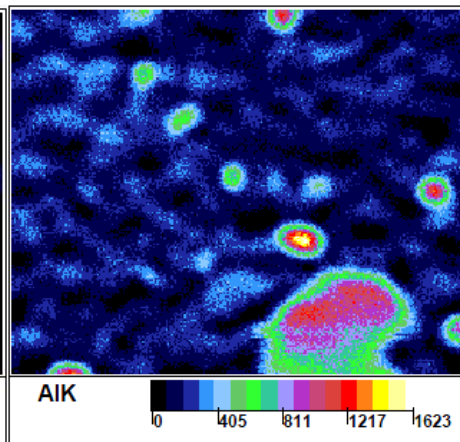
bottom



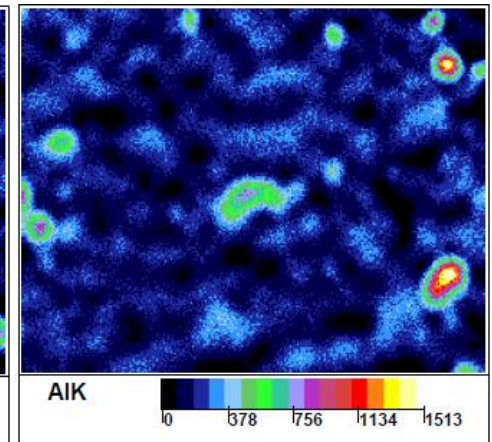
7 weeks
surface



middle



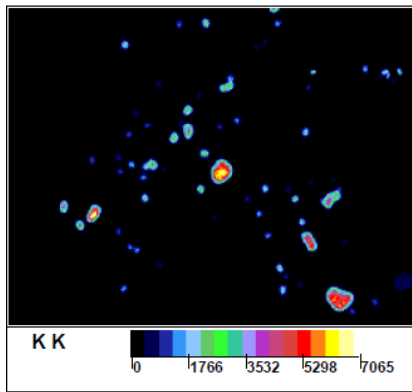
bottom



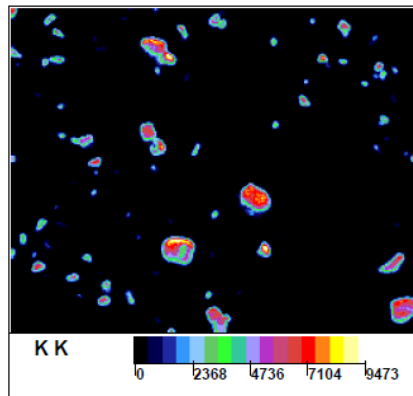
Micro XRF data sand samples K

3 weeks

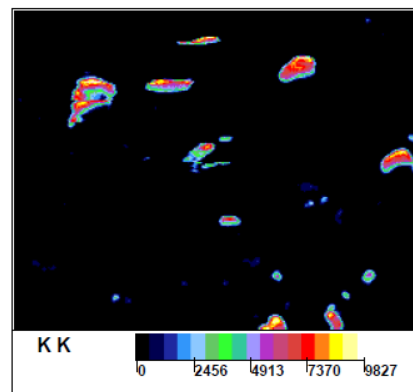
surface



middle

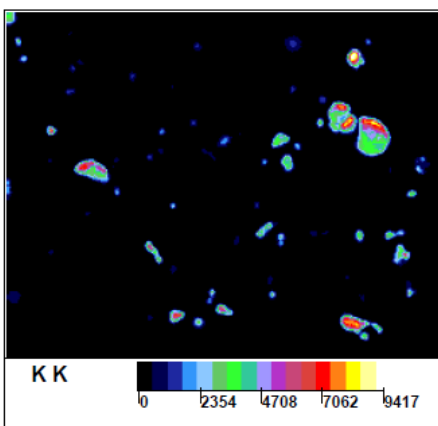


bottom

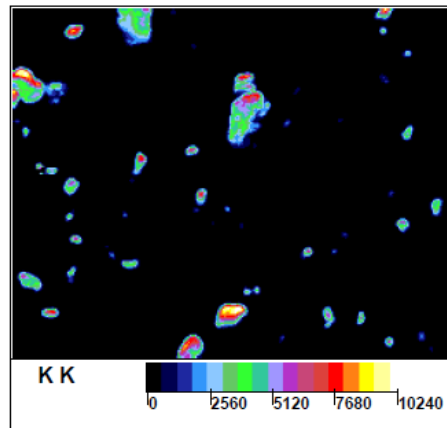


5 weeks

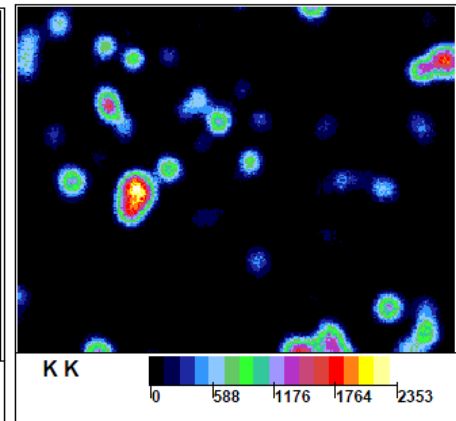
surface



middle

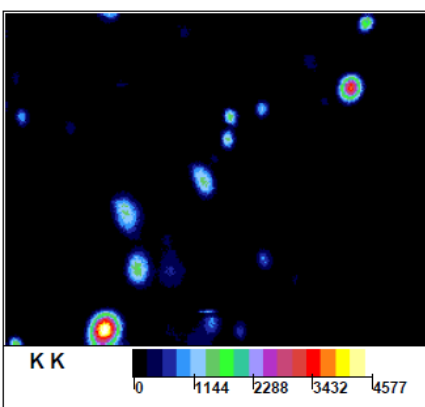


bottom

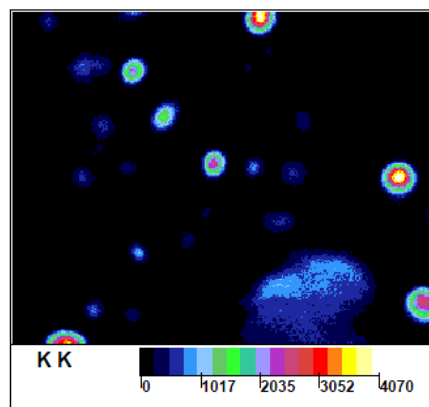


7 weeks

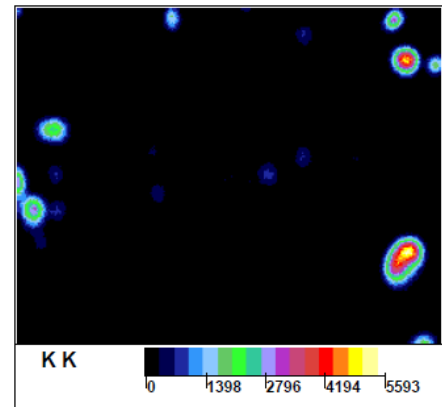
surface



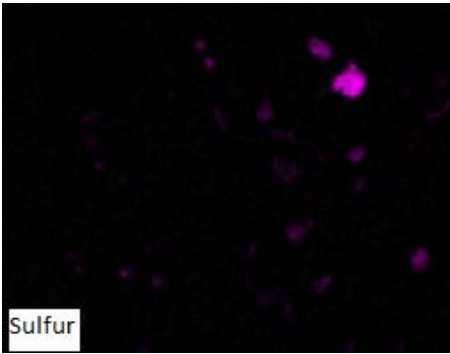
middle



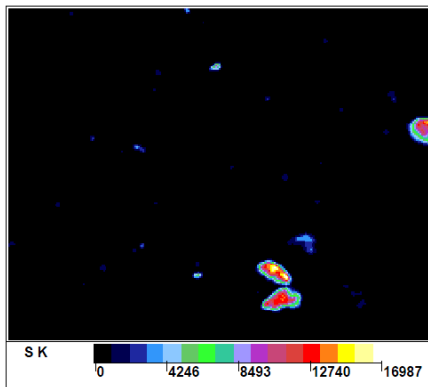
bottom



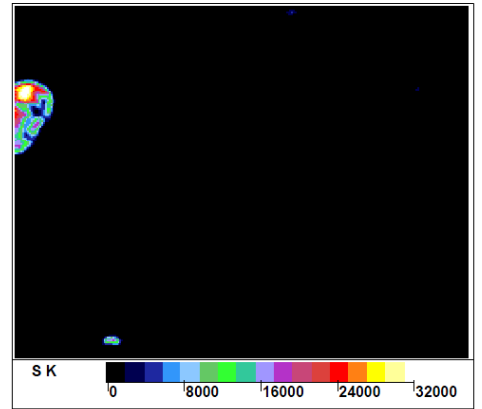
Micro XRF data sand samples S:
3 weeks
surface



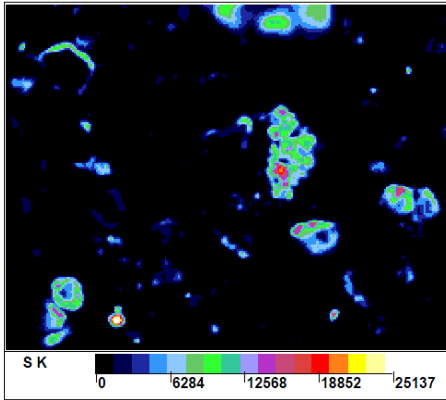
middle



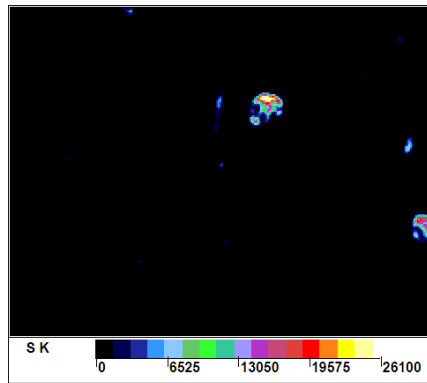
bottom



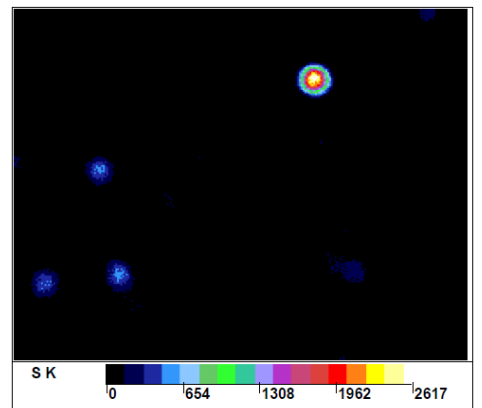
5 weeks
surface



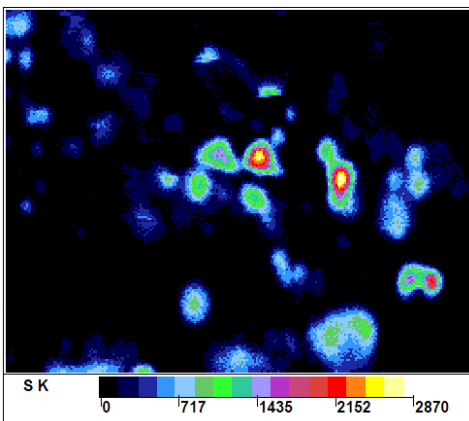
middle



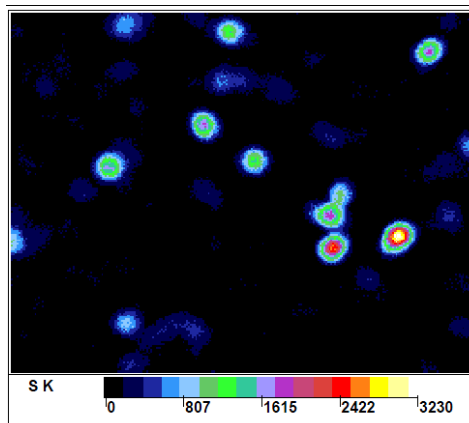
bottom



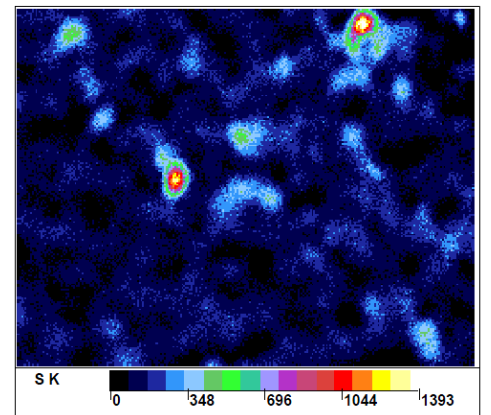
7 weeks
surface



middle



bottom



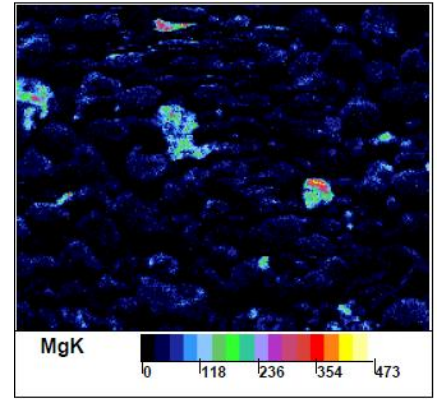
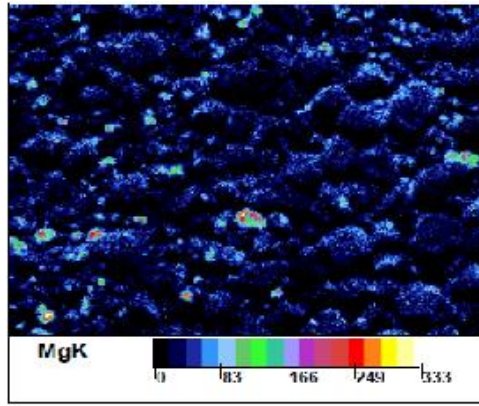
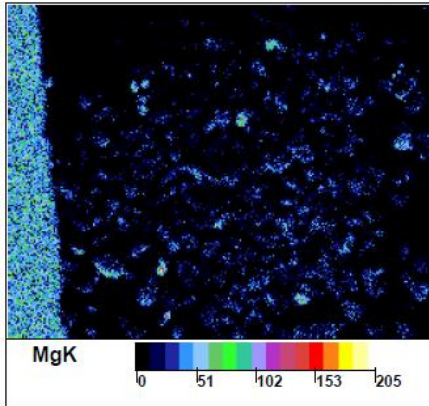
Micro XRF data sand samples Mg:

3 weeks

surface

middle

bottom

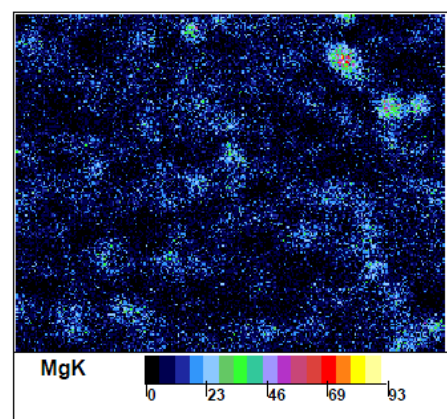
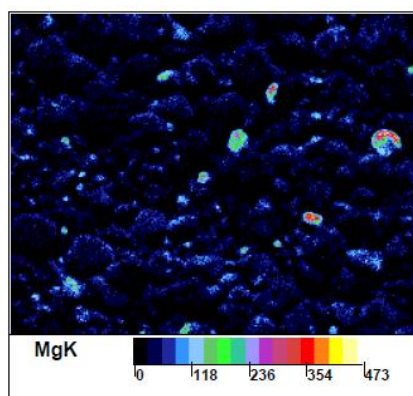
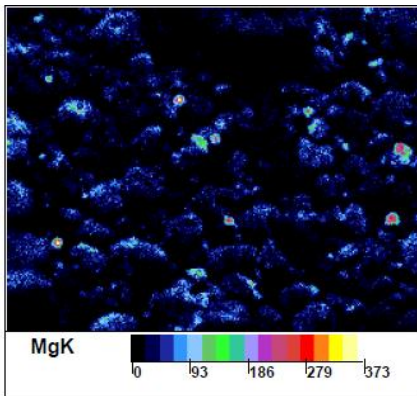


5 weeks

surface

middle

bottom

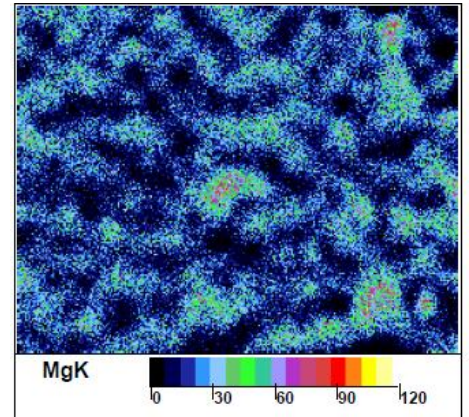
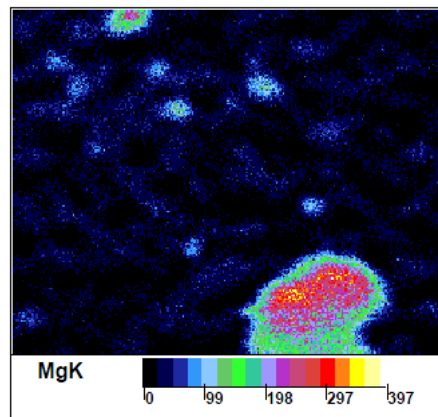
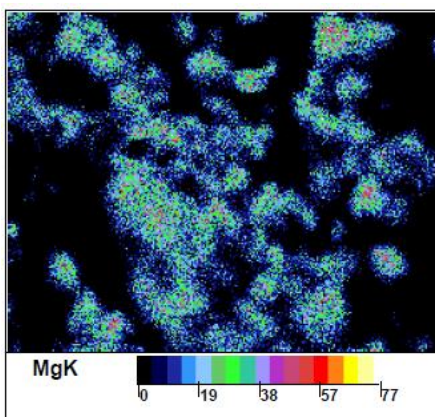


7 weeks

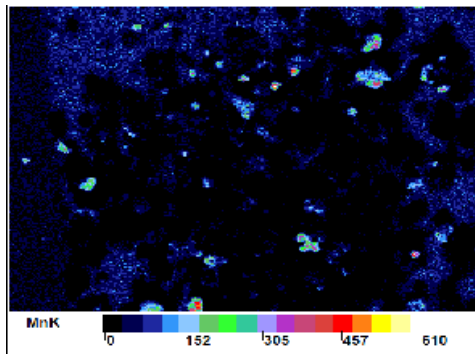
surface

middle

bottom

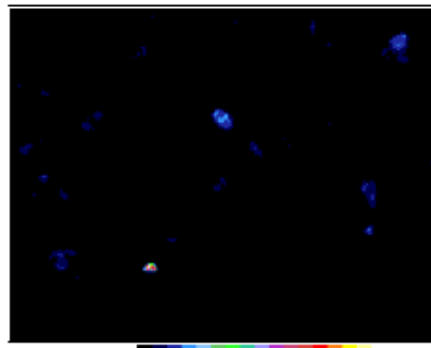


Micro XRF data sand samples Mn:
3 weeks
surface

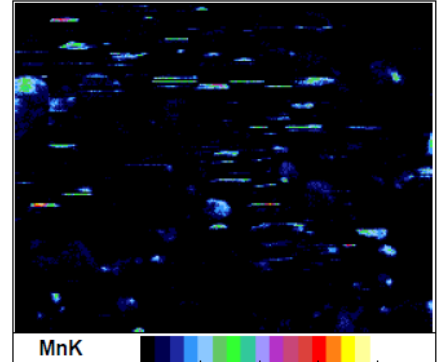


bottom

middle

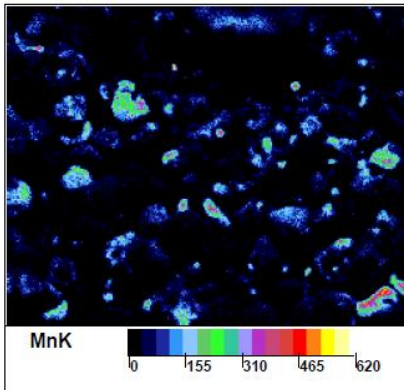


MnK 0 1130 2261 3392 4523

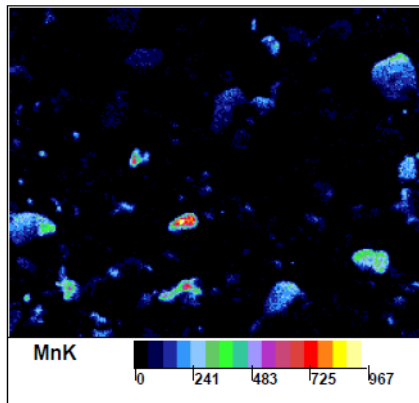


MnK 0 288 576 864 1153

5 weeks
surface

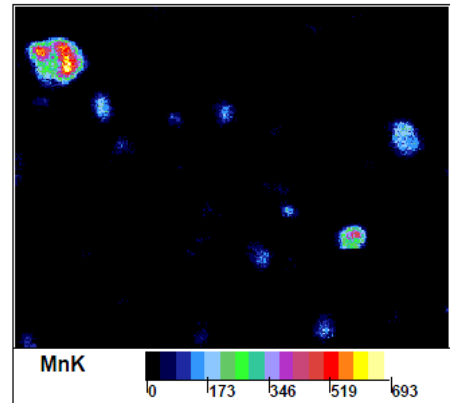


middle



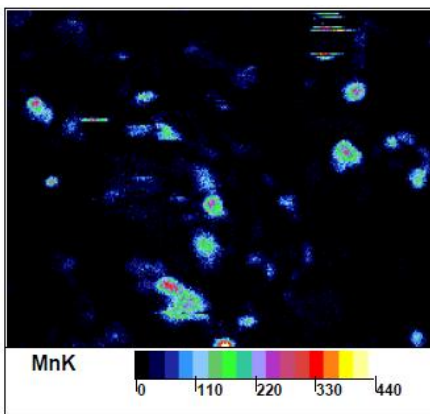
MnK 0 241 483 725 967

bottom

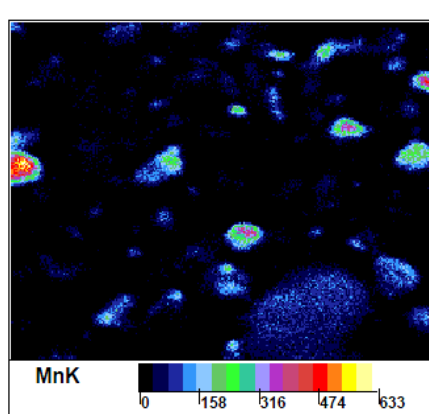


MnK 0 173 346 519 693

7 weeks
surface

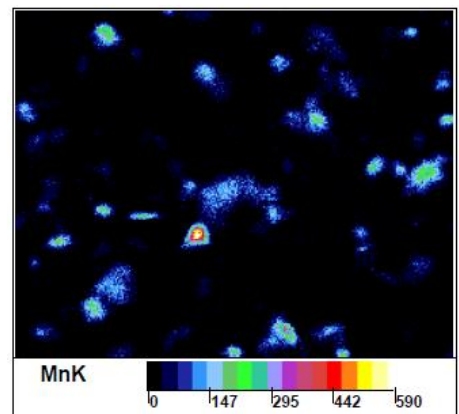


middle



MnK 0 158 316 474 633

bottom

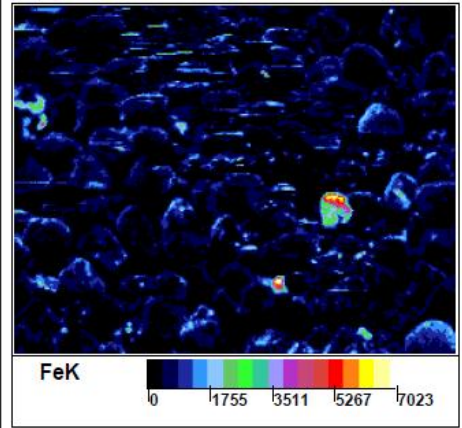
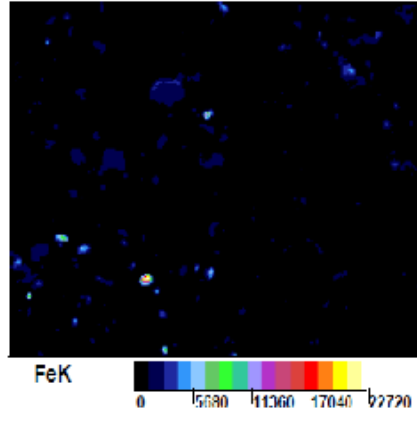
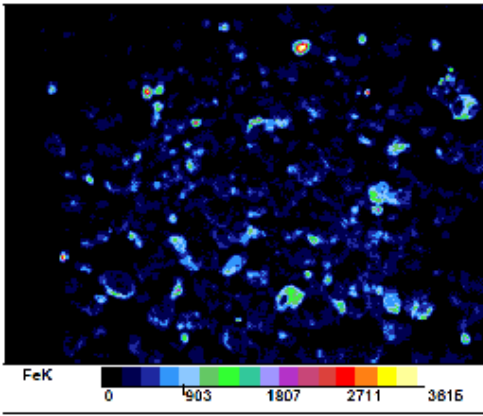


MnK 0 147 295 442 590

Micro XRF data sand samples Fe:
3 weeks
surface

middle

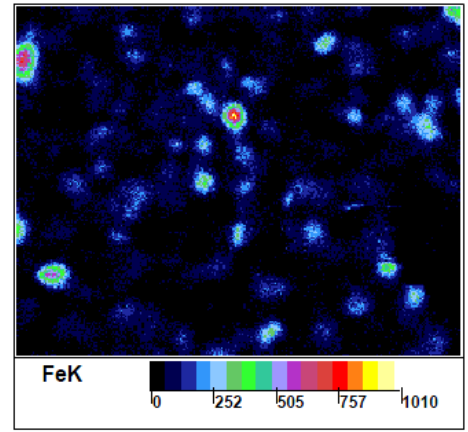
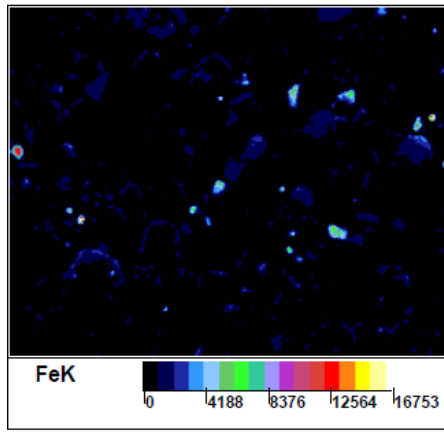
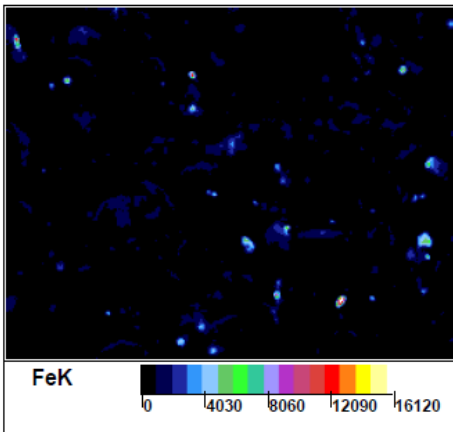
bottom



5 weeks
surface

middle

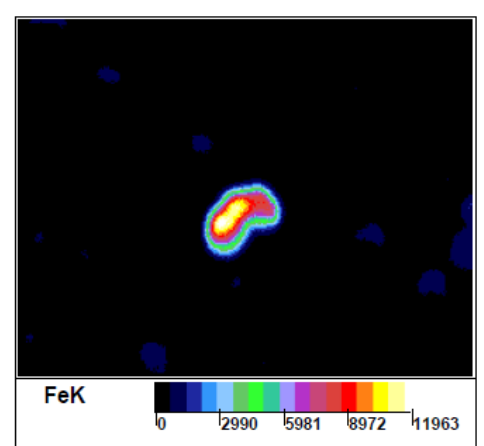
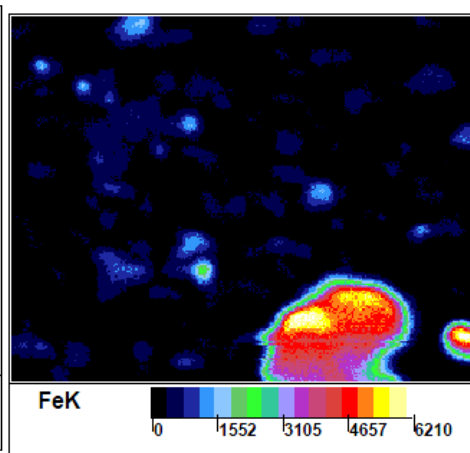
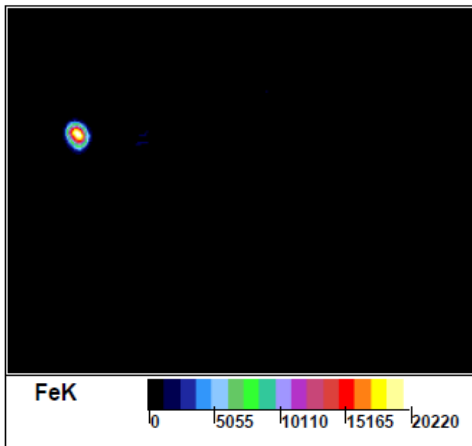
bottom



7 weeks
surface

middle

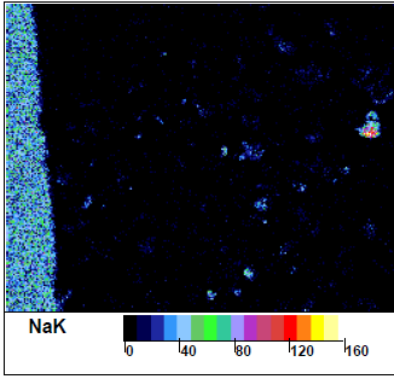
bottom



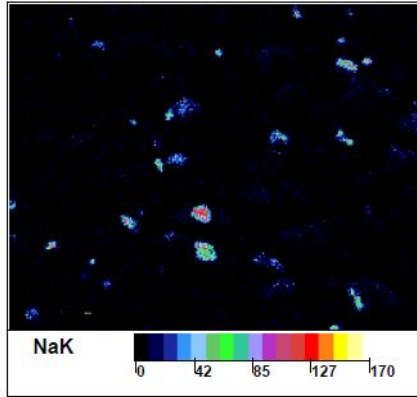
Micro XRF data sand samples Na:

3 weeks

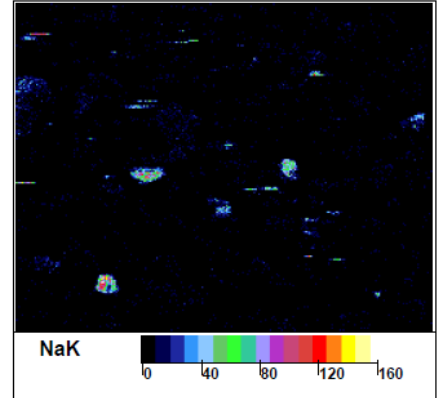
surface



middle

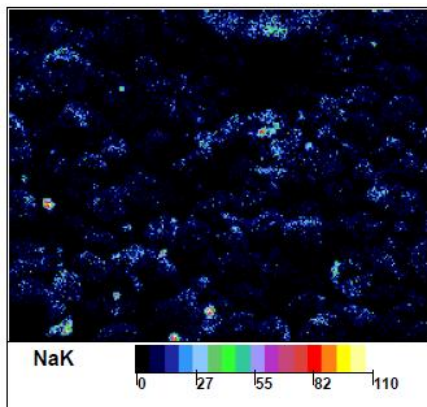


bottom

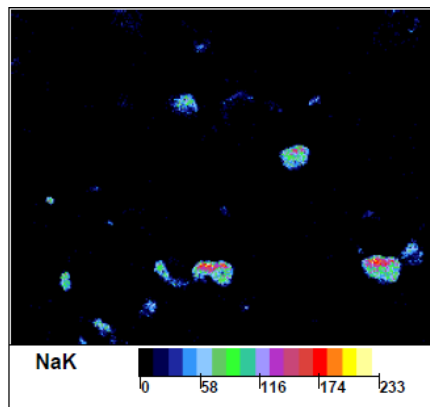


5 weeks

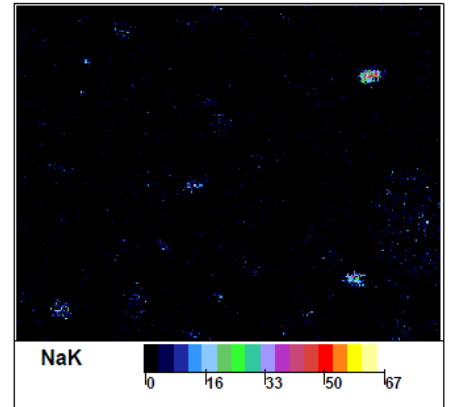
surface



middle

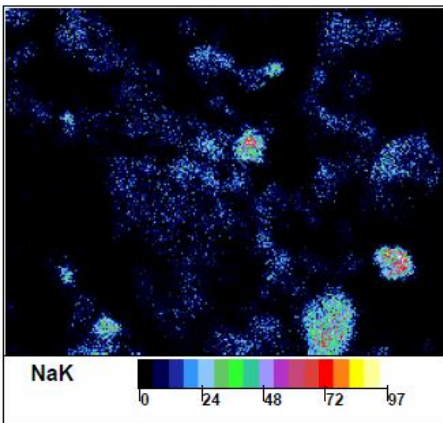


bottom

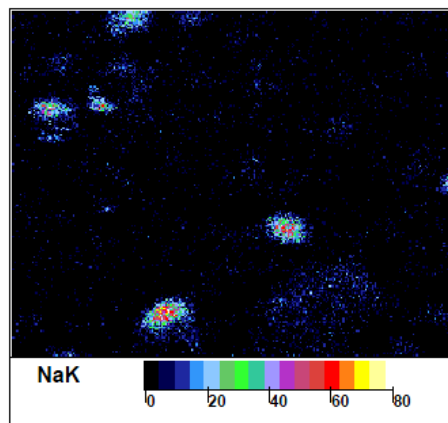


7 weeks

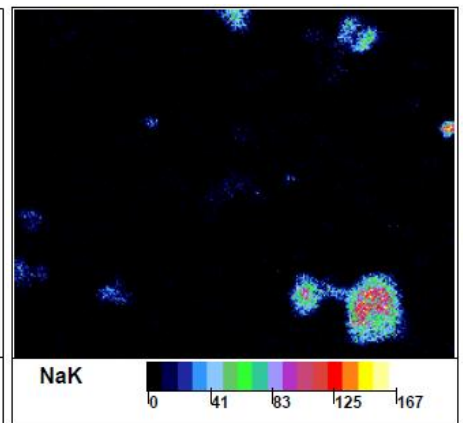
surface



middle



bottom

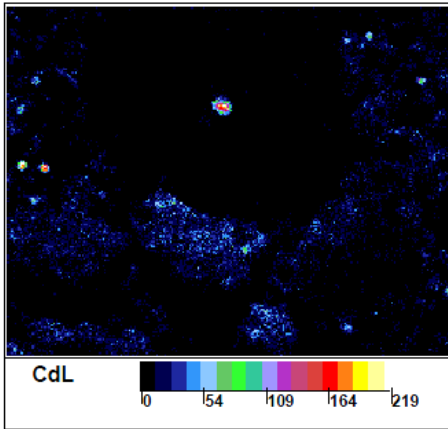


Appendix C-2 :Micro XRF data of the clay

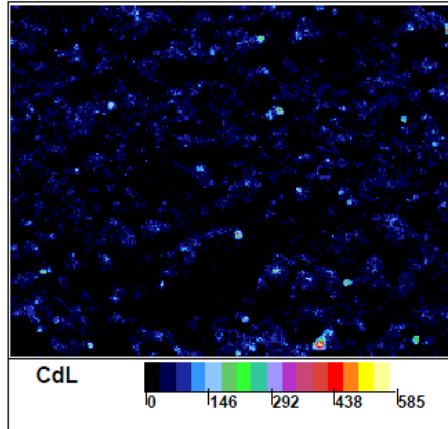
Micro XRF data clay samples Cd

3 weeks

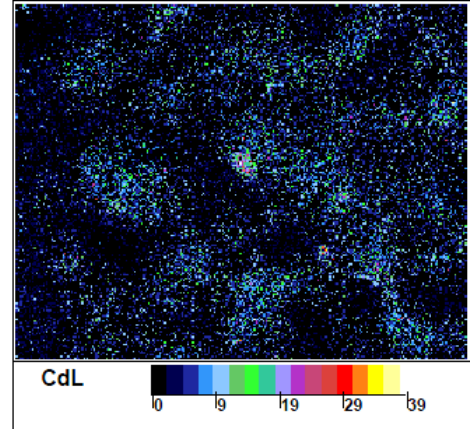
Surface



middle

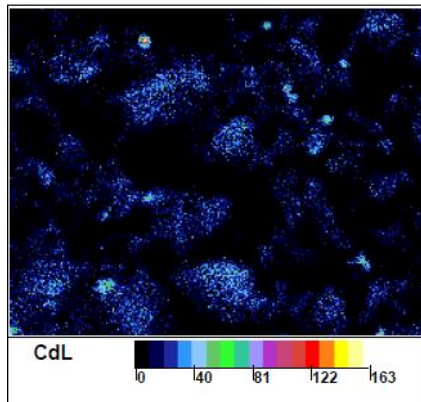


bottom

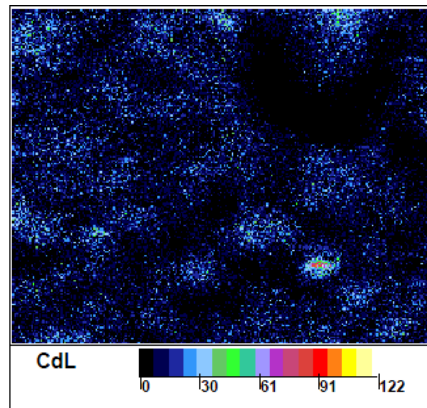


5 weeks

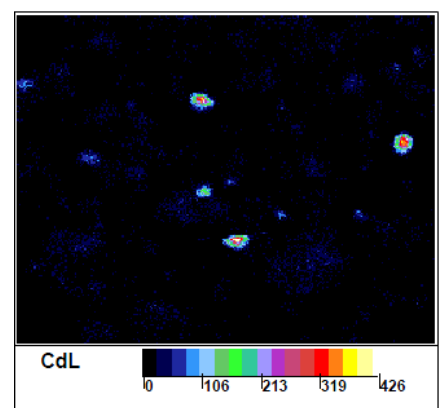
Surface



middle

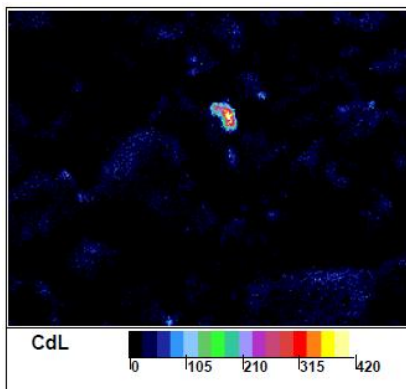


bottom

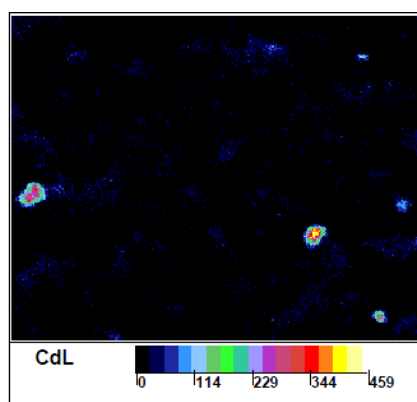


7 weeks

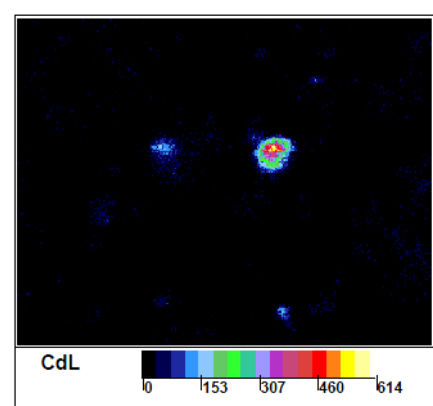
Surface



middle



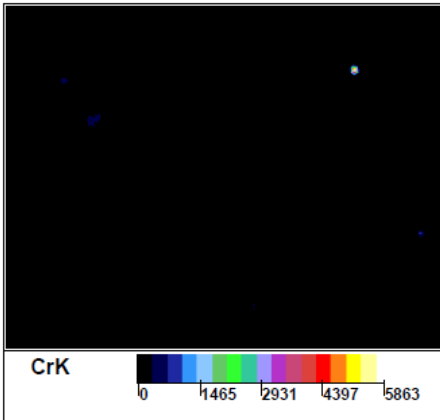
bottom



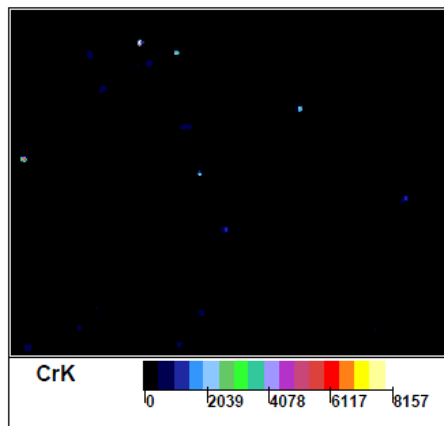
Micro XRF data clay samples Cr:

3 weeks

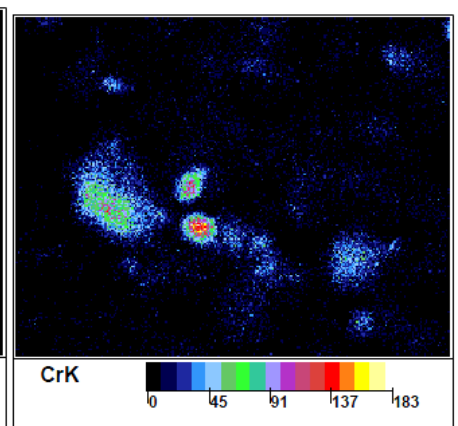
Surface



middle

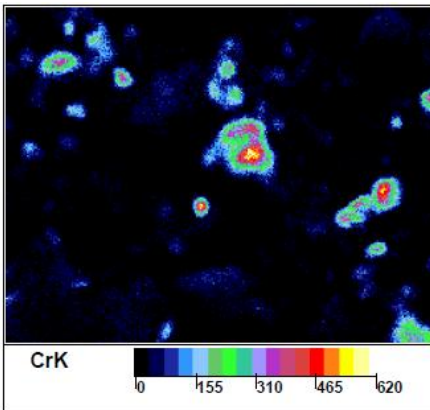


bottom

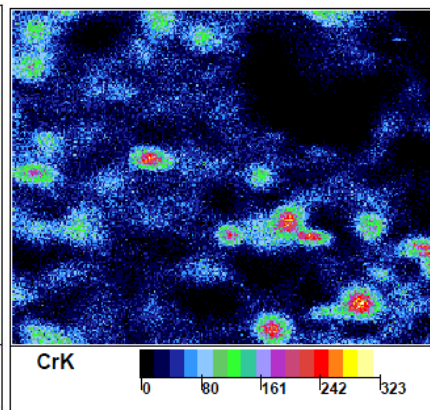


5 weeks

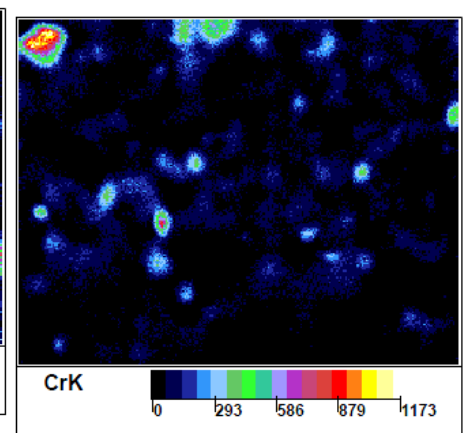
Surface



middle

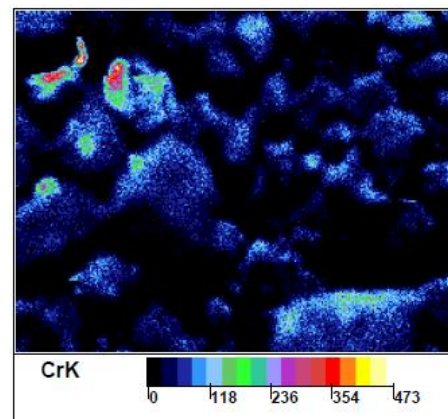


bottom

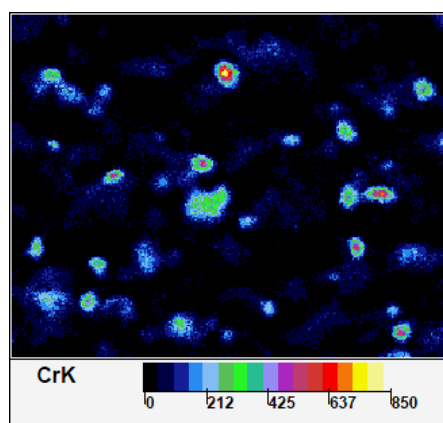


7 weeks

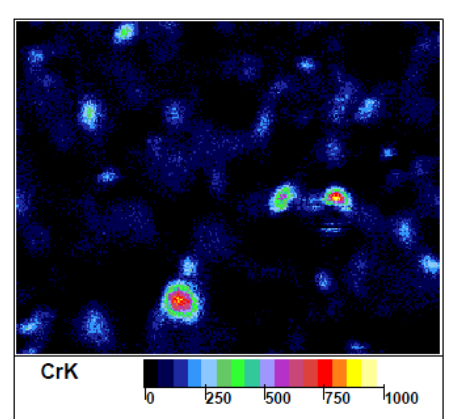
Surface



middle



bottom



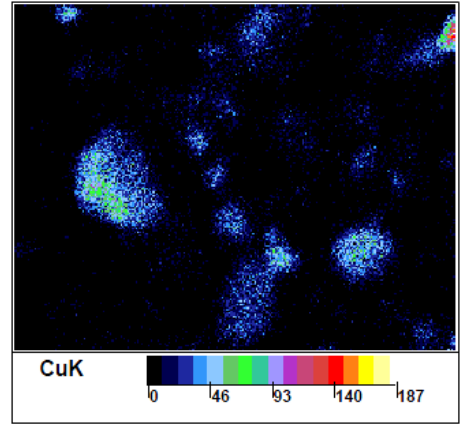
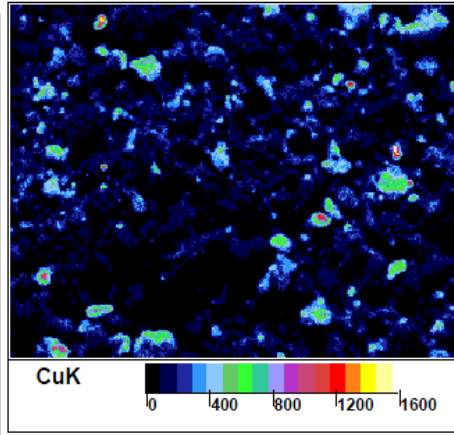
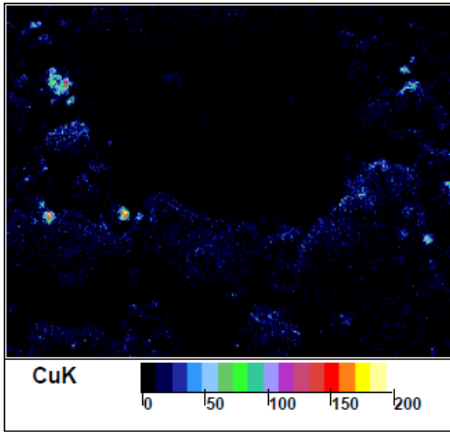
Micro XRF data clay samples Cu:

3 weeks

Surface

middle

bottom

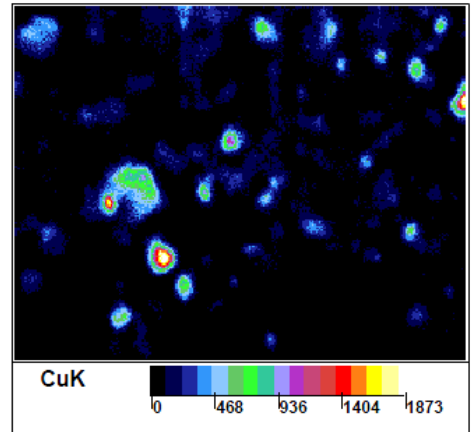
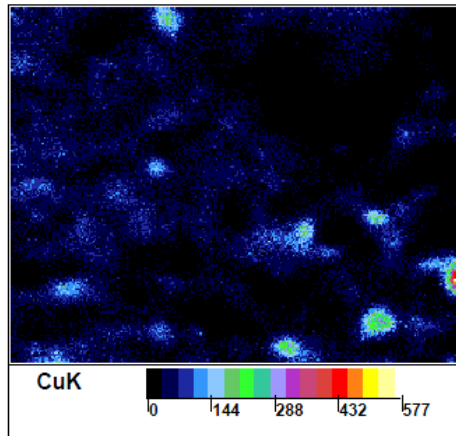
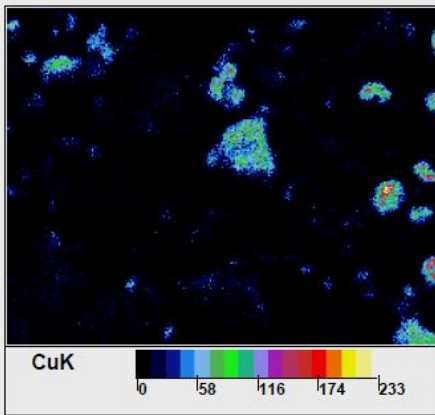


5 weeks

Surface

middle

bottom

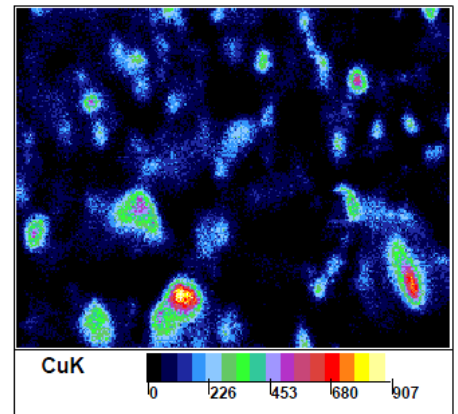
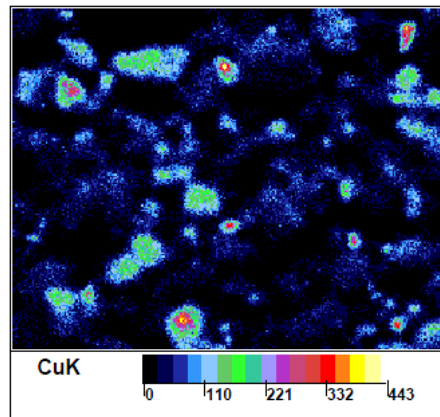
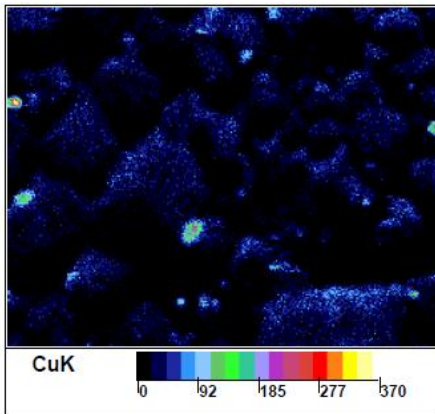


7 weeks

Surface

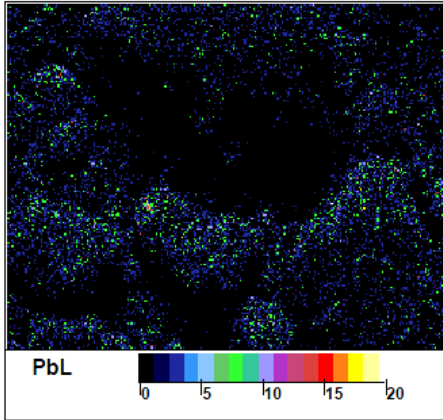
middle

bottom

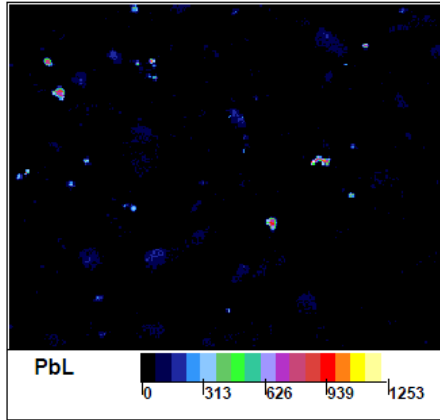


Micro XRF data clay samples Pb

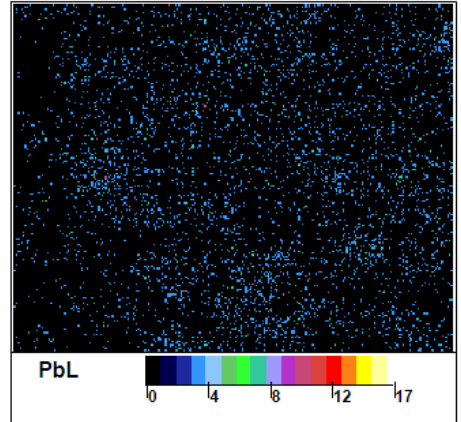
3 weeks
Surface



middle

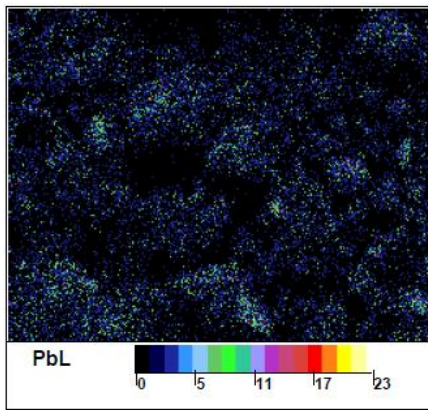


bottom

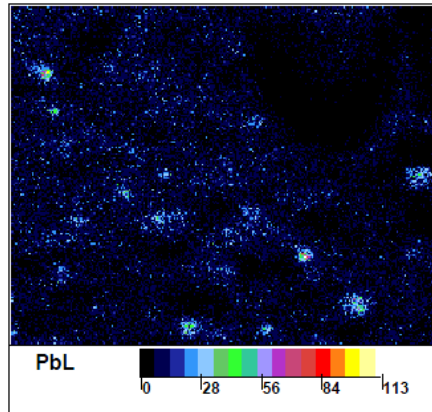


5 weeks

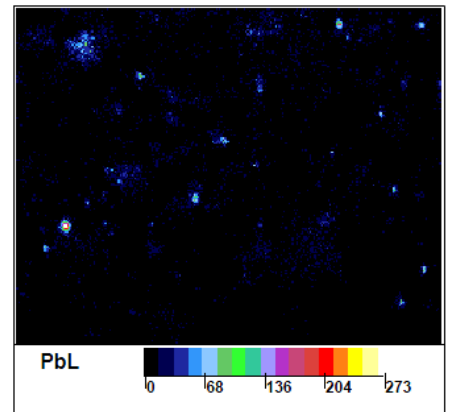
Surface



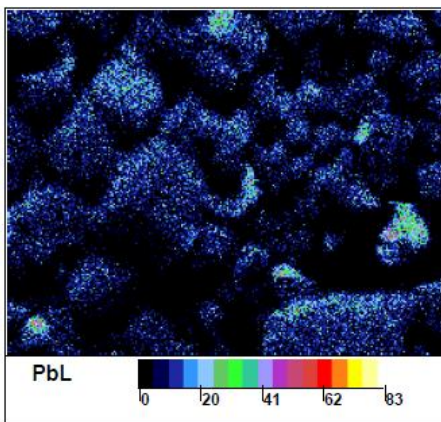
middle



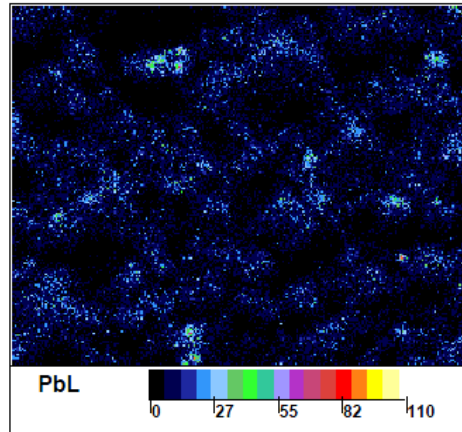
bottom



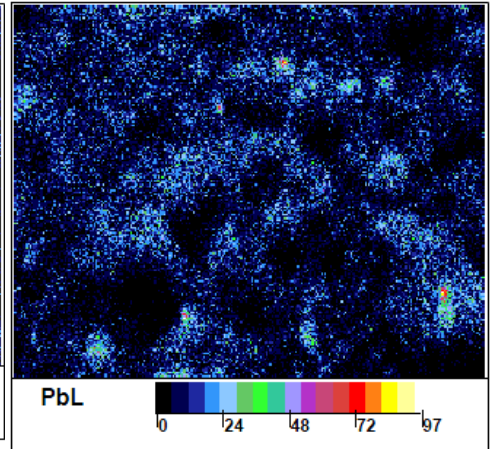
7 weeks
Surface



middle



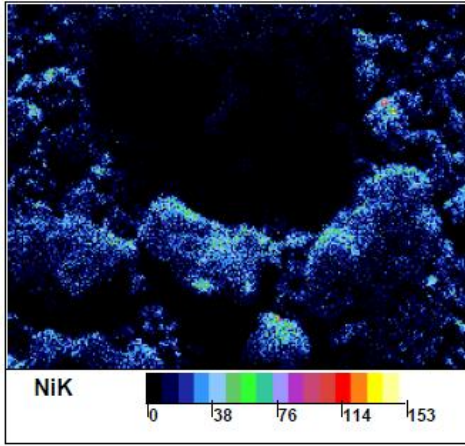
bottom



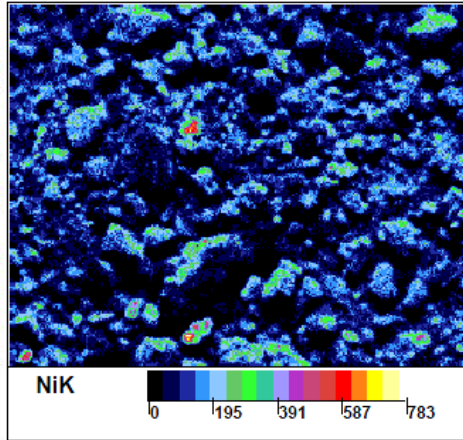
Micro XRF data clay samples Ni

3 weeks

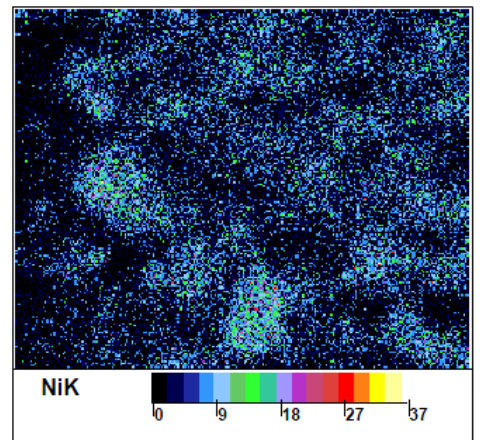
Surface



middle

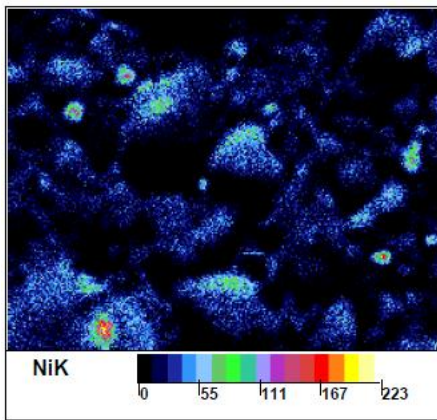


bottom

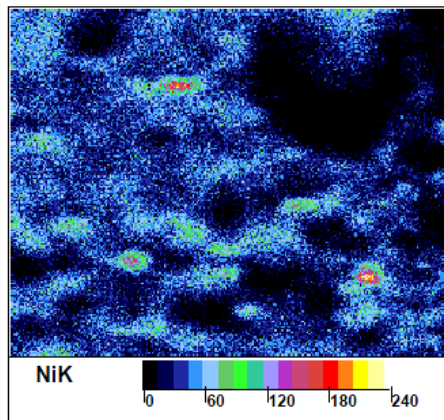


5 weeks

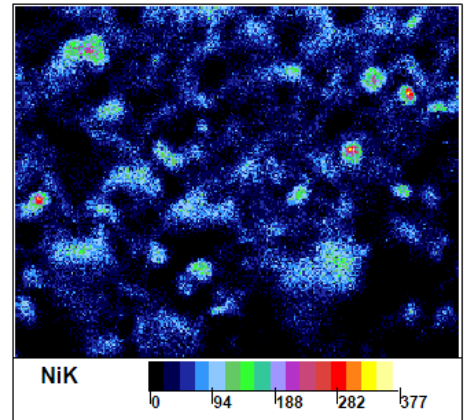
Surface



middle

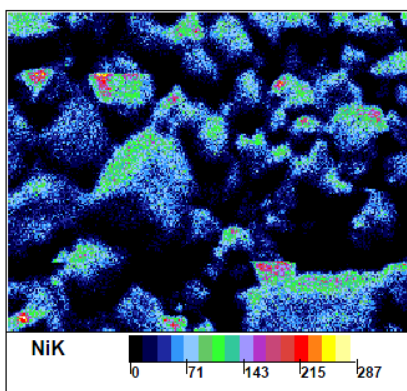


bottom

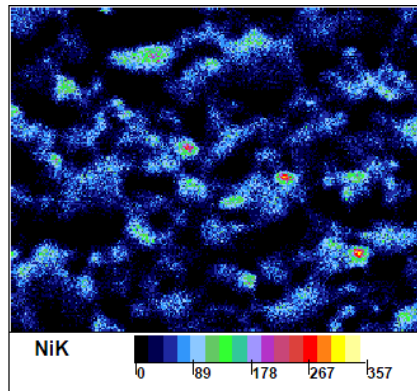


7 weeks

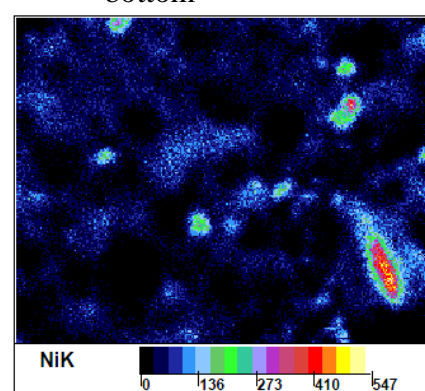
Surface



middle



bottom



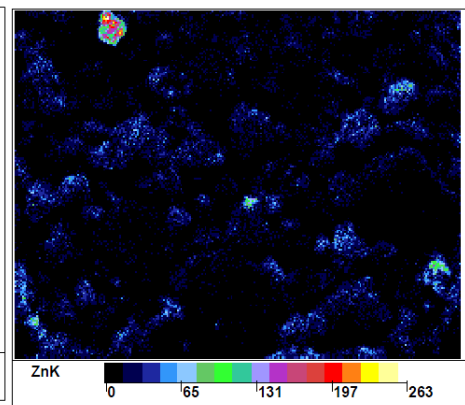
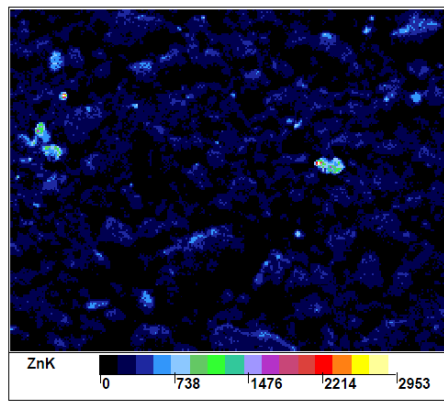
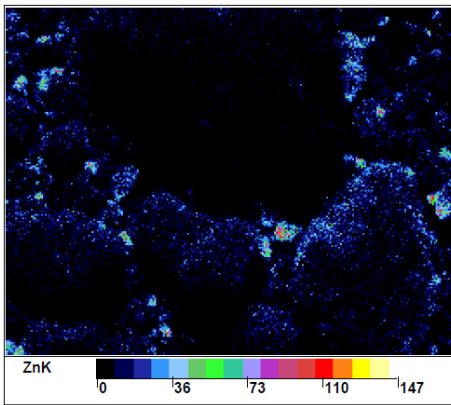
Micro XRF data clay samples Zn:

3 weeks

Surface

middle

bottom

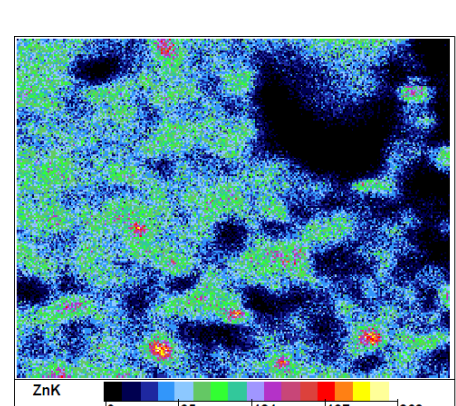
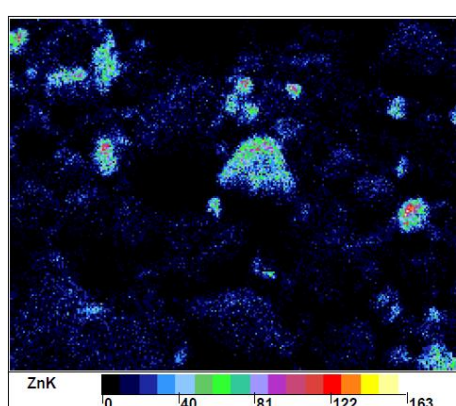
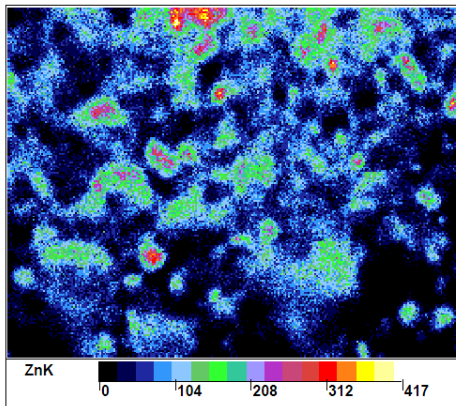


5 weeks

Surface

middle

bottom

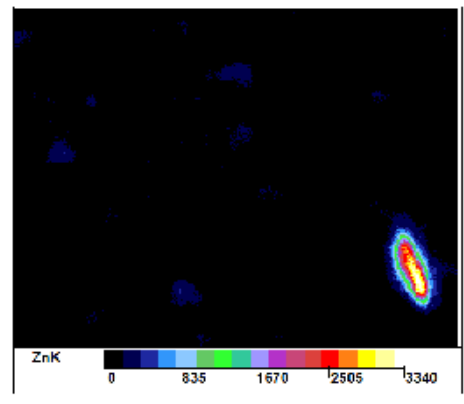
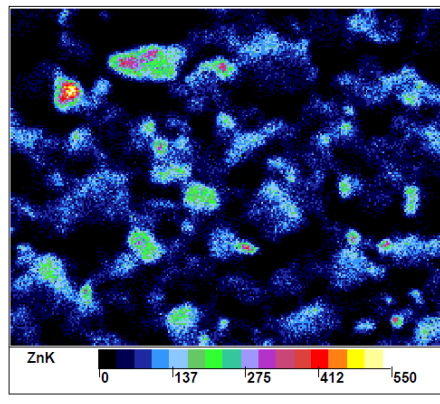
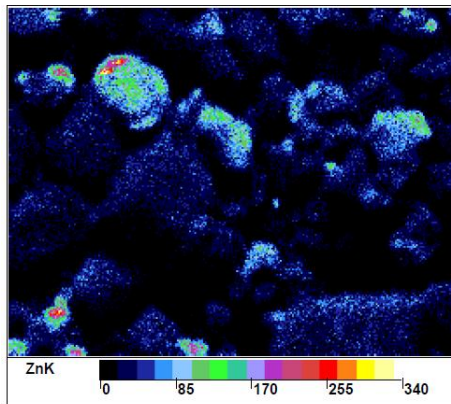


7 weeks

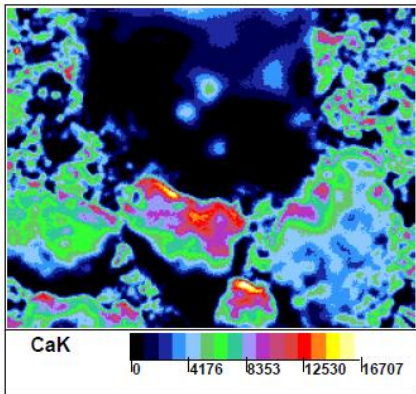
Surface

middle

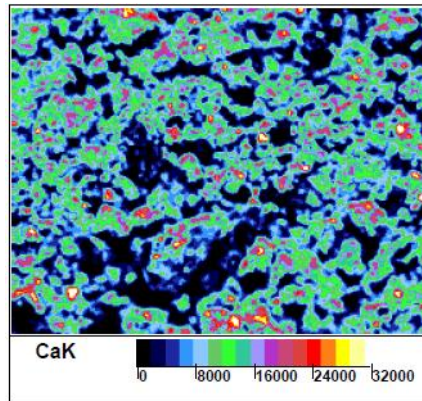
bottom



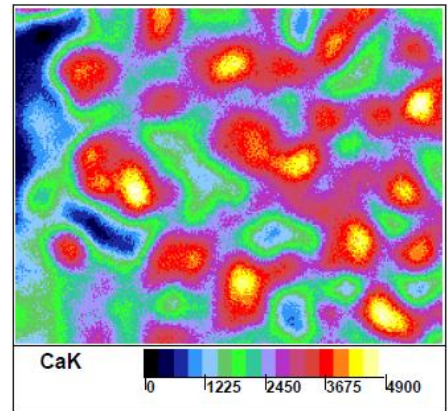
Micro XRF data clay samples Ca
3 weeks
Surface



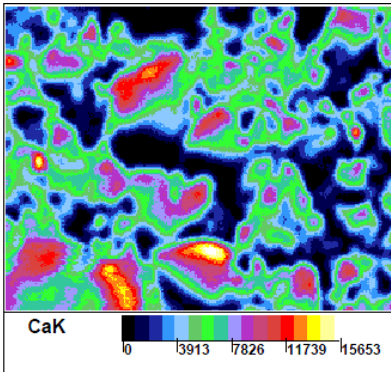
middle



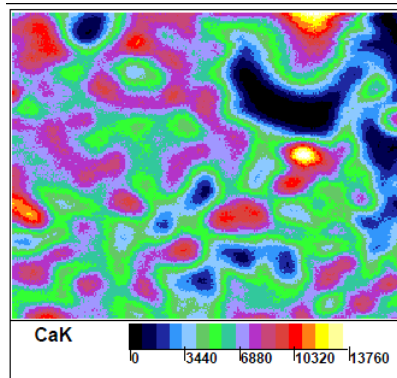
bottom



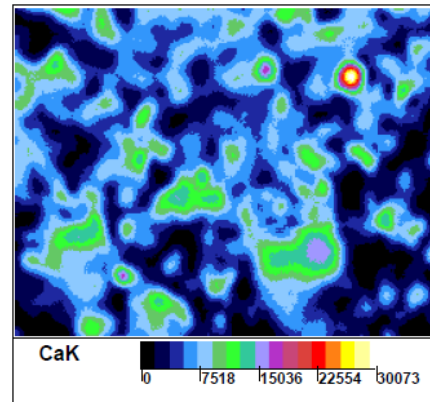
5 weeks
surface



middle

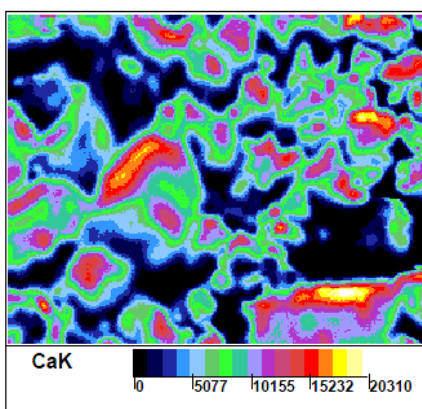


bottom

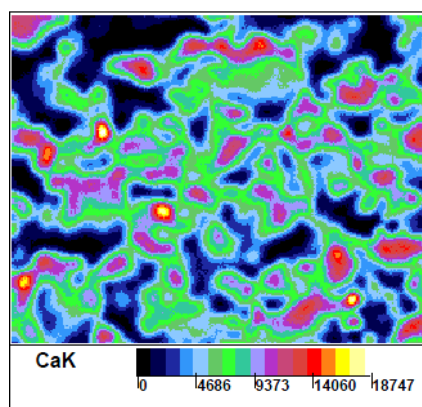


7 weeks

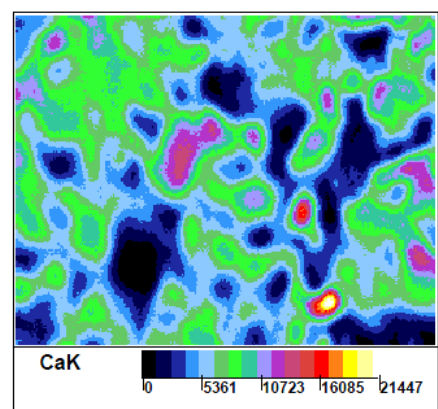
surface



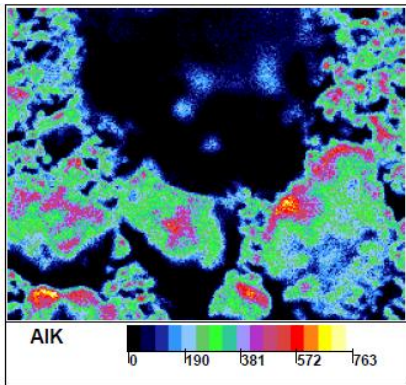
middle



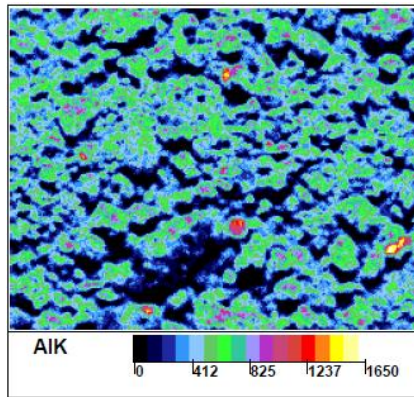
bottom



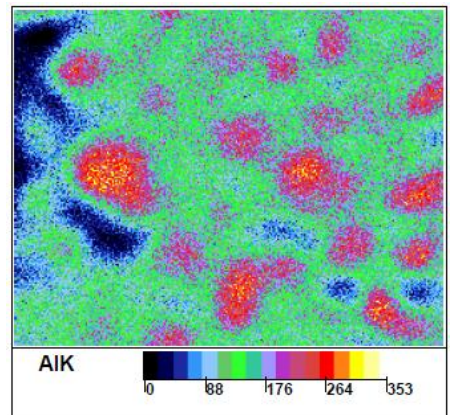
Micro XRF data clay samples AI
3 weeks
Surface



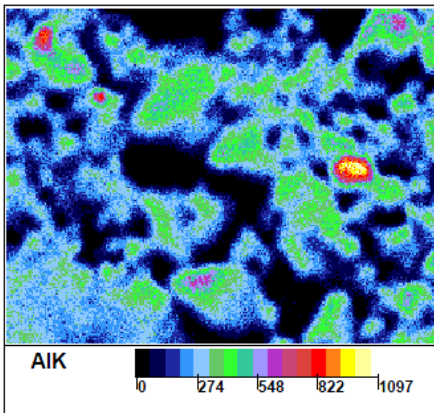
middle



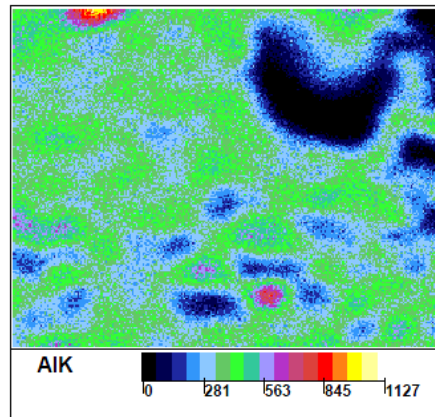
bottom



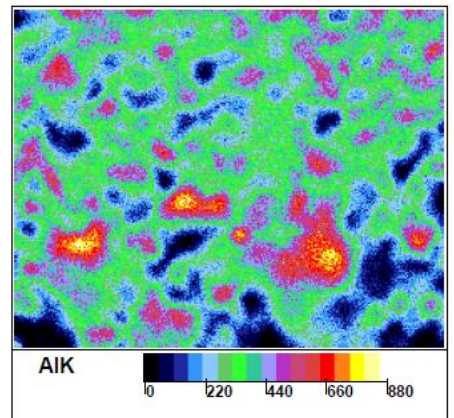
5 weeks
surface



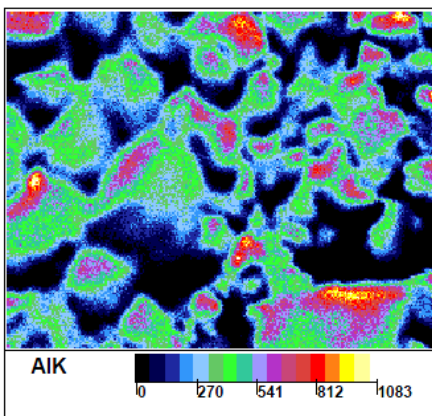
middle



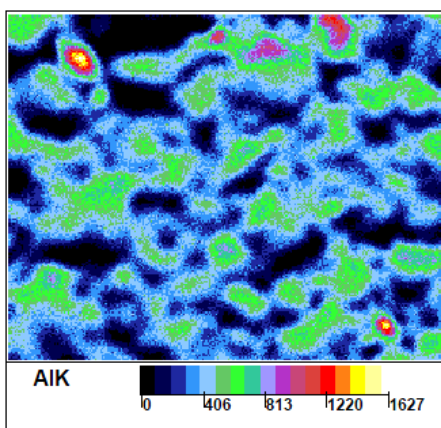
bottom



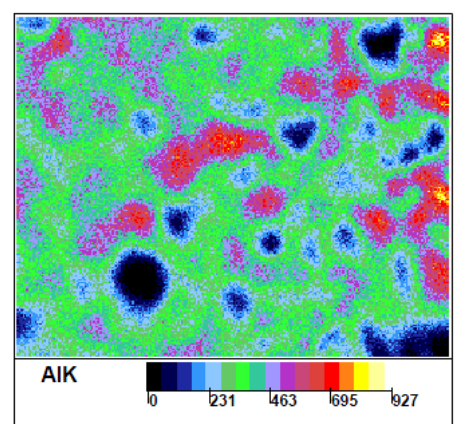
7 weeks
surface



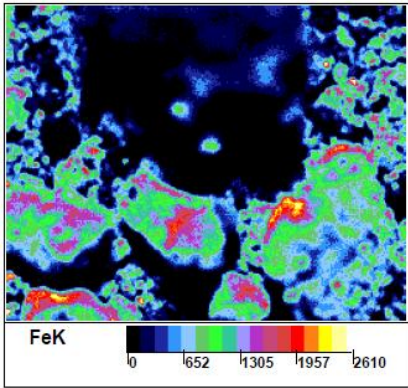
middle



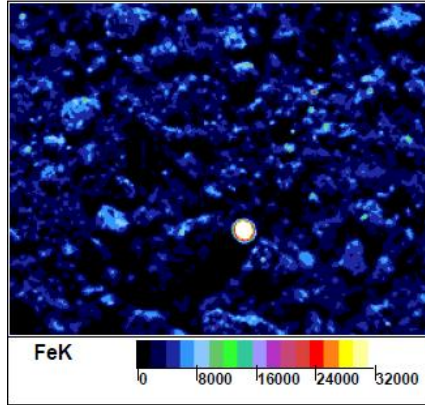
bottom



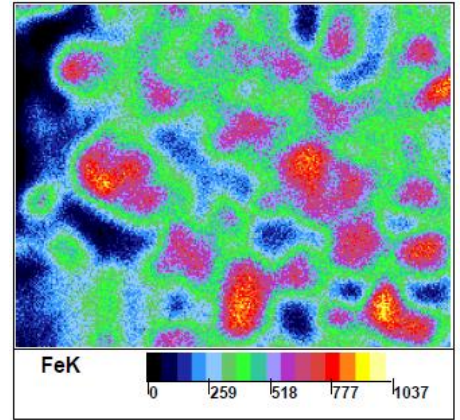
Micro XRF data Fe
3 weeks
Surface



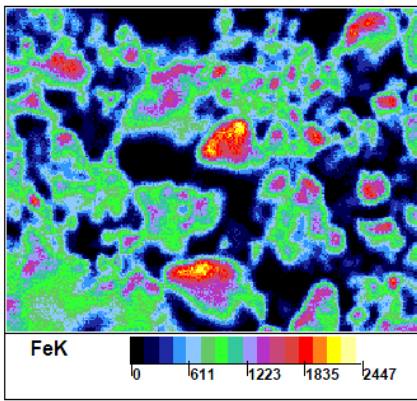
middle



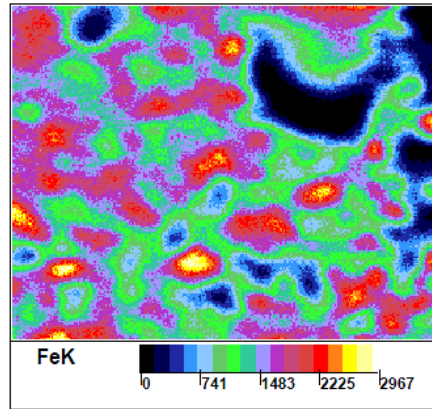
bottom



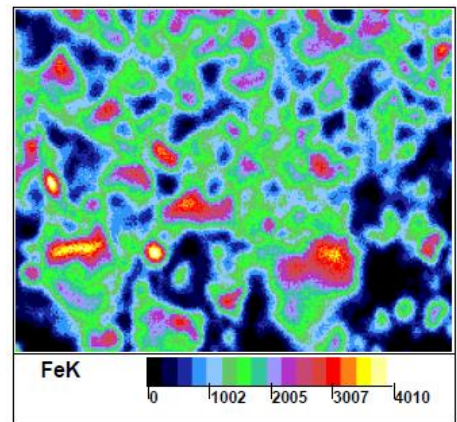
5 weeks
surface



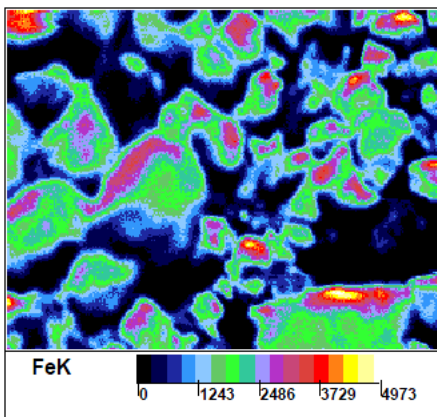
middle



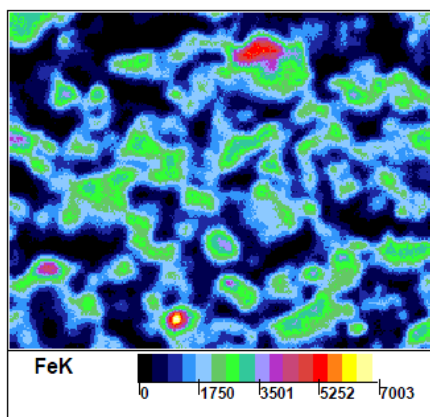
bottom



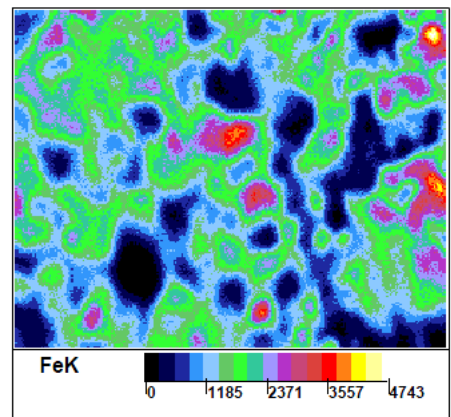
7 weeks
surface



middle



bottom



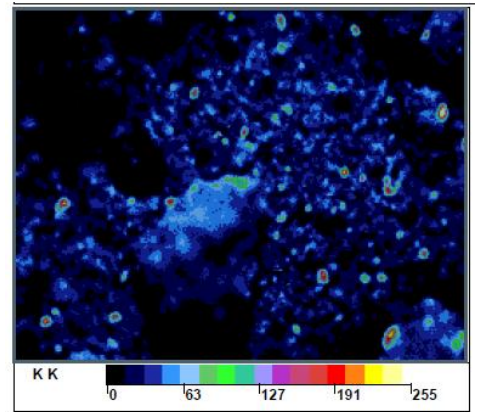
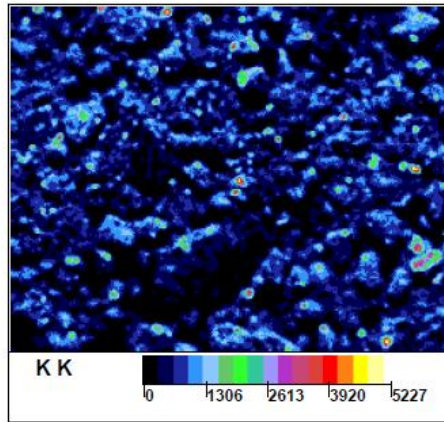
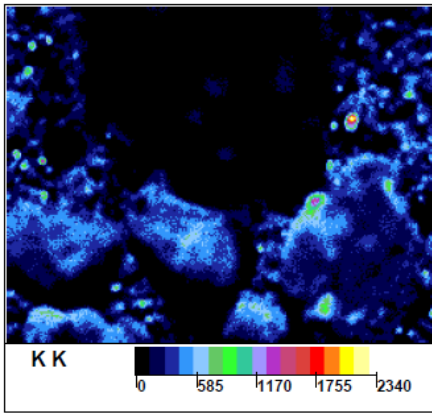
Micro XRF data clay samples K

3 weeks

Surface

middle

bottom

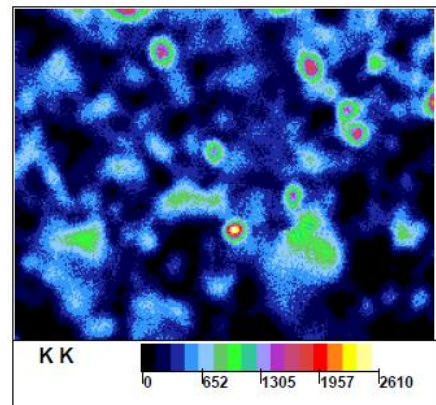
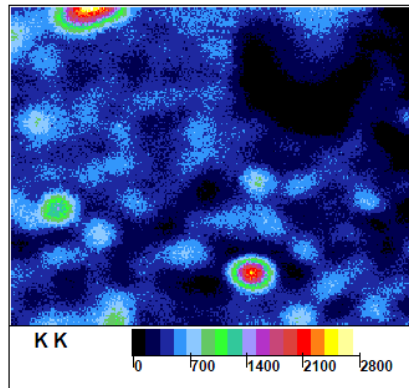
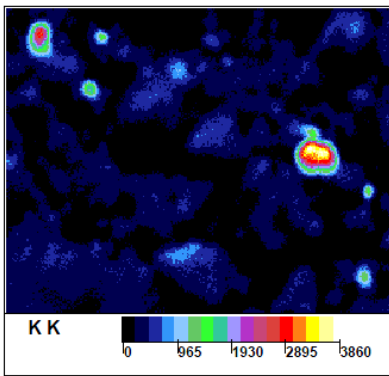


5 weeks

surface

middle

bottom

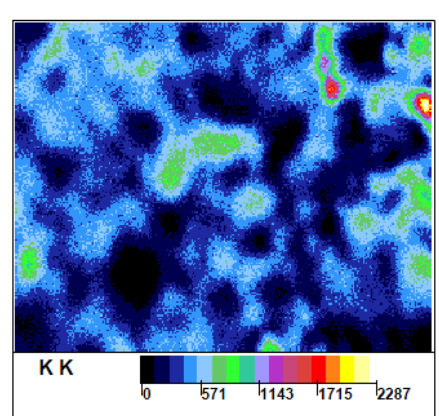
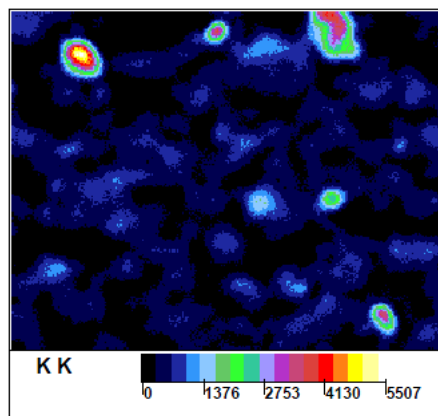
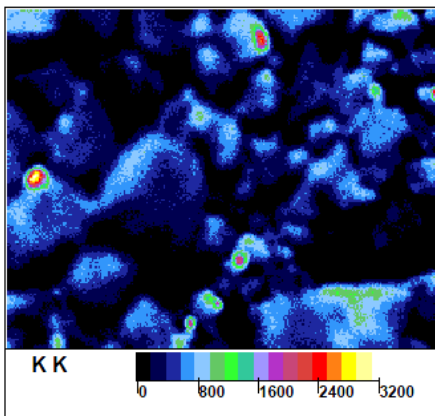


7 weeks

surface

middle

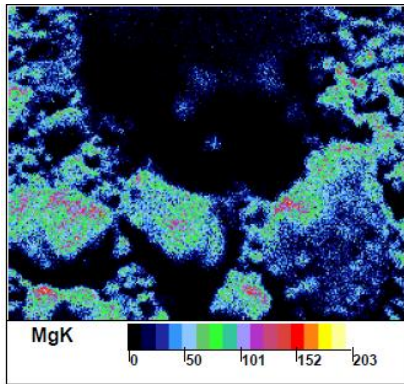
bottom



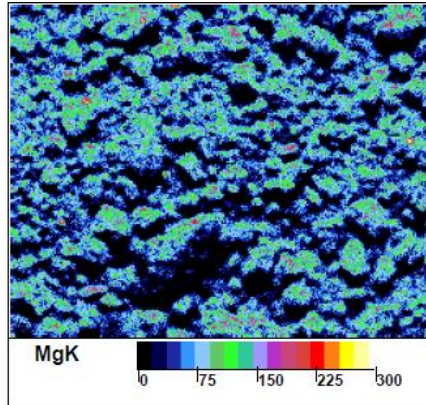
Micro XRF data clay samples Mg:

3 weeks

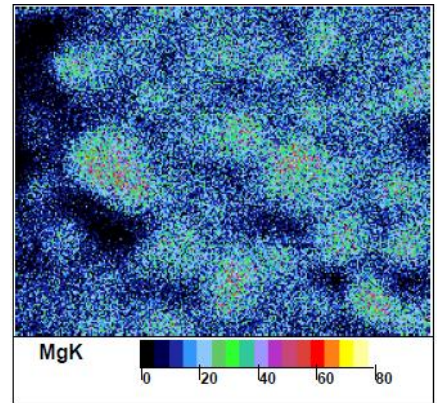
Surface



middle

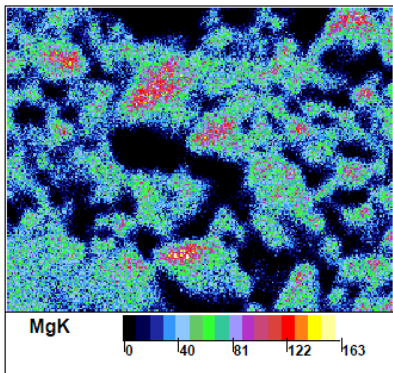


bottom

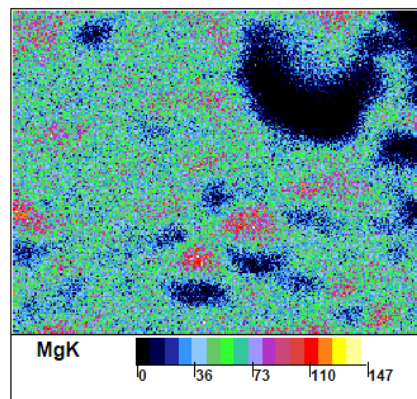


5 weeks

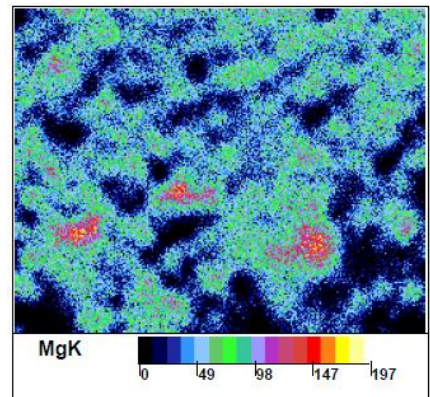
surface



middle

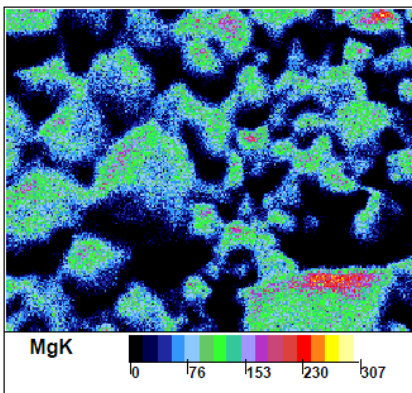


bottom

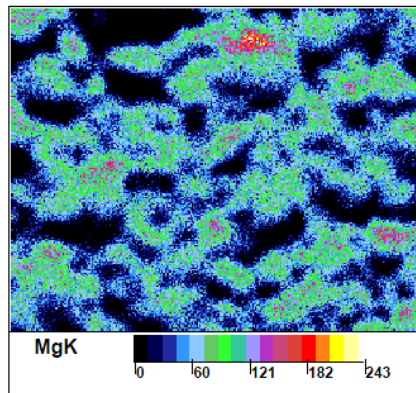


7 weeks

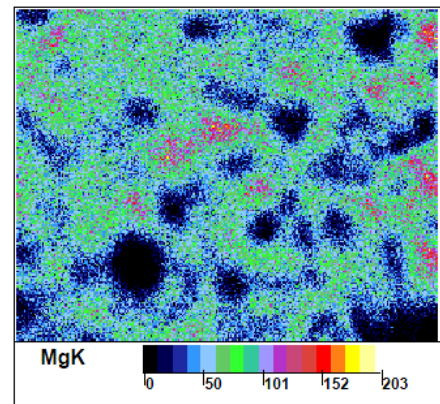
surface



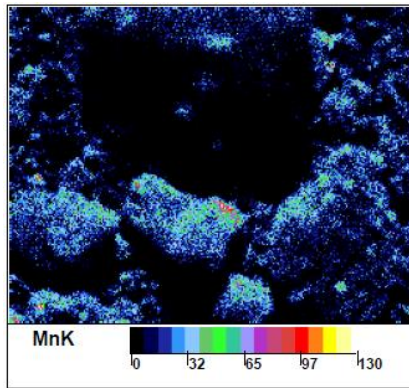
middle



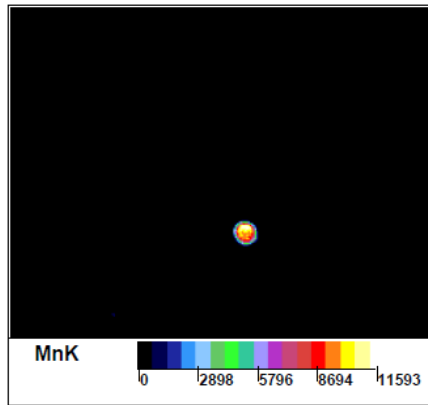
bottom



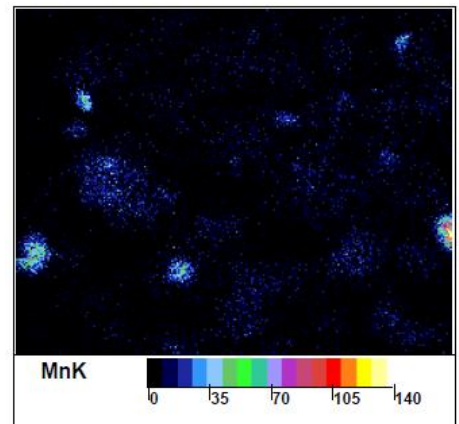
Micro XRF data clay samples Mn
3 weeks
Surface



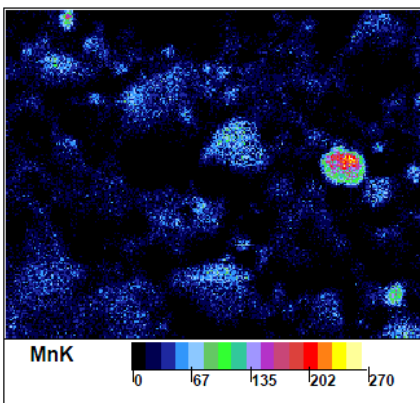
middle



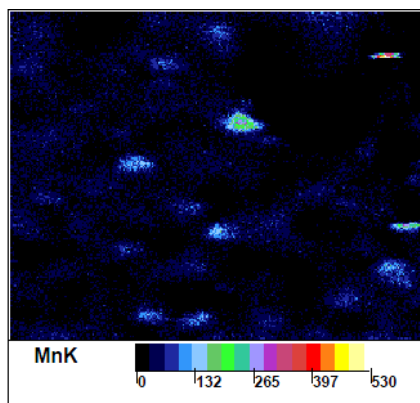
bottom



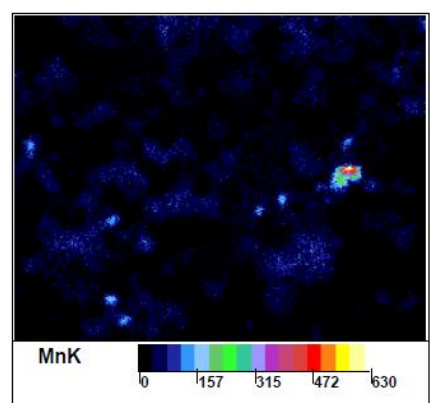
5 weeks
surface



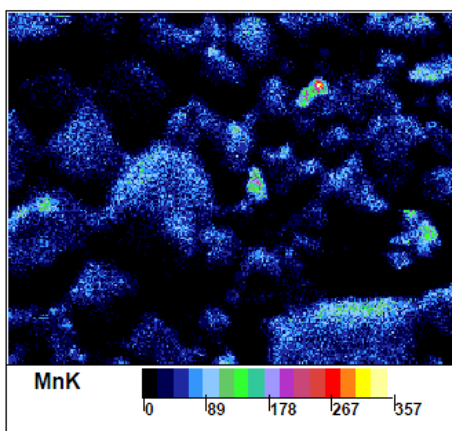
middle



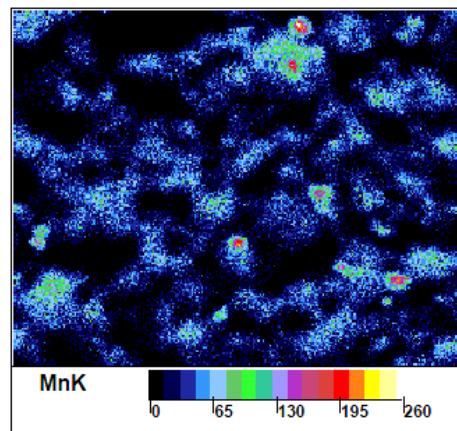
bottom



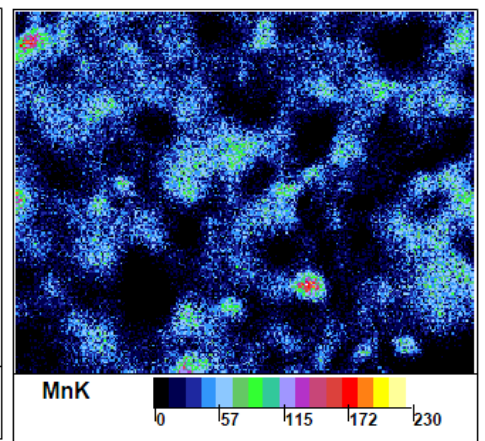
7 weeks
surface



middle



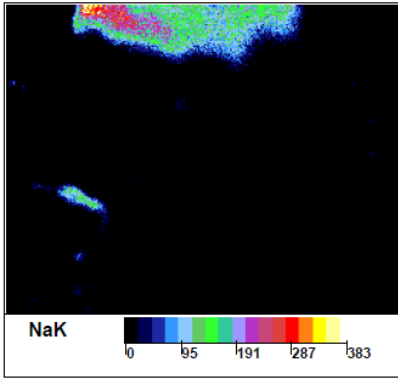
bottom



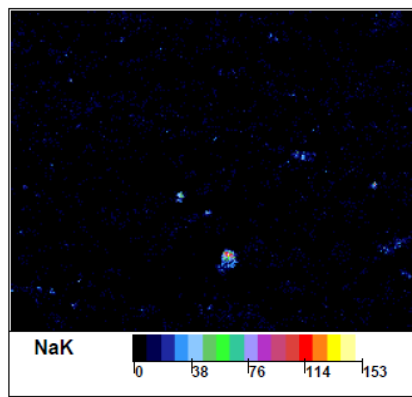
Micro XRF data clay samples Na

3 weeks

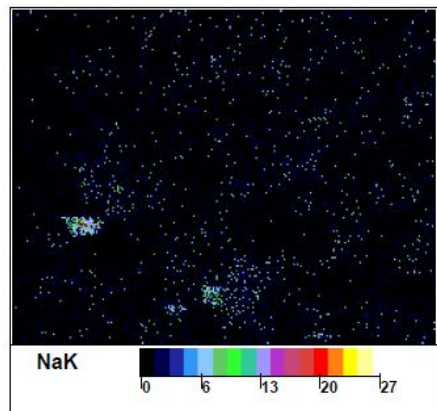
surface



middle

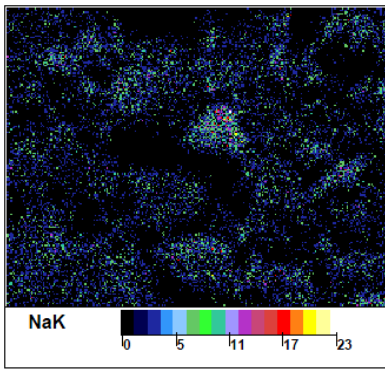


bottom

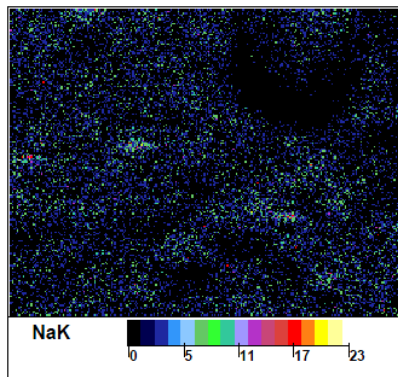


5 weeks

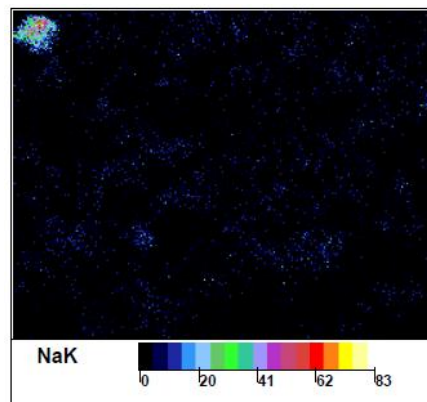
surface



middle

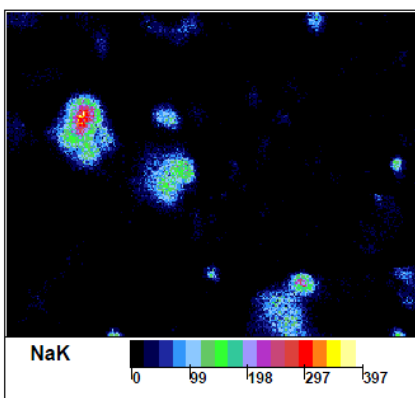


bottom

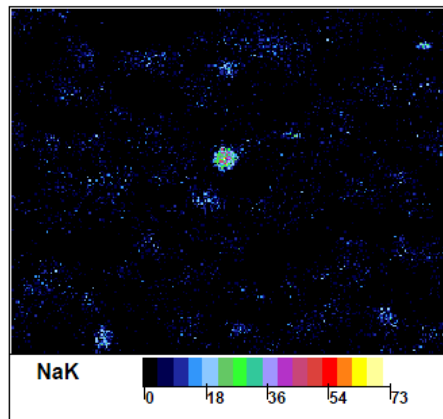


7 weeks

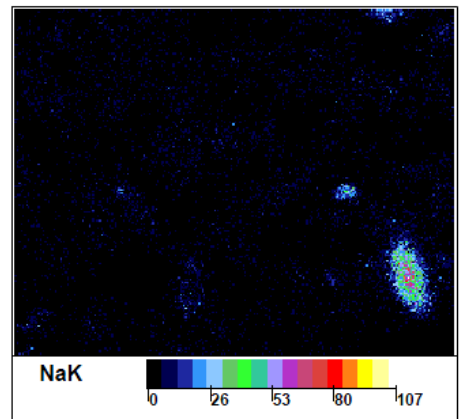
surface



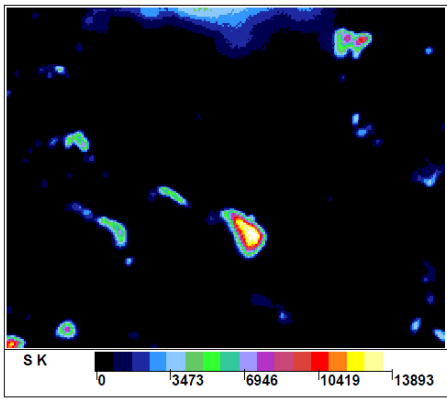
middle



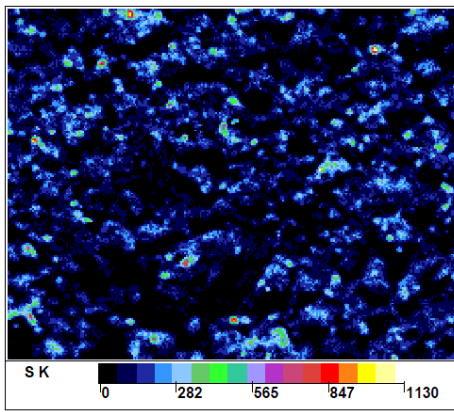
bottom



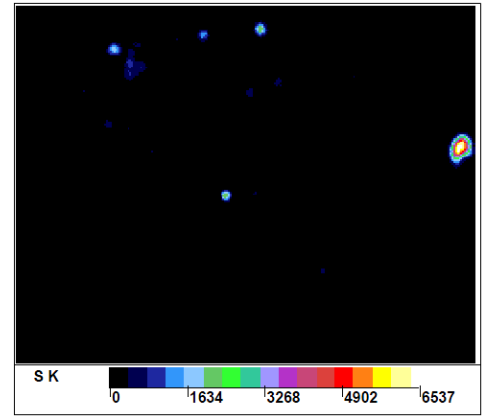
Micro XRF data clay samples S
3 weeks
Surface



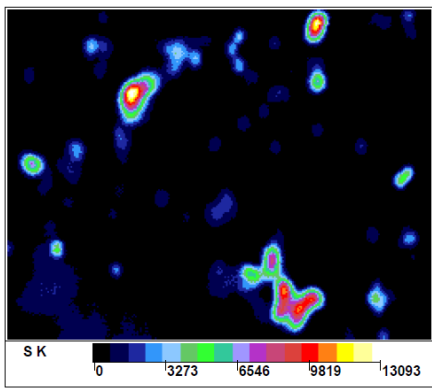
middle



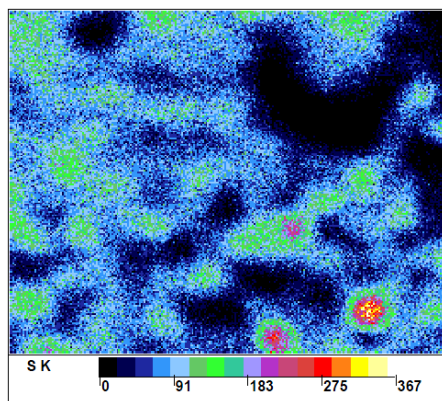
bottom



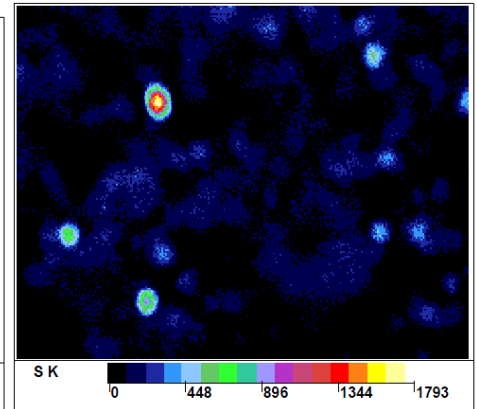
5 weeks
surface



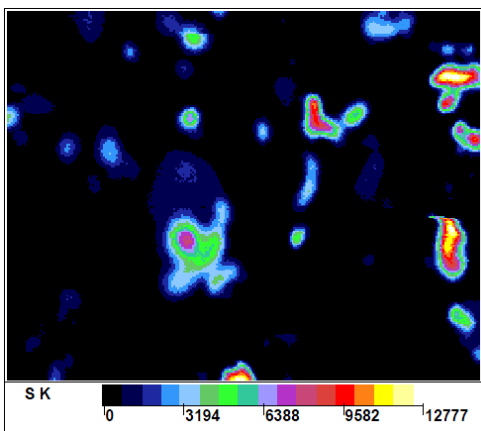
middle



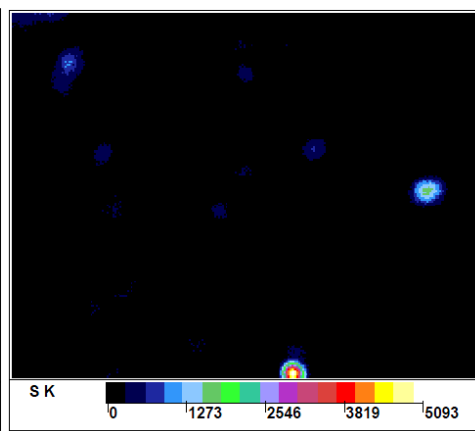
bottom



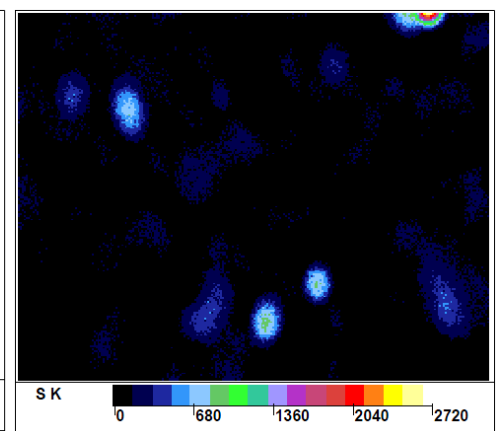
7 weeks
surface



middle

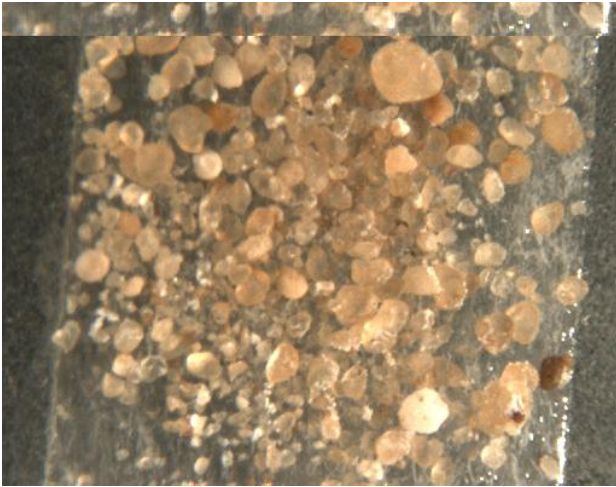


bottom



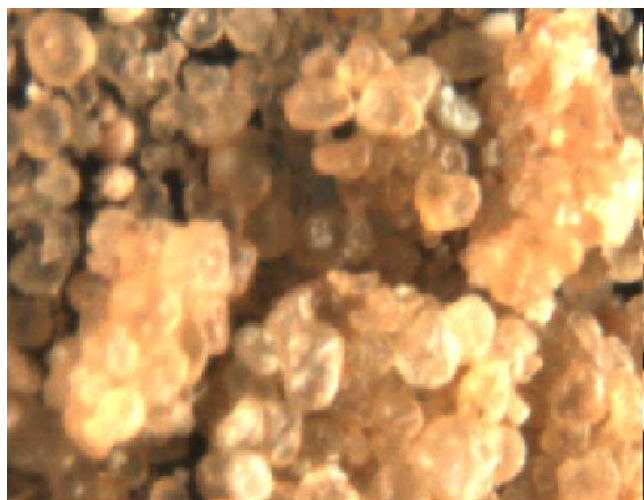
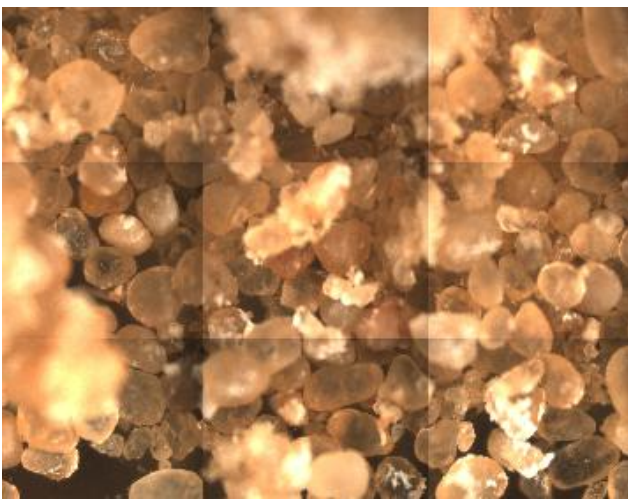
Some of the surface sample pictures:

3 weeks dried sand:

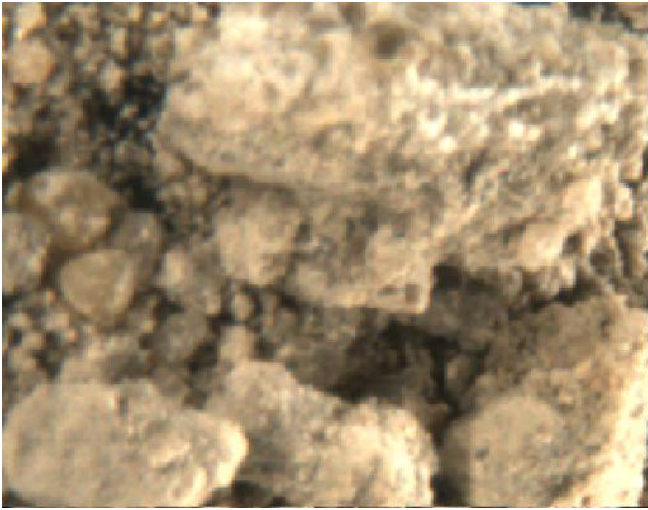


5 weeks dried sand:

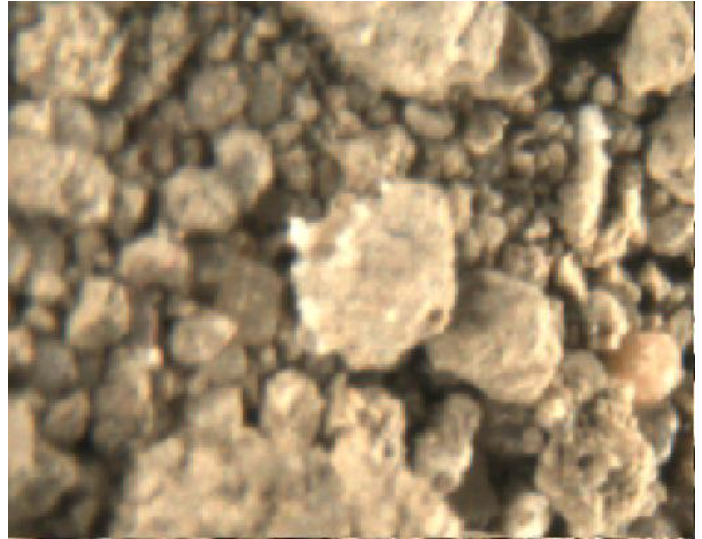
7 weeks dried sand:



3 weeks dried clay:



5 weeks dried clay:

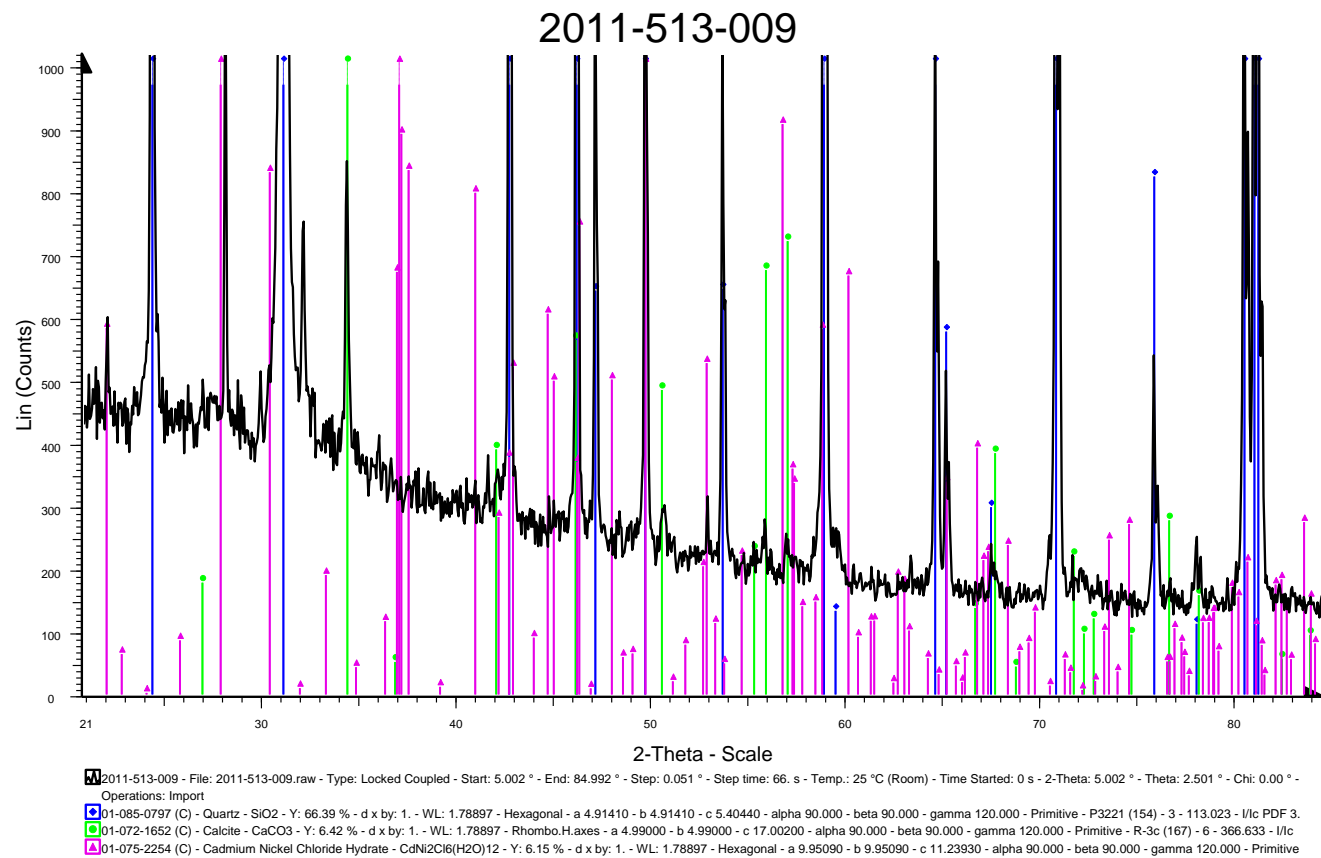


7 weeks dried clay:



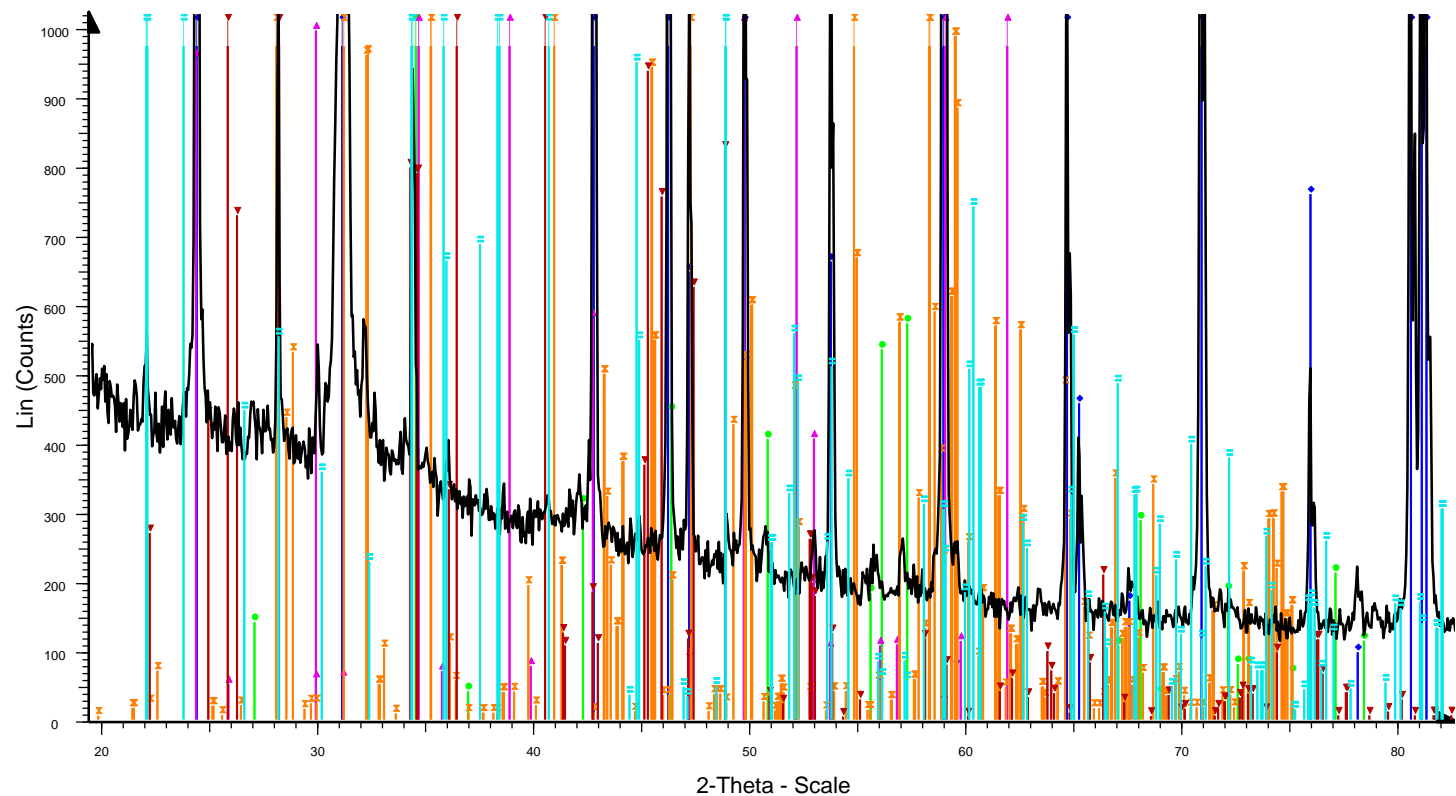
Appendix D: XRD data (sand)

3 weeks surface



3 weeks middle slice

2011-513-0010

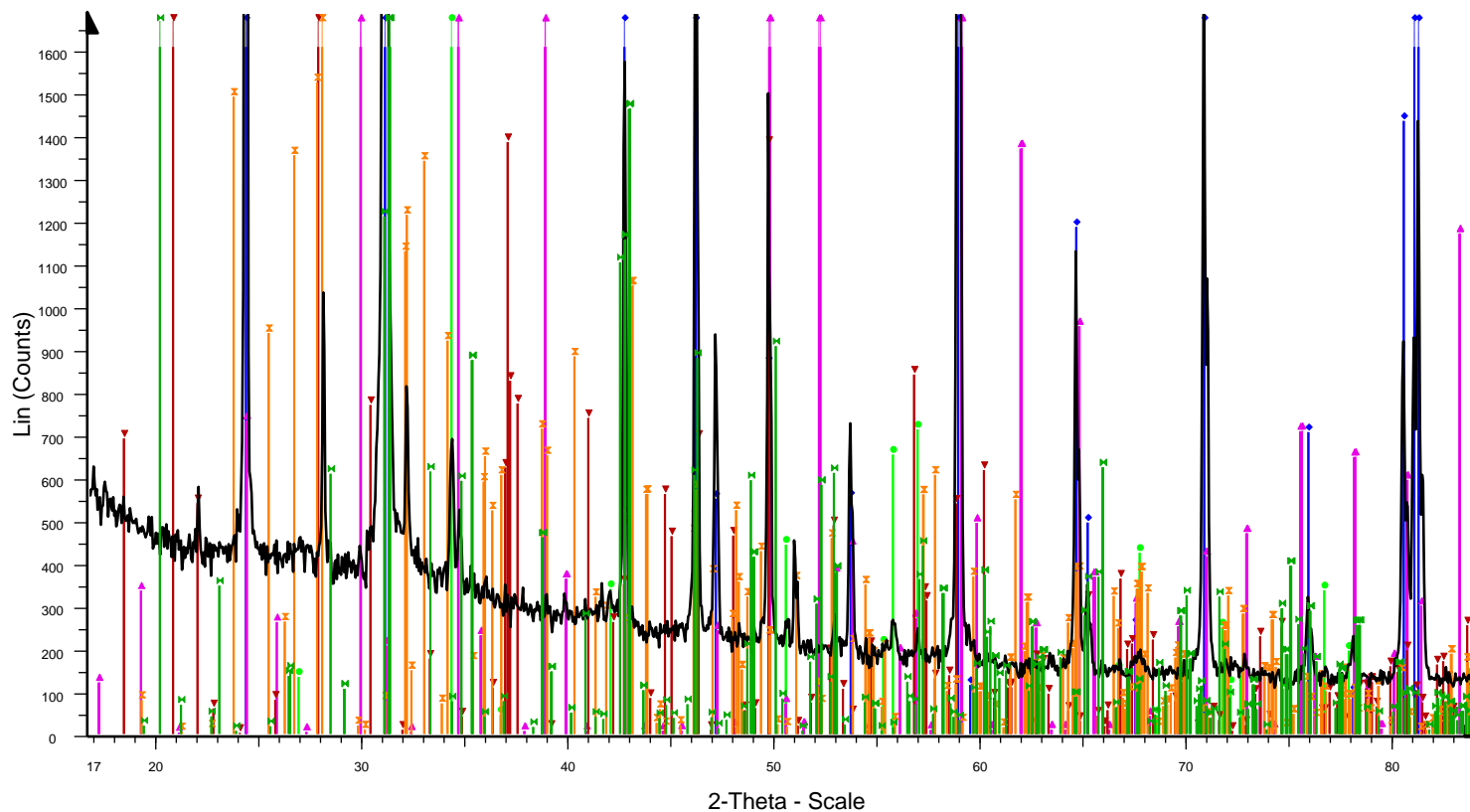


2011-513-0010 - File: 2011-513-010.raw - Type: Locked Coupled - Start: 5.002 ° - End: 84.992 ° - Step: 0.051 ° - Step time: 66. s - Temp.: 25 °C (Room) - Time Started: 0 s - 2-Theta: 5.002 ° - Theta: 2.501 ° - Chi: 0.00 °
Operations: Import

- 01-085-0796 (C) - Quartz - SiO₂ - Y: 58.31 % - d x by: 1. - WL: 1.78897 - Hexagonal - a 4.91180 - b 4.91180 - c 5.40340 - alpha 90.000 - beta 90.000 - gamma 120.000 - Primitive - P3221 (154) - 3 - 112.896 - I/c PDF 3.
- 01-086-2335 (C) - Calcite magnesien - (Mg_{0.064}Ca_{0.936})(CO₃) - Y: 5.38 % - d x by: 1. - WL: 1.78897 - Rhombo.H.axes - a 4.96730 - b 4.96730 - c 16.96310 - alpha 90.000 - beta 90.000 - gamma 120.000 - Primitive - R-3
- 00-028-0694 (I) - Nickel Chloride Borate - Ni₃B₇O₁₃Cl - Y: 19.16 % - d x by: 1. - WL: 1.78897 - Orthorhombic - a 8.51700 - b 8.51700 - c 12.03700 - alpha 90.000 - beta 90.000 - gamma 90.000 - 873.155 - I/c PDF 1. -
- 01-070-2217 (C) - Cadmium Chloride Hydrate - CdCl₂(H₂O)₄ - Y: 12.49 % - d x by: 1. - WL: 1.78897 - Orthorhombic - a 12.88900 - b 7.28100 - c 15.01000 - alpha 90.000 - beta 90.000 - gamma 90.000 - Primitive - P212
- 01-084-1180 (C) - Lead Chloride Bromide - PbCl₆Br_{1.4} - Y: 6.49 % - d x by: 1. - WL: 1.78897 - Orthorhombic - a 7.90710 - b 9.33500 - c 4.65130 - alpha 90.000 - beta 90.000 - gamma 90.000 - Primitive - Pnam (62) - 4
- 01-070-2348 (C) - Zinc Chlorate Hydrate - Zn(ClO₄)₂(H₂O)₂ - Y: 6.65 % - d x by: 1. - WL: 1.78897 - Monoclinic - a 6.42500 - b 6.89200 - c 6.45400 - alpha 90.000 - beta 94.700 - gamma 90.000 - Primitive - P21/n (14) -

3 weeks bottom

2011-513-0011

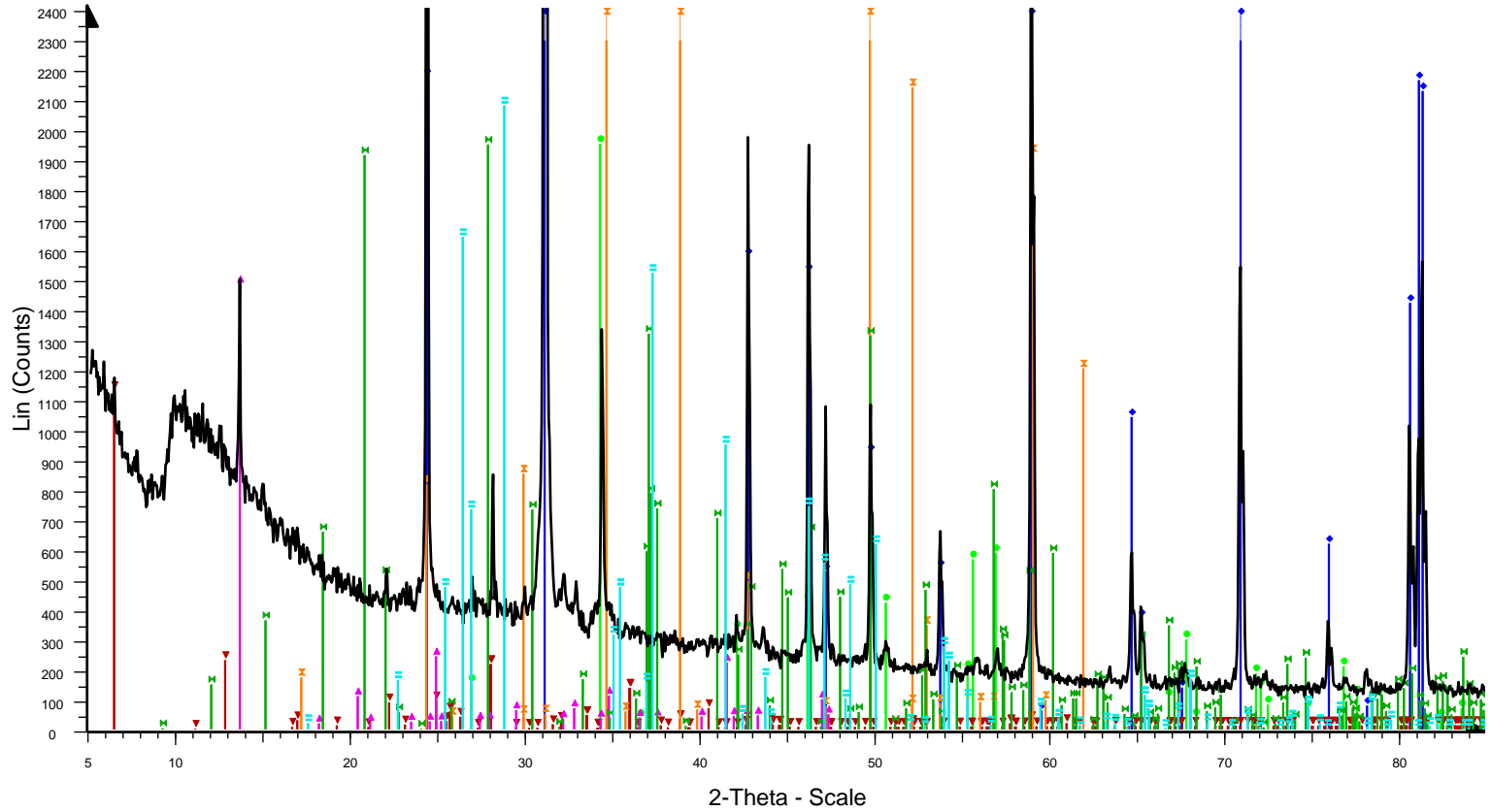


2011-513-0011 - File: 2011-513-011.raw - Type: Locked Coupled - Start: 5.002 ° - End: 84.992 ° - Step: 0.051 ° - Step time: 66. s - Temp.: 25 °C (Room) - Time Started: 0 s - 2-Theta: 5.002 ° - Theta: 2.501 ° - Chi: 0.00 °
Operations: Import

- 01-085-0797 (C) - Quartz - SiO₂ - Y: 64.77 % - d x by: 1. - WL: 1.78897 - Hexagonal - a 4.91410 - b 4.91410 - c 5.40440 - alpha 90.000 - beta 90.000 - gamma 120.000 - Primitive - P3221 (154) - 3 - 113.023 - I/c PDF 3.
- 00-047-1743 (C) - Calcite - CaCO₃ - Y: 6.01 % - d x by: 1. - WL: 1.78897 - Rhombo.H.axes - a 4.98960 - b 4.98960 - c 17.06100 - alpha 90.000 - beta 90.000 - gamma 120.000 - Primitive - R-3c (167) - 6 - 367.847 - I/c
- 01-081-0218 (C) - Nickel Borate Chloride - Ni₃(B₇O₁₃)Cl - Y: 17.28 % - d x by: 1. - WL: 1.78897 - Orthorhombic - a 8.51050 - b 8.49840 - c 12.03240 - alpha 90.000 - beta 90.000 - gamma 90.000 - Primitive - Pca21 (29)
- 01-075-2254 (C) - Cadmium Nickel Chloride Hydrate - CdNi₂Cl₆(H₂O)₁₂ - Y: 6.49 % - d x by: 1. - WL: 1.78897 - Hexagonal - a 9.95090 - b 9.95090 - c 11.23930 - alpha 90.000 - beta 90.000 - gamma 120.000 - Primitive
- 01-070-1965 (C) - Cesium Zinc Chloride - Cs₂ZnCl₄ - Y: 5.85 % - d x by: 1. - WL: 1.78897 - Orthorhombic - a 9.75770 - b 12.97040 - c 7.40040 - alpha 90.000 - beta 90.000 - gamma 90.000 - Primitive - Pnam (62) - 4 - 9
- 01-085-1566 (C) - Lead Iron Chloride Hydroxide Hydrate - Pb₂FeCl₃(OH)₄(H₂O) - Y: 8.90 % - d x by: 1. - WL: 1.78897 - Monoclinic - a 8.03300 - b 6.25300 - c 9.22100 - alpha 90.000 - beta 102.980 - gamma 90.000 - Pr

5 weeks surface

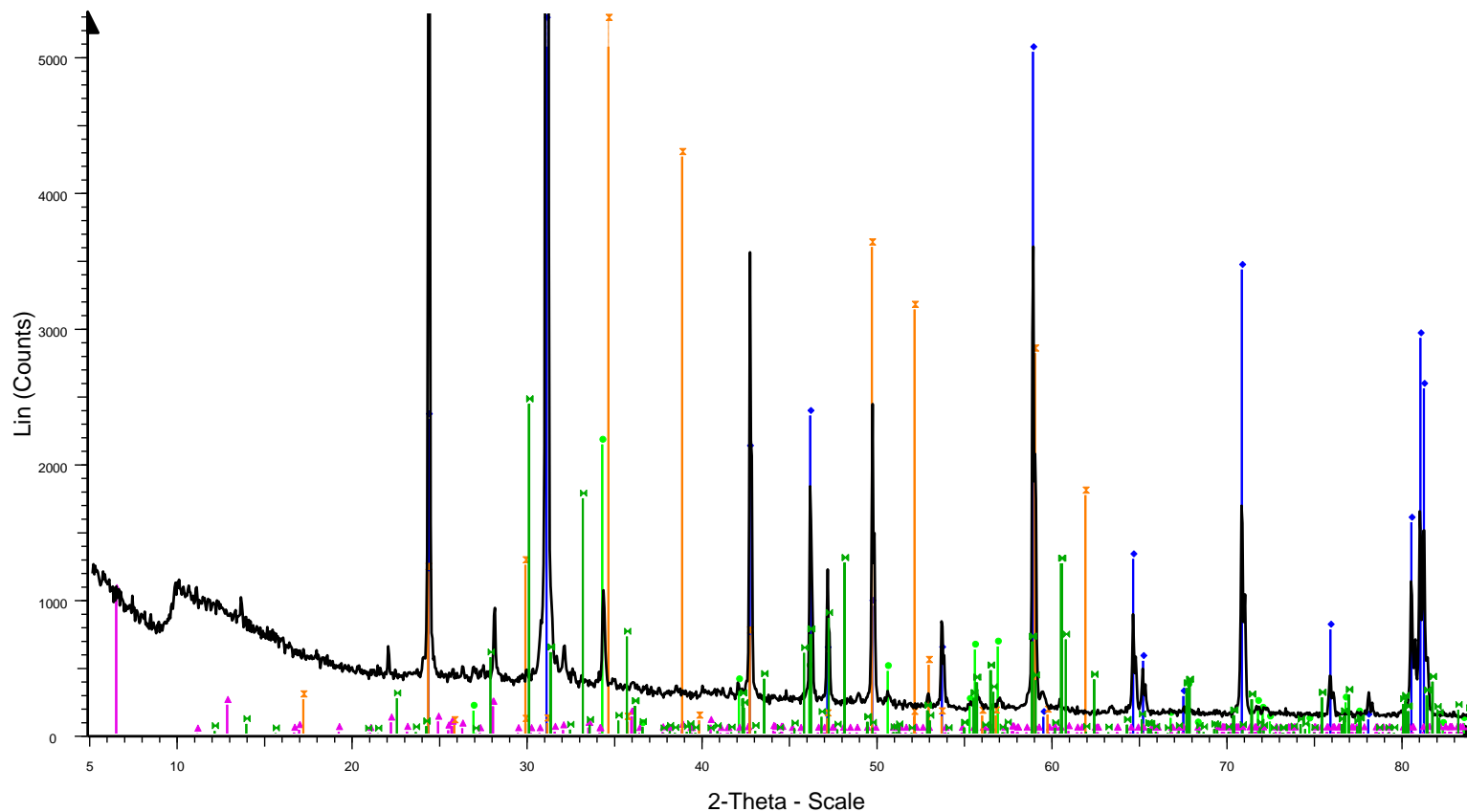
2011-513-006



- 2011-513-006 - File: 2011-513-006.raw - Type: Locked Coupled - Start: 5.002 ° - End: 84.992 ° - Step: 0.0 01-084-1178 (C) - Lead Chloride Bromide - PbCl1.52Br.48 - Y: 9.60 % - d x by: 1. - WL: 1.78897 - Orthorh
Operations: Import
- 01-085-0796 (C) - Quartz - SiO₂ - Y: 77.44 % - d x by: 1. - WL: 1.78897 - Hexagonal - a 4.91180 - b 4.911
 - 01-086-2339 (C) - Calcite - Ca(CO₃) - Y: 9.01 % - d x by: 1. - WL: 1.78897 - Rhombo.H.axes - a 4.98400 -
 - 01-079-2334 (C) - Aluminum Phosphate Hydrate - Al(PO₄)(H₂O).3333 - Y: 5.22 % - d x by: 1. - WL: 1.788
 - 00-030-0053 (*) - Ammonium Aluminum Hydrogen Phosphate - NH₄AlH₂PO₄ - Y: 6.85 % - d x by: 1. - W
 - 00-028-0694 (I) - Nickel Chloride Borate - Ni₃B₇O₁₃Cl - Y: 26.73 % - d x by: 1. - WL: 1.78897 - Orthorho
 - 01-075-2254 (C) - Cadmium Nickel Chloride Hydrate - CdNi₂Cl₆(H₂O)₁₂ - Y: 9.00 % - d x by: 1. - WL: 1.7

5 weeks middle slice

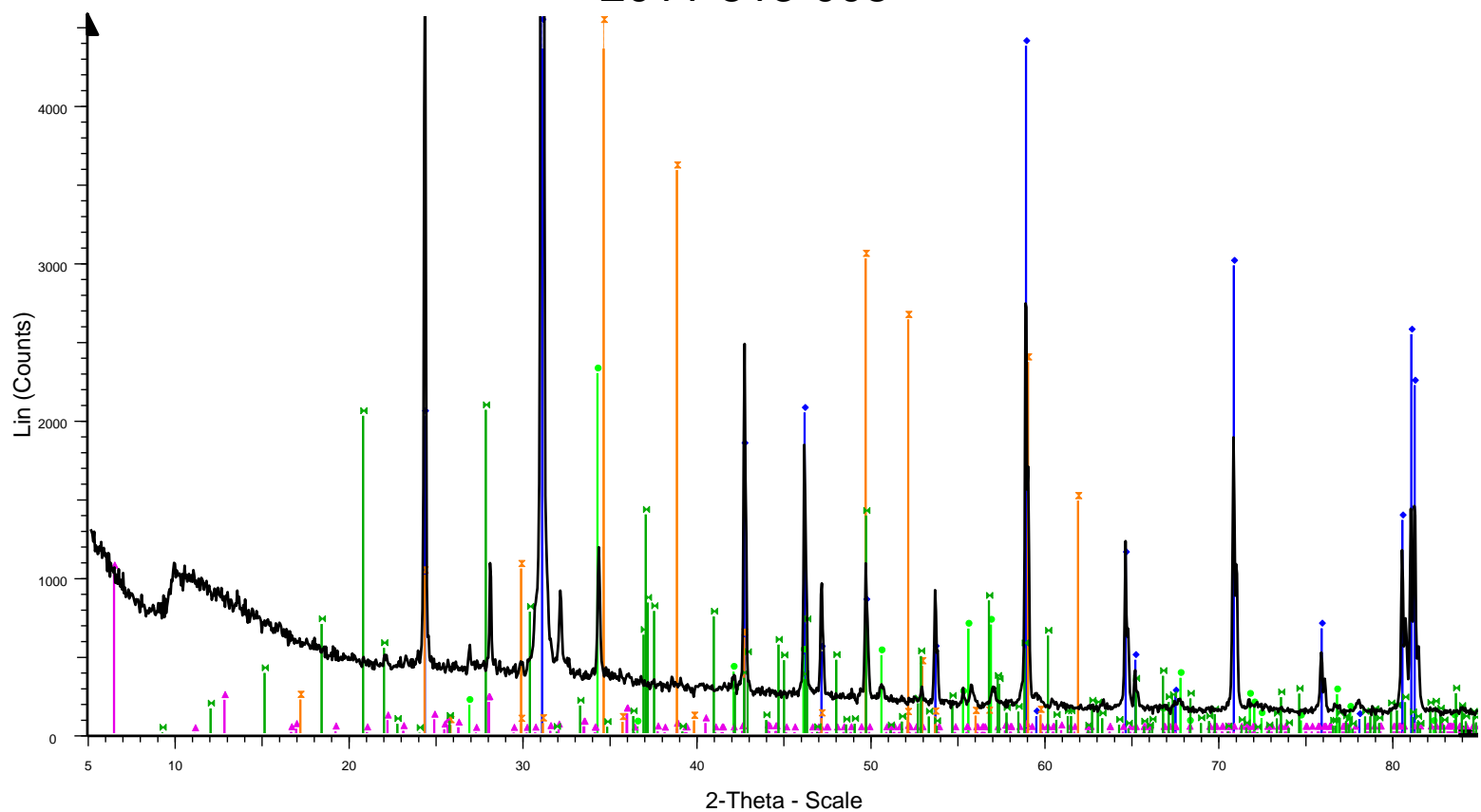
2011-513-007



2011-513-007 - File: 2011-513-007.raw - Type: Locked Coupled - Start: 5.002 ° - End: 84.992 ° - Step: 0.051 ° - Step time: 66. s - Temp.: 25 °C (Room) - Time Started: 0 s - 2-Theta: 5.002 ° - Theta: 2.501 ° - Chi: 0.00 ° -
Operations: Import
01-085-0797 (C) - Quartz - SiO₂ - Y: 92.63 % - d x by: 1. - WL: 1.78897 - Hexagonal - a 4.91410 - b 4.91410 - c 5.40440 - alpha 90.000 - beta 90.000 - gamma 120.000 - Primitive - P3221 (154) - 3 - 113.023 - I/c PDF 3.
01-086-2339 (C) - Calcite - Ca(CO₃) - Y: 8.90 % - d x by: 1. - WL: 1.78897 - Rhombo.H.axes - a 4.98400 - b 4.98400 - c 17.12100 - alpha 90.000 - beta 90.000 - gamma 120.000 - Primitive - R-3c (167) - 6 - 368.312 - I/c
01-079-2334 (C) - Aluminum Phosphate Hydrate - Al(PO₄)(H₂O).3333 - Y: 4.34 % - d x by: 1. - WL: 1.78897 - Hexagonal - a 18.65760 - b 18.65760 - c 8.32840 - alpha 90.000 - beta 90.000 - gamma 120.000 - Primitive -
00-028-0694 (I) - Nickel Chloride Borate - Ni₃B₇O₁₃Cl - Y: 35.30 % - d x by: 1. - WL: 1.78897 - Orthorhombic - a 8.51700 - b 8.51700 - c 12.03700 - alpha 90.000 - beta 90.000 - gamma 90.000 - 873.155 - I/c PDF 1. -
01-083-0392 (C) - Barium Manganese Nickel Chloride Fluoride - Ba₂(MnNiF₇C) - Y: 10.15 % - d x by: 1. - WL: 1.78897 - Monoclinic - a 7.76600 - b 5.84400 - c 8.93200 - alpha 90.000 - beta 106.640 - gamma 90.000 - P

5 weeks bottom

2011-513-008

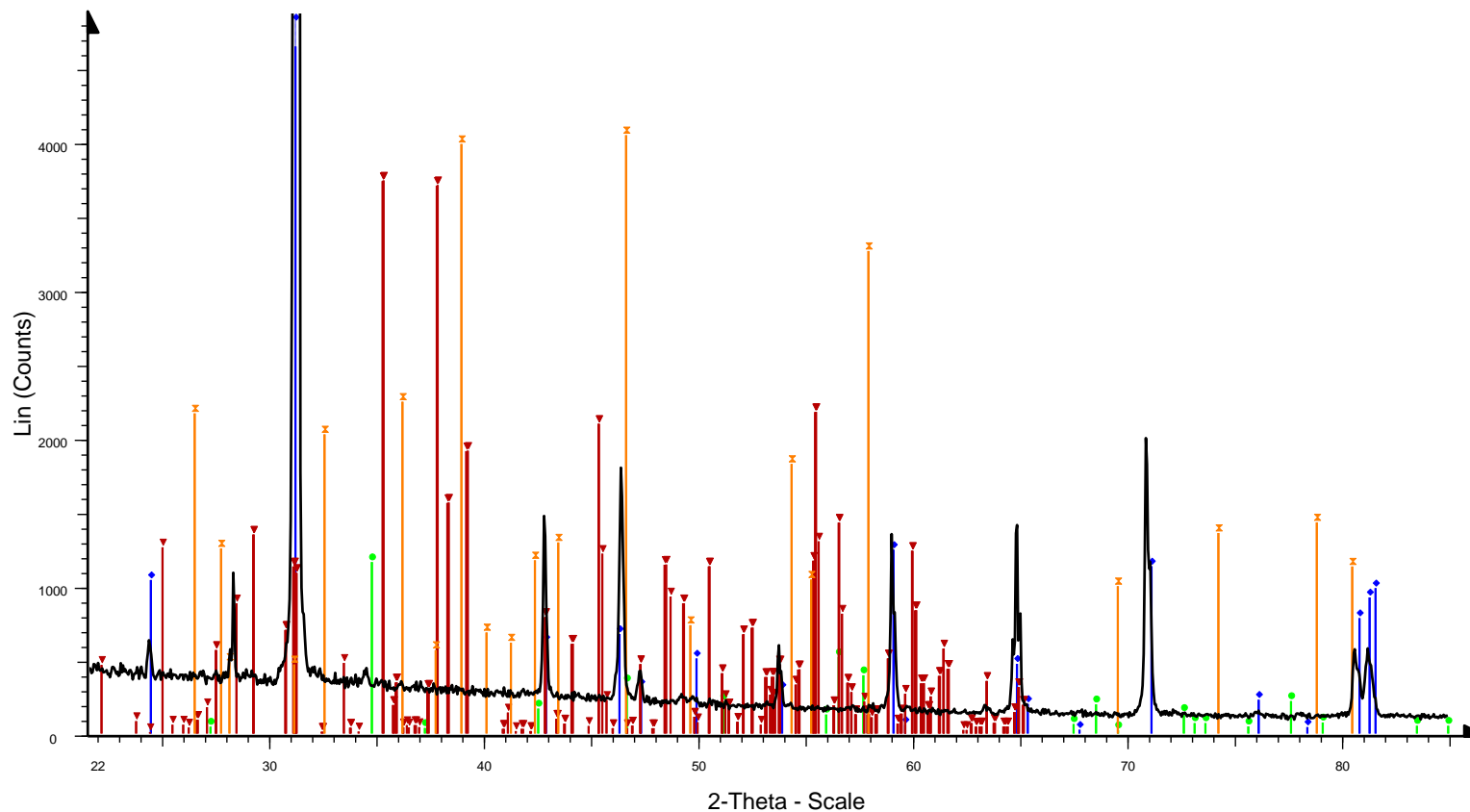


2011-513-008 - File: 2011-513-008.raw - Type: Locked Coupled - Start: 5.002 ° - End: 84.992 ° - Step: 0.051 ° - Step time: 66. s - Temp.: 25 °C (Room) - Time Started: 0 s - 2-Theta: 5.002 ° - Theta: 2.501 ° - Chi: 0.00 ° - Operations: Import

- 01-085-0797 (C) - Quartz - SiO₂ - Y: 62.88 % - d x by: 1. - WL: 1.78897 - Hexagonal - a 4.91410 - b 4.91410 - c 5.40440 - alpha 90.000 - beta 90.000 - gamma 120.000 - Primitive - P3221 (154) - 3 - 113.023 - I/lc PDF 3.
- 01-086-2339 (C) - Calcite - Ca(CO₃) - Y: 7.46 % - d x by: 1. - WL: 1.78897 - Rhombo.H.axes - a 4.98400 - b 4.98400 - c 17.12100 - alpha 90.000 - beta 90.000 - gamma 120.000 - Primitive - R-3c (167) - 6 - 368.312 - I/lc
- 01-079-2334 (C) - Aluminum Phosphate Hydrate - Al(PO₄)(H₂O).3333 - Y: 3.38 % - d x by: 1. - WL: 1.78897 - Hexagonal - a 18.65760 - b 18.65760 - c 8.32840 - alpha 90.000 - beta 90.000 - gamma 120.000 - Primitive -
- 00-028-0694 (I) - Nickel Chloride Borate - Ni₃B₇O₁₃Cl - Y: 23.19 % - d x by: 1. - WL: 1.78897 - Orthorhombic - a 8.51700 - b 8.51700 - c 12.03700 - alpha 90.000 - beta 90.000 - gamma 90.000 - 873.155 - I/lc PDF 1. -
- 01-075-2254 (C) - Cadmium Nickel Chloride Hydrate - CdNi₂Cl₆(H₂O)₁₂ - Y: 6.70 % - d x by: 1. - WL: 1.78897 - Hexagonal - a 9.95090 - b 9.95090 - c 11.23930 - alpha 90.000 - beta 90.000 - gamma 120.000 - Primitive

7 weeks surface

Sand surface 7 weeks



W Sand surface 7 weeks - File: 2011-513-003.raw - Type: Locked Coupled - Start: 5.002 ° - End: 84.992 ° - Step: 0.051 ° - Step time: 66. s - Temp.: 25 °C (Room) - Time Started: 0 s - 2-Theta: 5.002 ° - Theta: 2.501 ° - Chi: Operations: Import

B 01-086-1628 (C) - Quartz low - SiO₂ - Y: 20.25 % - d x by: 1. - WL: 1.78897 - Hexagonal - a 4.90210 - b 4.90210 - c 5.39970 - alpha 90.000 - beta 90.000 - gamma 120.000 - Primitive - P3121 (152) - 3 - 112.374 - I/c PD

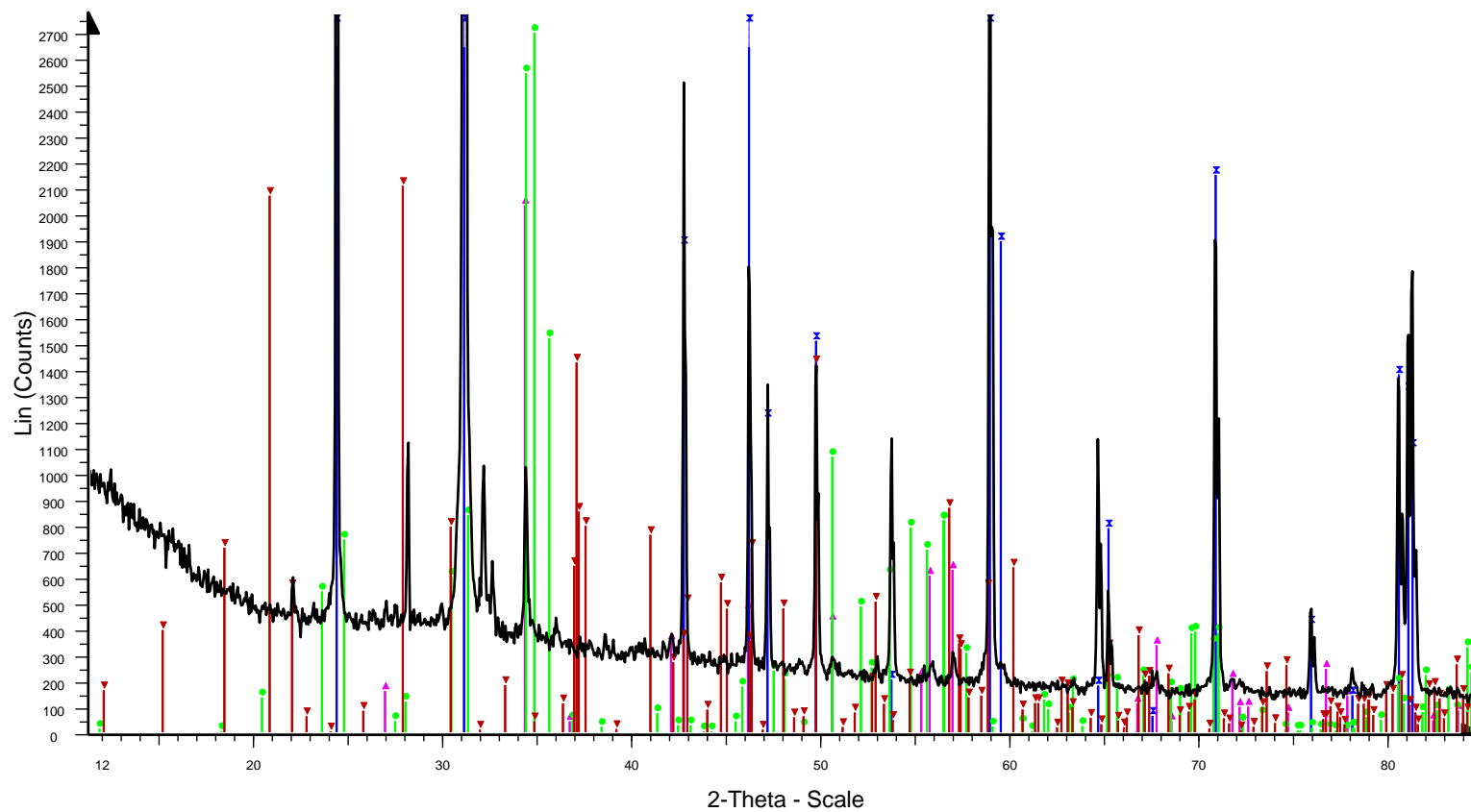
G 00-043-0697 (*) - Calcite, magnesian - (Ca,Mg)CO₃ - Y: 3.79 % - d x by: 1. - WL: 1.78897 - Rhombo.H.axes - a 4.94260 - b 4.94260 - c 16.85200 - alpha 90.000 - beta 90.000 - gamma 120.000 - Primitive - R-3c (167) -

V 01-079-0673 (C) - Cadmium Calcium Chloride Hydrate - Cd₂CaCl₆(H₂O)₆ - Y: 12.86 % - d x by: 1. - WL: 1.78897 - Triclinic - a 11.13700 - b 7.69300 - c 9.38700 - alpha 90.070 - beta 111.100 - gamma 99.930 - Primitive

X 00-042-0721 (I) - Copper Chromium Ammine Chloride Hydrate - Cr(NH₃)₅CuCl₅·H₂O - Y: 13.22 % - d x by: 1. - WL: 1.78897 - Cubic - a 22.18092 - b 22.18092 - c 22.18092 - alpha 90.000 - beta 90.000 - gamma 90.000

7 weeks middle slice

2011-513-005

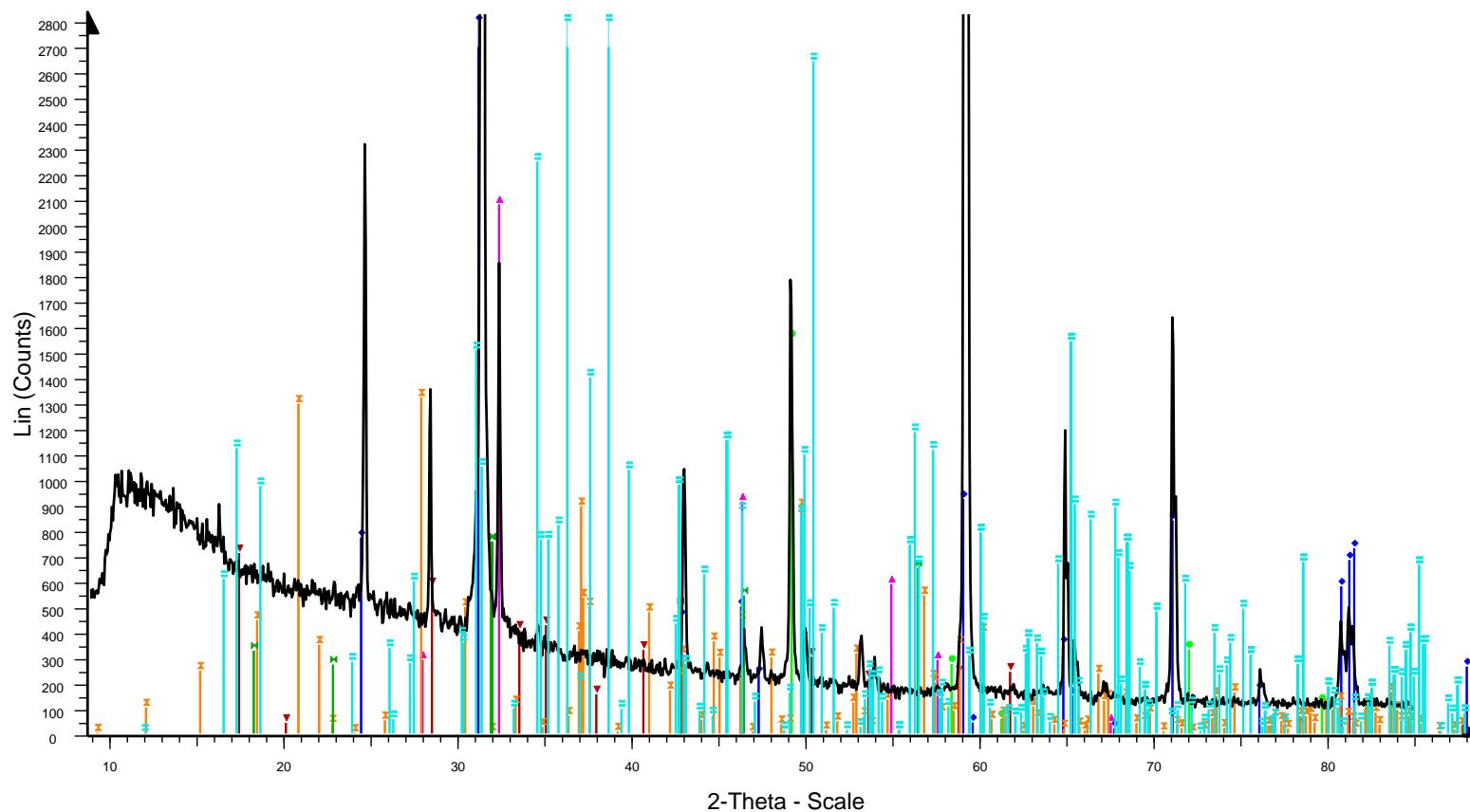


2011-513-005 - File: 2011-513-005.raw - Type: Locked Coupled - Start: 5.002 ° - End: 84.992 ° - Step: 0.051 ° - Step time: 66. s - Temp.: 25 °C (Room) - Time Started: 0 s - 2-Theta: 5.002 ° - Theta: 2.501 ° - Chi: 0.00 ° - Operations: Import

- 01-086-0174 (C) - Calcite, syn - $\text{Ca}(\text{CO}_3)$ - Y: 5.96 % - d x by: 1. - WL: 1.78897 - Rhombo.H.axes - a 4.98800 - b 4.98800 - c 17.06800 - alpha 90.000 - beta 90.000 - gamma 120.000 - Primitive - R-3c (167) - 6 - 367.761
- 01-087-2096 (C) - Quartz - SiO_2 - Y: 87.93 % - d x by: 1. - WL: 1.78897 - Hexagonal - a 4.91270 - b 4.91270 - c 5.40450 - alpha 90.000 - beta 90.000 - gamma 120.000 - Primitive - P3221 (154) - 3 - 112.961 - I/c PDF 4.
- 01-080-2149 (C) - Lead Chromium Oxide Silicate Chloride - $\text{Pb}_5(\text{Cr}_{1.5}\text{Si}_{1.5}\text{O}_{12})\text{Cl}$ - Y: 7.91 % - d x by: 1. - WL: 1.78897 - Hexagonal - a 10.14600 - b 10.14600 - c 7.41400 - alpha 90.000 - beta 90.000 - gamma 120.0
- 01-075-2254 (C) - Cadmium Nickel Chloride Hydrate - $\text{CdNi}_2\text{Cl}_6(\text{H}_2\text{O})_{12}$ - Y: 6.18 % - d x by: 1. - WL: 1.78897 - Hexagonal - a 9.95090 - b 9.95090 - c 11.23930 - alpha 90.000 - beta 90.000 - gamma 120.000 - Primitive

7 weeks bottom

Sand 7 weeks bottom



- Sand 7 weeks bottom - File: 2011-513-002.raw - Type: Locked Coupled - Start: 5.002 ° - End: 84.992 ° - S
- 01-075-1196 (C) - Potassium Copper Chloride - K_2CuCl_3 - Y: 10.57 % - d x by: 1. - WL: 1.78897 - Orthorh
- Operations: Import
- 01-086-1628 (C) - Quartz low - SiO_2 - Y: 10.88 % - d x by: 1. - WL: 1.78897 - Hexagonal - a 4.90210 - b 4.
- 00-047-1298 (*) - Copper Gold Zinc - $Au_{0.21}Cu_{0.35}Zn_{0.44}$ - Y: 3.68 % - d x by: 1. - WL: 1.78897 - Cubic -
- 00-048-1667 (*) - Potassium Hydrogen Fluoride - HKF_2 - Y: 4.93 % - d x by: 1. - WL: 1.78897 - Cubic - a 6
- 00-016-0195 (*) - Nickel Chlorate Hydrate - $Ni(ClO_3)_2 \cdot 6H_2O$ - Y: 1.68 % - d x by: 1. - WL: 1.78897 - Cubic -
- 01-075-2254 (C) - Cadmium Nickel Chloride Hydrate - $CdNi_2Cl_6(H_2O)_{12}$ - Y: 3.13 % - d x by: 1. - WL: 1.7
- 00-039-1255 (I) - Cadmium Aluminum Chloride - $Cd_2(AlCl_4)_2$ - Y: 1.79 % - d x bv: 1. - WL: 1.78897 - Tricli

Appendix E: concentrations alkali metals of other elements present in the soil

